17177

c.1

CONTINUOUS MICROBIOLOGICAL LEACHING OF A ZINC SULPHIDE CONCENTRATE

by

LYNTON SPENCER GORMELY

B. A. Sc., University of British Columbia, 1968

A THESIS SUBMITTED IN PARTIAL FULFILMENT OF THE REQUIREMENTS FOR THE DEGREE OF DOCTOR OF PHILOSOPHY

in the Department of CHEMICAL ENGINEERING

We accept this thesis as conforming to the required standard

THE UNIVERSITY OF BRITISH COLUMBIA

February, 1973

In presenting this thesis in partial fulfilment of the requirements for an advanced degree at the University of British Columbia, I agree that the Library shall make it freely available for reference and study. I further agree that permission for extensive copying of this thesis for scholarly purposes may be granted by the Head of my Department or by his representatives. It is understood that copying or publication of this thesis for financial gain shall not be allowed without my written permission.

Department of Chemical Engineering

The University of British Columbia
Vancouver 8, Canada

Date July 6, 1973

Abstract

A zinc sulphide concentrate was leached microbiologically by Thiobacillus ferrooxidans in a continuous stirred tank reactor. A model was developed to predict the leaching kinetics when the bacterial growth rate was not limited by any substrate other than the zinc concentrate, and it was modified to explain the observed results.

It was possible to obtain stable steady-states over a range of dilution rates. Because a solid substrate was used, the specific growth rate of the bacteria was not a unique function of the substrate concentration, and conventional continuous culture theory based on the Monod equation therefore did not apply to this system. The bacterial concentration did not limit the growth rates under the conditions of these experiments. The leaching rates and bacterial growth rates are thus first order in mineral surface area concentration.

The highest specific growth rate observed was 0.1038 hr^{-1}; the highest oxygen uptake coefficient ($Q_{O_2}(N)$) calculated was 7650. Both of these values are higher than any reported previously for T. ferrooxidans growing on a solid substrate. The highest zinc release rate obtained was 1.3 g/l-hr. None of these values is necessarily the maximum achievable.

Total carbon and non-distillable ammonium ion concentrations proved to be satisfactory measures of biomass concentration. Yield coefficients calculated from these data were constant for the dilution rates investigated, indicating a low maintenance energy requirement for the organism. The value of the net ammonium ion yield constant suggests that addition of ammonium ion above the level present in the medium 9K of Silverman and Lundgren should be beneficial when zinc concentrations exceed 68 g/l.

Percentage zinc extractions increased with decreasing dilution rate, but sufficiently low dilution rates to achieve extractions which would be competitive with conventional processes were not used. Recommendations are given for achieving competitive extractions by altering the process configuration. When the percentage zinc extraction was known for one dilution rate, it was possible to use a calculation method given by Levenspiel to predict the extractions at other dilution rates.

Contents

List of Tables

List of Figures

Acknowledgements

With pleasure I acknowledge the contributions of the following people and organizations:

Dr. D. W. Duncan, Dr. R. M. R. Branion, and Dr. K. L. Pinder provided guidance, instruction and friendship throughout the course of this work. I am indebted to B. C. Research for allowing me full use of their facilities for the research program. The technical instruction of Hilde Kurtz and Margaret Lewis is appreciated. I have had many valuable discussions with Dr. R. O. McElroy which have given me a better perspective on the field of hydrometallurgy. The Chemical Engineering workshop and stores personnel have been most cooperative in all aspects of equipment design and maintenance. Mr. Bruce Bowen supplied a sample of silica spheres for one of the experiments. The zinc concentrate was provided by Cominco Ltd. I wish to thank my wife Pat for her support during my graduate studies.

Financial support for this research was provided by the National Research Council of Canada and Shell Canada Limited.

NOMENCLATURE

a	= activity
A	= constant
b	= stoichiometric coefficient
B	= constant
D	= dilution rate, F/V, or diameter
E	= rate constant for maintenance energy metabolism, or electrode potential
f	= surface area occupied per unit of concentration of attached bacteria, or a polynomial function
F	= volumetric rate of removal of material from fermentor, or free energy
FEE	= free energy efficiency
G	= G-mass, structural/genetic biomass, or G-mass concentration
h	= constant
H	= enthalpy, or height
k	= rate constant
K	= saturation constant
L	= length
M	= dead biomass
N	= cell number concentration
pd	= pulp density
P	= P-mass, synthetic biomass, or P-mass concentration
Q	= oxygen uptake coefficient
r	= growth rate, release rate, or substrate consumption rate
s	= surface area concentration

S = substrate, or substrate concentration

SSA = specific surface area

t = time, or residence time

T = toxicant

TC = total carbon concentration

V = viable biomass, or viable biomass concentration, or volume of fermentor

W = width

X = cell mass concentration, or fractional extraction

y = an observation

Y = yield of cell mass or numbers based on substrate consumption

GREEK

α = constant

Δ = change in

κ = k_{-1}/k_1

μ = specific growth rate, r_X/X, or r_N/N

ν = specific growth rate for bacteria which are attached to mineral

ρ = density

σ = concentration of bacteria attached to mineral

τ = time for total consumption of particle

ϕ = constant

SUBSCRIPTS

b	baseline chemical leaching, or baffle
B	barrel
c	total carbon
C	critical dilution rate
CH	chemical leaching
G	G-mass
i	impeller
I	inhibitor
L	liquid
m	maximum specific growth rate
n	net ammonium ion
N	cell numbers
o	initial, or feed
OX	leaching of oxidized zinc mineral
P	P-mass
s	slurry
S	substrate
t	tank
T	toxicant
X	cell mass
Z	dissolved zinc

I. INTRODUCTION

The bacterium Thiobacillus ferrooxidans is of interest to the mining industry because it participates in the leaching of a variety of metals from their sulfide ores. Much research effort has been directed towards developing processes using T. ferrooxidans for microbiological leaching of heaps or dumps of low grade mineralization which cannot be handled economically by conventional mineral dressing techniques.

It has been proposed that microbiological leaching could be used to advantage in treating mineral concentrates as well as low grade material (1). This type of leaching would take place in a batch or continuous flow chemical reactor in which the process could be more readily controlled than could be a dump leaching system.

In chemical engineering, it is common to model processes mathematically. This permits mathematical manipulations to replace time consuming and costly experimentation in the search for the best configuration and optimum values of operating parameters for the process. In addition, because mathematical models may be based on hypotheses about the mechanisms which determine process behaviour, comparison of predicted and experimental results yields greater understanding of these mechanisms.

The objective of this work is to develop a mathematical model for *T. ferrooxidans* growing on zinc sulphide concentrate in continuous culture.

II. LITERATURE REVIEW

A. Mathematical Models For Microbial Growth

1. Types of Models

Many of the models to be considered seek to represent all phases of batch growth, and will be judged in part on whether or not they do this. The importance of this criterion when the batch models are adapted to continuous culture lies in the fact that all aspects of batch growth must manifest themselves in continuous culture (2). For example, if we consider the lag phase to be a period of adaptation for the bacterium, then the transient response to a step change of a variable in continuous culture should show the effect of adaptation of the bacterium to the new conditions existing in the fermentor. There are a number of different assumptions which can lead to models which will (qualitatively) predict all phases of batch growth.

Tsuchiya et al. (2) discussed possible approaches to the problem of dynamic modelling of microbial cell populations, and proposed several classifications for models. They noted that life is segregated into structural and functional units called cells which can only arise from preexisting cells. Therefore, in any complete theory of cellular population dynamics, the number of cells per unit volume will be the fundamental dependent

variable.

In bacterial leaching of mineral sulphides, firm attachment of cells to the surface of the mineral makes cell counts virtually impossible. Thus, the cell number will need to be replaced by some more easily attainable measure of population such as bacterial carbon or nitrogen analysis. The model for correlating the data will use such empirical measures of concentration of living substance, and will treat life as something distributed throughout the medium in which the cells are growing. This gives us the first means of classifying a model: it may be either a segregated model or a distributed model. A segregated model recognizes the existence of cells and uses cell number as the fundamental dependent variable. A distributed model does not recognize the segregation of biomass into cells and uses a measure of biomass other than cell numbers as the fundamental dependent variable. While the process of growth can be treated in both models, the process of reproduction can only be treated by segregated models.

A second basis for classification is that the living material may be assumed to be either structured or unstructured. A segregated model contains structure if some means is specified for distinguishing a cell from its fellows. A distributed model contains structure if the composition of the living substance (or biomass) varies with conditions of propagation. The

inclusion of structure is a recognition that a cell is not of homogeneous composition; it is differentiated, and the proportions of the differentiated structures may vary. The physiological state of a cell is determined by its structure. In a structured model, specification of the state of the population requires specification of more than one quantity.

Finally, we may use either stochastic or deterministic models. In fact, a cell population is always segregated and structured, and its growth and reproduction are random processes which should be treated stochastically. Predictions of stochastic models are in the form of frequency distributions; there is a range of possible results due to randomness of biological processes. Deterministic models predict only discrete results for any given set of conditions; they assume that in a large cell population the randomness will average out to the predicted results every time. A stochastic model containing all aspects of structure is beyond the scope of our biological and mathematical sophistication, so that simplified approaches are necessary to give useful results.

2. Stochastic Models

Tsuchiya et al. (2) derived a segregated, unstructured, stochastic model. This simple model simulated the exponential phase of growth only. By investigating the moments of the

distribution, they concluded that for small inocula, observations on many identical systems would be widely scattered about the mean. However, for inocula of the sizes usually encountered, they concluded that for practical purposes the growth process can be regarded as deterministic.

Fredrickson and Tsuchiya (3) presented a segregated, structured, stochastic model in which the structure was provided by considering age as an index of physiological state of the cell. Cell division, death, and autolysis probability densities were thus considered as functions of cell age. The resulting equations were solved for the cell age distribution in a continuous fermentor at steady-state. The steady-state obtained was probably stable with no oscillations, but this was not proved. Expressions for calculating gross metabolic rates and cell size distributions were derived.

Eakman *et al.* (4) modified the above model by considering cell mass to be a better index of physiological state than cell age. This allowed them to treat the rate of increase of mass of a single cell by existing deterministic models, so that explicit account could be taken of the interaction between population and environment. The equations were solved for the case of the steady-state continuous fermentor. They concluded that distributed models are adequate to describe the results when the dilution rate is not near the critical dilution rate.

The stochastic models which have been discussed are only valid when environmental conditions are constant or changing slowly, that is, when growth is balanced (4). They cannot predict a lag phase in batch culture, nor can they correctly predict transient conditions in continuous culture[1]. Elaborate experiments are necessary to obtain the distribution functions for cell division and death (e.g. synchronous culture studies (3)). These objections, together with the mathematical complexity of the stochastic models, have resulted in deterministic models being more popular in the literature.

3. Unstructured Deterministic Models

In many of the models to be discussed below, the following cell mass (or cell numbers) balance and limiting substrate balance equations will be combined with an expression for growth rate to derive expressions for bacterial growth in a continuous stirred fermentor with no recycle or feed of bacteria.

---

[1] These objections may be removed by the inclusion of a limited amount of biochemical structure into the models. The equations for such a model have been developed, but not yet solved (4).

$$\frac{dX}{dt} = r_X - DX \qquad \text{(cell mass concentration)} \tag{1}$$

$$\frac{dN}{dt} = r_N - DN \qquad \text{(cell numbers concentration)} \tag{2}$$

$$\frac{dS}{dt} = DS_o - DS - \frac{r_X}{Y} \qquad \text{(substrate concentration)} \tag{3}$$

Tsuchiya *et al.* (2) discussed two simple deterministic models in which the growth rate is a function only of the number of cells present. The first yields only the exponential phase in batch growth:

$$r_N = \mu N \tag{4}$$

If the bacteria are considered to be growing in a continuous stirred fermentor, the cell number balance gives

$$\frac{dN}{dt} = \mu N - DN \tag{5}$$

so that at steady-state

$$\mu = D \tag{6}$$

Since μ is a constant (here) there can be only one steady state, and the population density is indeterminate. This contradicts the experimental observation that different steady-states may be attained over a range of dilution rates.

The second model assumes the "logistic law":

$$r_N = \alpha N (1 - hN) \tag{7}$$

where α and h are positive constants. In batch growth (D = 0), this may be integrated to give the logistic curve:

$$N = \frac{N_o e^{\alpha t}}{1 - hN_o (1 - e^{\alpha t})} \tag{8}$$

As $t \rightarrow \infty$, N approaches 1/h, giving a stationary phase following the exponential growth. No lag phase is predicted.

In continuous culture, at steady-state,

$$D = \alpha (1 - hN) \tag{9}$$

In contrast to equation 6, a steady-state can be obtained for

any dilution rate less than α . At $D = \alpha$, a steady-state is also attained, but $N = 0$.

This result is much more satisfactory than the previous one, but it is suspect because no allowance is made for the reciprocal effect of bacteria on environment and environment on bacteria. This objection can be overcome by making assumptions first suggested by M'Kendrick and Pai (5). They postulated that exponential growth can occur only when unlimited nutrient is available, and that when this was exhausted, growth must stop. Their expression gave growth rate as

$$r_N = \phi NS \tag{10}$$

where S is the growth limiting substrate concentration. The concentration of growth limiting substrate is influenced by the rate of consumption of substrate which is assumed to be

$$r_S = -\frac{1}{Y} r_N \tag{11}$$

In batch growth, equations 10 and 11 lead to the logistic equation 8 where $\alpha = \phi (S_o + (1/Y) N_o)$ and $h = (1/Y)/(S_o + (1/Y) N_o)$. Now α and h have a physical significance.

Monod (6,7) improved on the theory of M'Kendrick and Pai in

two ways. He realized that they were in effect postulating a chemical reaction between the cell material and the substrate, so that cell mass concentration, not population density should be the dependent variable; i.e., a distributed model was required. He also recognized that there was a limit to how fast a cell could grow, so he postulated that substrate dependence of growth follow the Michaelis-Menten enzyme kinetics expression:

$$r_X = \frac{\mu_m XS}{K + S} \tag{12}$$

This, together with

$$r_X = - Y r_S \tag{13}$$

constituted Monod's model. Monod was very careful to explain that equation 12 was an empirical relation which was found to explain the data quite well. Monod considered it to be an extremely remote possibility that only one of all the reactions involved in growth should be so slow as to be rate controlling. Therefore equation 12 should not be considered as representing the Michaelis-Menten kinetics of a one enzyme catalyzed "master reaction".

In batch growth, X increases exponentially at first, but a stationary phase occurs when substrate is exhausted. There is no

lag phase. The maximum concentration of protoplasm is

$$X = X_o + YS_o \simeq YS_o \tag{14}$$

Herbert et al. (8) developed Monod's model for the continuous case. Using equations 12 and 13 in equations 1 and 3, they derived the differential equations

$$\frac{dX}{dt} = X \{\mu_m \frac{S}{K + S} - D\} \tag{15}$$

$$\frac{dS}{dt} = D (S_o - S) - \frac{\mu_m X}{Y} (\frac{S}{K + S}) \tag{16}$$

Setting these to zero, they obtained the steady-state cell mass concentration and substrate concentration:

$$X = Y (S_o - K (\frac{D}{\mu_m - D})) \tag{17}$$

$$S = K (\frac{D}{\mu_m - D}) \tag{18}$$

and also

$$S = S_o \tag{19}$$

$$X = 0 \tag{20}$$

Tsuchiya et al. (2) showed that the first steady-state (equations 17 and 18) is stable if

$$\frac{\mu_m S_o}{K+S_o} > D \tag{21}$$

and unstable if the inequality is reversed. When it is stable, no oscillations will be observed in the approach to steady-state. The second steady-state (equations 19 and 20) is stable if

$$\frac{\mu_m S_o}{K+S_o} < D \tag{22}$$

and unstable if the inequality is reversed. This corresponds to complete washout of cells, so that one is normally more interested in the first steady-state. The point of equality

$$\frac{\mu_m S_o}{K + S_o} = D = D_C \qquad (23)$$

gives the critical dilution rate. Because the critical dilution rate is that at which cells wash out, it is an operating parameter of considerable practical importance.

Herbert et al. (8) used Aerobacter cloacae to make quantitative experimental tests of the model. The model was adequate to explain the data except near the critical dilution rate. Steady-state was obtained at dilution rates higher than the predicted critical dilution rate. The reason for the discrepancy was believed to be non-ideal mixing in the fermentor as well as wall growth on the fermentor. The yield constant was similar to the value obtained in batch experiments for low dilution rates, but decreased at higher dilution rates.

Dabes et al. (9) developed a general model of a series of linked reversible enzymatic reactions dependent on the concentration of a single external substrate. Applying the master reaction concept and using different simplifying assumptions, they were able to derive the following three models:

-when two slow enzymatic steps are separated by a series of

fast reactions that together can be described by an equilibrium constant that is not large,

$$\mu = \frac{B + A\mu_m + S - \sqrt{(B + A\mu_m + S)^2 - 4\,A\mu_m S}}{2\,A} \qquad (24)$$

where A, B, and μ_m are defined in terms of parameters of the assumed enzymatic pathway.

-when the equilibrium constant for the intermediate reactions is large, Blackman kinetics result:

$$\mu = \frac{S}{A}\ , \quad \text{when} \quad S < A\mu_m \qquad (25)$$

$$\mu = \mu_m\ , \quad \text{when} \quad S > A\mu_m \qquad (26)$$

-when the maximum forward rate of one enzymatic reaction in the cell may be assumed to be much less than the maximum forward rate of any other reaction in the pathway, Monod's model (equation 12) results.

These workers then examined twelve sets of experimental data from the literature and showed that the Monod model gave a poorer fit than the Blackman model in nine of the twelve cases

as determined by a non-linear least-squares fitting technique.

Sinclair et al. (10) have modified Monod's model to account for utilization of substrate to provide maintenance energy for the bacteria. The steady-state bacterial concentration predicted is

$$X = \frac{YD}{D + E}\left[S_o - \frac{K\,(D + E)}{\mu_m - (D + E)}\right] \qquad (27)$$

This predicts that the yield of bacteria per unit of substrate consumed decreases at low dilution rates as a greater portion of the energy released is diverted for maintenance requirements.

Ware (11) developed Monod's model to handle mixed cultures (more than one strain of bacteria), mutations, and the addition of antimicrobial agents. Initial lag was introduced by creating an artificial delay in the organism's response to substrate. A certain maximum concentration of cells (the M-concentration) could not be exceeded even if substrate was not yet exhausted; a rate modifying factor was introduced to ensure this. The effect of bactericides was given by another rate modifying factor. The actual growth rate at any time was calculated after considering these three modifying effects. Other modifications included provision for death of cells naturally and by bactericides, and adsorption of bactericides by dead cells. The equations for batch culture were solved in Algol 60 on a digital computer.

Continuous culture was not treated.

It is felt that Ware's simulation, although able to reproduce all phases of bacterial growth and to account for numerous other factors, has lost much of its potential usefulness because of the arbitrary manner in which some of the effects were taken into account. It may be useful in a predictive sense, but it gives no insight into the reasons for the appearance of a lag phase or a maximum population.

Consideration will now be given to alternative unstructured deterministic models which give better understanding of how properties of the culture can determine the appearance of various batch growth phases.

We have seen that the Monod model predicts exponential growth initially while substrate concentration is high, followed by a stationary phase when substrate is exhausted. Andrews (12) observed that high concentrations of substrates could initially be inhibitory to organisms metabolizing them, and that this could result in a lag phase in their growth curve. Just as Monod's empirical relation was similar to the Michaelis-Menten expression for enzyme kinetics, Andrews chose an "inhibition function" similar in form to one used to describe substrate inhibition in enzyme kinetics:

$$\mu = \frac{\mu_m S}{K + S + S^2/K_I} \qquad (28)$$

This expression was used in formulation of differential equations for batch and continuous growth. The equations were solved numerically on a digital computer.

In batch growth, substrates with low values of K_I produced pronounced lag phases. In continuous culture it was found that there were two possible steady states, one of which was unstable. Successful startups required a minimum inoculum size below which the process failed. If start-up took the form of a ramp change in substrate concentration rather than a step change, successful start-ups could be achieved with lower inoculum sizes.

As with the Monod model, a stationary phase should occur at substrate exhaustion, although this was not demonstrated.

Besides exhaustion of substrate, stationary phase may occur as a result of accumulation in the medium of toxic or inhibitory products of the cells' metabolism. Thus, a phase of decline may occur as the cells are killed by a toxicant.

Ramkrishna *et al.* (13) developed a model in which the reactions representing growth were given as

$$V + b_S S \rightarrow 2\,V + b_T\,T + \ldots. \qquad (29)$$

$$V + T \rightarrow M + (1 + b_{T1})\,T \qquad (30)$$

In reaction 29 viable biomass and substrate react to produce more viable biomass plus toxicant and other metabolic products. In reaction 30, viable biomass and toxicant react to form dead biomass, and toxicant may be consumed or produced, depending on the sign of b_{T1}. The kinetics for reaction 29 are assumed to be given by the Monod equation.

With b_{T1} positive, all growth phases except lag phase are present in simulated batch growth. b_{T1} negative or zero gives a curve showing no lag or stationary phases.

In continuous culture, two steady-states are predicted by this model; one is at washout and the other is the "normal" steady-state. A critical dilution rate is predicted equal to that predicted by Monod's model. Damped oscillations about the normal steady-state may occur for smaller dilution rates.

Luedeking (14) in a review of fermentation process kinetics presented a graphical method for predicting continuous culture results from batch culture data. The method is presented in Figure 1. The bacterial growth rate is plotted against the bacterial concentration for the entire batch cycle. A line having slope equal to the desired dilution rate and passing through the origin (the operating line) is then drawn over this curve. The intersection of the operating line with the growth curve represents a steady-state mass balance on bacteria for a continuous stirred tank reactor operating at the chosen dilution rate. The bacterial growth rate and bacterial concentration at this point should be those existing in the continuous reactor if the feed has the same conditions as the initial conditions for the batch experiment. Luedeking and Piret (15) have verified this method for a single-stage continucus lactic acid fermentation.

Assumptions necessary for the accurate prediction of continuous results by this method are that conditions in the continuous culture are the same as those in the corresponding stage of batch cultivation and that bacterial concentration is a valid parameter for determining the rate of bacterial growth.

The second assumption is really an indirect way of expressing bacterial growth rate as a function of both substrate

Figure 1

LUEDEKING'S GRAPHICAL SOLUTION FOR CONTINUOUS FERMENTATION IN A SINGLE VESSEL (14)

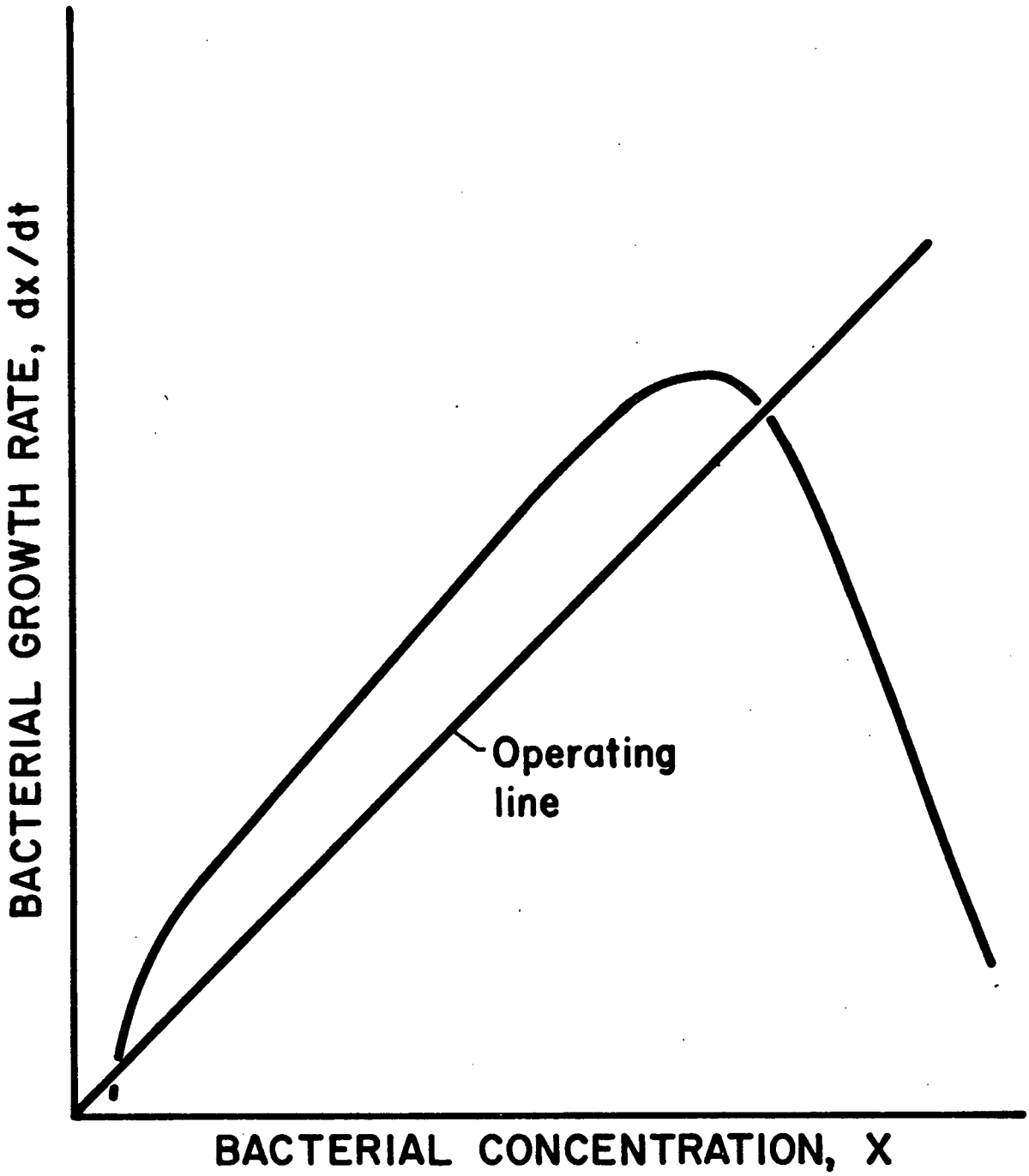

concentration and bacterial concentration. As bacterial concentration increases, the substrate concentration decreases until exhaustion of substrate terminates the fermentation. Such curves are therefore unique only to a given initial substrate concentration.

For the special case of the fermentation of a heterogeneous substrate, the growth rate should depend on concentration of substrate surface available to the bacteria, not on the substrate concentration (16). The utility of this method then depends on whether the relation between bacterial growth rate and bacterial concentration will be the same in both batch and continuous culture under this special constraint.

For a single substrate particle exposed to bacterial attack, the substrate surface area and amount of substrate used are a function of the time the particle has been exposed to the bacteria. In a batch reaction, if all the particles are the same size initially, one simply multiplies the surface area and amount of substrate used for one particle by the total particle concentration to obtain the relation between the reduction in substrate concentration and the surface area concentration at any time.

In a continuous reactor, however, there is a distribution of particle ages, and the surface area concentration for any

reactor residence time must be determined by summing the surface areas of the particles over all the ages. Similarly, the reduction in substrate concentration must be calculated by summing the reductions for particles of all ages (17).

Evidently, the relationship between surface area concentration (and hence bacterial growth rate) and substrate utilization (and hence bacterial concentration) will not need to be the same in batch as in continuous culture. It is dependent on the distributions of residence times which are quite different for the two cases. Therefore, conditions in a batch culture at a particular time are not the same as those in a continuous culture having that residence time when bacteria are consuming a heterogeneous substrate, and the method should not successfully predict the continuous leaching results from the batch data.

4. Structured Deterministic Models

Up to now we have considered only deterministic models which lack structure. When structure is added to a model, the cell composition changes with changing culture conditions. Therefore the behaviour of the biomass may be affected by its history. This enables structured models to predict a large number of observed phenomena of bacterial growth.

One of the simplest structured models to appear in the literature is that of Williams (18). The viable biomass is divided into two components, G-mass and P-mass. G-mass is the structural/genetic portion of the cell and P-mass is the synthetic portion. G-mass is seen as consisting mainly of protein and DNA, while P-mass is thought of as the sum total of small metabolites in the cell, together with the ribosomal particles and RNA involved in protein synthesis. Cell division is said to occur if and only if the G portion has doubled its size. The reactions which comprise growth are

$$G + b_S S + P \rightarrow 2\ P + G + \ldots. \tag{31}$$

$$b_P P + G \rightarrow 2\ G \tag{32}$$

Assuming bimolecular first order reactions in a continuous fermentor, the differential equations are

$$\frac{dS}{dt} = D\ (S_o - S) - k_1 S V \tag{33}$$

$$\frac{dP}{dt} = k_1SV - k_2 PG - DP \qquad (34)$$

$$\frac{dG}{dt} = k_2 PG - DG \qquad (35)$$

where V = G+P and batch fermentation is simulated by putting D = 0. Adding equations 33 and 34

$$\frac{dP}{dt} + \frac{dG}{dt} = \frac{dV}{dt} = k_1 SV - DV \qquad (36)$$

which in batch culture is similar to equation 10 with V substituted for N. Thus, in batch culture, the growth curve for viable biomass is given by the logistic equation. The model therefore gives results like those of M'Kendrick and Pai (5) except that viable biomass is substituted for cell numbers. Because of its structure, however, this model will predict a lag based on cell numbers, with the increase in viable biomass going into making the existing cells larger rather than increasing their number. No phase of decline is predicted.

This simple model illustrates a number of other experimentally observed features of cell population growth. It shows differences in response lag of different cellular

components following a change in environmental conditicns, and general growth curve shapes for both steady-state and transient conditions in either batch or continuous cultures. There is an absence of lag phase when the culture medium is inoculated with already rapidly growing cells. Cells are able to continue dividing after being placed in non-nutrient medium.

Some shortcomings of the model include the difficulty of determining what shall constitute G-mass and P-mass, the lack of provision for a maximum growth rate (e.g. as in the Mcnod equation), and the fact that the lag phase is nct perfect - there is always some cell division occurring.

We have already mentioned the first part of a paper by Ramkrishna et al. (13), in which they postulated that stationary phase and phase of decline are the result of toxicants released into the medium by the growing cells. In the seccnd part of that paper, by adding structure to the model, they were able to predict all phases of batch growth, including a lag phase in the viable biomass. They divided the cell into two parts, G- and P-mass, as did Williams, but they formulated the growth reactions and the growth reaction kinetics in a different manner. Ignoring the toxicant, growth was postulated as

$$G + b_S S + P \rightarrow 2\,G + P \tag{37}$$

$$G + b'_S\,S + P \rightarrow 2\,P + G + \ldots. \tag{38}$$

Here, growth of G did not occur at the expense of P as it did in Williams' model. The kinetics for these reactions were given by a double substrate Michaelis-Menten type expression:

$$r_G = \frac{\mu_G SGP}{(K + S)(K_G + G)} \tag{39}$$

$$r_P = \frac{\mu_P SGP}{(K' + S)(K'_G + G)} \tag{40}$$

so that there was a maximum growth rate at high substrate concentrations.

In another paper (19), these authors assumed that the stationary phase was a result of exogenous substrate exhaustion, and that the decline phase did not begin until stores of an endogenous substrate were depleted. Using the same type of structure (G-mass and P-mass), all phases of batch growth could

be predicted.

Which of these last two models is better for a given situation should be determinable by experimentation since some differences in behaviour in both batch and continuous culture are expected, even though each can predict qualitatively the same batch curves. The toxicant model predicts a large change in growth pattern as the initial substrate concentration is changed, while the endogenous metabolism model predicts little difference. With the toxicant model, viable biomass concentration at steady-state falls off at low dilution rates; with the endogenous metabolism model, a fairly constant viable biomass level is maintained. Oscillations in continuous culture viable biomass concentration are possible with the toxicant assumption, but not with the endogenous metabolism assumption.

One other interesting approach to the problem of modelling a growing bacterial population is that of Swanson et al. (20). They consider the problem of bacterial growth to be similar to certain optimization problems in economics, termed "bottleneck" problems. In this view, the rate of growth of the biomass is controlled by the concentration in the cell of a critical intermediate which is produced at the expense of substrate. It is postulated that the bacteria produce the critical intermediate ("bottleneck product") in such a way as to maximize the net increase in biomass by the time that the limiting

nutrient is exhausted. Solution of this problem leads to two sets of differential equations; one for lag phase, when the concentration of bottleneck product is building up but no growth occurs, and the other for the remaining phases when no bottleneck product is produced. Since provision for cell death is included, this model can predict all phases of cell population growth.

The model has been solved only for batch culture. Because the point at which lag phase gives over to exponential growth is a function of the initial concentrations of substrate and bottleneck product, adaptation to continuous culture is not quite so straightforward as it has been in some of the previous models. Intuitively, it seems that it should be possible, invoking lag equations only for transient behaviour. This model is intriguing because it assumes that natural selection has led to an optimal growth pattern. The optimal growth pattern turns out to be (qualitatively) that which is observed experimentally.

5. Models for Heterogeneous Fermentations

Chakravarty *et al.* (21) have presented a kinetic model for growth on a solid hydrocarbon substrate. The model is based on the assumption that a metabolite produced by the growing cells helps the dissolution of the solid substrate in the aqueous medium so that it can be used by the bacteria. The growth rate

of the bacteria is related to the concentration of dissolved hydrocarbon according to the Monod model. The concentration of the metabolite in the medium is assumed to be proportional to the number of cells present. The linear behaviour of the growth curve predicted by the model was verified experimentally.

Erickson and Humphrey (22) have formulated three batch models for growth on a substrate which forms a second phase in the fermentor. The second phase is assumed to be a pure substrate, and the interfacial area is assumed to decrease due to substrate consumption. No cells are in the continuous phase until the surface of the dispersed phase becomes saturated with cells.

The first model assumes all growth occurs at the interface of the dispersed phase, and the specific growth rate for cells at the surface is a constant. The second model assumes substrate equilibrium between the two phases and growth occurs both at the interface and in the continuous phase. The third model assumes substrate consumption in the continuous phase is limited by mass transfer of substrate into that phase, and growth occurs both at the interface and in the continuous phase.

By comparing these models to experimental results they conclude that the concept of a growth rate proportional to the surface area of the dispersed liquid phase may be useful in

explaining rates of growth on n-alkanes. Surface area may limit growth either by allowing only a fraction of the total cell population to be at a drop surface or by limiting the rate of substrate transport to the continuous phase, or both. They observed with yeast cultures that a large number of cells are in the continuous phase even when there are not enough cells to cover the drop surface. An equilibrium should exist between those cells at the drop surface and those in the continuous phase.

Erickson et al. (23) developed a model for growth on a hydrocarbon substrate which is dissolved in a dispersed phase. The model accounts for drop size distribution, coalescence and redispersion, growth in the continuous phase and at the interface, and adsorption and desorption of bacteria at the interface. The adsorption rate is assumed to be proportional to the product of the cell concentration in the continuous phase and the free surface area per unit volume. The rate of desorption is assumed to be proportional to the number of cells on the drops. The differential equations describing the model have been solved numerically for the case of batch growth only. It should be possible to adapt this model to the case of continuous bacterial leaching of sulphide minerals.

If a solid or liquid dispersed phase surface were saturated with cells and no growth were occurring in the continuous phase,

then the reaction could be modelled by the methods provided by Levenspiel (17) for heterogeneous reacting systems. His model for a shrinking spherical particle when chemical reaction at the surface is controlling should apply to this system. He supplies the solutions for both batch reactors and continuous stirred tank reactors.

B. Bacterial Leaching

1. Introduction

Throughout the discussion of models, bacterium-environment interaction has been described by means of interaction between the bacterium and a limiting substrate. Thus, the models have been concerned not only with growth rates but also with yields of bacteria when a given amount of substrate has been consumed. We now wish to consider specifically the bacterium used in this study, *T. ferrooxidans*, its nutritional requirements, possible limiting substrates, and yield and rate data which have appeared in the literature. We will conclude by reviewing the work done by Torma (16) which was the basis for the present study.

While examining acidic coal mine drainage waters for a pollution study, Colmer and Hinkle (24) noted the presence of a bacterium involved in the oxidation of ferrous iron to the ferric form. In subsequent papers, Colmer *et al.* (25), and

Temple and Colmer (26) described morphological and cultural characteristics of the organism, demonstrated its autotrophic nature on thiosulphate and ferrous iron media, and suggested the specific name T. ferrooxidans.

Two organisms similar to T. ferrooxidans have been isolated and described (27,28). These were given the names Ferrobacillus ferrooxidans and F. sulfooxidans, but the validity of this new genus has been questioned (29,30). It is now generally accepted that the three are the same organism. Moreover, any slight differences between them are negligible in mineral applications (31). They are, however, distinct from the morphologically similar T. thiooxidans due to the latter's inability to oxidize ferrous iron (32).

2. Nutritional Requirements

Nutritional requirements of T. ferrooxidans have been reviewed by Tuovinen and Kelly (33). Energy is derived from oxidation of iron, sulphur, and reduced sulphur compounds. The ultimate electron acceptor in the oxidation of these substances is oxygen dissolved in the medium. Carbon for the creation of biomass can be supplied entirely by carbon dioxide dissolved in the medium. Nitrogen may be supplied as ammonium ion; some amino acids may be substituted as a nitrogen source. Fixation of atmospheric nitrogen has been cited. Phosphate requirements are

satisfied by orthophosphate ion. Magnesium is required as a trace element theoretically, but no one has demonstrated a measureable requirement. Sulphate is required as a source of sulphur for biosynthesis; an additional role in the metabolism of T. ferrooxidans as a complexing agent in ferrous iron oxidation has been postulated.

For purposes of modelling, we may consider only those nutrients whose concentrations might exert an effect on the leaching rate; i.e., the possible limiting substrates. The most likely limiting substrates are sulphide mineral (expressed as surface area), oxygen, and carbon dioxide. All other nutrients can be made to be in excess.

3. Mechanism of Bacterial Leaching

The release of zinc ion into solution during biological leaching is due to bacterial oxidation of the sulphide sulphur to sulphate:

$$ZnS + 2\ O_2 \rightarrow ZnSO_4 \qquad (41)$$

Zinc sulphide concentrates usually contain some iron, and this will also be released into solution during sulphide oxidation by the bacteria. Since ferrous iron is an acceptable energy source for the bacteria, it may be oxidized by them either directly on

the mineral surface (34) or in solution according to

$$Fe^{++} + {}^{1}/_{4}\, O_2 + H^{+} \rightarrow {}^{1}/_{2}\, H_2O + Fe^{+++} \qquad (42)$$

Some investigators (35,36) attribute the oxidation of metallic sulphides solely to the chemical action of acidic ferric iron solutions:

$$MS + 2\, Fe^{+++} \rightarrow M^{++} + S^{o} + 2\, Fe^{++} \qquad (43)$$

The bacteria would participate in the process only by regenerating the ferric iron which becomes reduced to ferrous iron during the leaching reaction. Sulphur produced may be oxidized by the bacteria to give sulphuric acid:

$$S^{o} + {}^{3}/_{2}\, O_2 + H_2O \rightarrow H_2SO_4 \qquad (44)$$

There is considerable evidence to show that the bacteria are able to attack the sulphide minerals directly. *T. ferrooxidans* has been shown to accelerate metal release from sulphides containing no iron (32,37). Duncan *et al.* (34) used selective inhibition of enzymes in the bacteria to show that the iron and sulphide in chalcopyrite and pyrite were attacked simultaneously and independently by the bacteria and that

sulphide oxidation was the rate controlling step. Additional support of the direct action theory is provided by the carbon dioxide fixation efficiency studies of Beck and Brown (38) who found that the efficiency of carbon dicxide fixation by T. ferrooxidans growing on pyrite and chalcopyrite was higher than would be expected if the bacteria were simply regenerating ferric iron in the system.

Levels of ferric iron in the latter two experiments were not reported but they were prcbably not tco high. Duncan and Walden (39) have determined that high levels of ferric iron contribute little to release of copper and zinc from sulphide minerals in a microbiological leaching system. There is thus little doubt that direct bacterial attack of the mineral is the major contributor to leaching of sulphide ores when ccnditions are favourable for growth of the organisms.

Evidence for the attachment of bacteria to the mineral surface has been given by McGoran et al. (40). They state that in excess of 96% of a bacterial populaticn grcwn cn chalcopyrite and 77% of a population grown cn sulphur were associated with insoluble material. The chalcopyrite data are suspect (41) since it has been shown that inorganic nitrogen may be precipitated as ammonio-jarosite, $NH_4Fe_3(SO_4)_2(OH)_6$ (42). This would have reported as bacterial nitrogen in their procedure.

MacDonald and Clark (36) encountered severe wall growth on their fermentor, which demonstrates the ability of the bacterium to attach to solid surfaces. Duncan et al. (43) have shown that the lag that occurs before leaching of chalcopyrite begins can be shortened by addition of the surfactant Tween 20. They concluded that the ability to contact the sulphide surface apparently was aided by the surfactant. Jones and Benson (44) isolated phosphatidyl glycerol from medium in which T. thiooxidans had been growing. They concluded that this lipid could provide surfactant activity essential for metabolic attack at sulphur surfaces. Agate et al. (45) have isolated similar compounds from medium in which F. ferrooxidans had been growing. Schaeffer et al. (46) presented electron micrographs of replicas of sulphur crystals before and after attack by T. thiooxidans which showed that the bacteria eroded the crystal immediately adjacent to the cell. Since direct contact appears to be necessary, the observed increase in leaching rate with mineral surface area (16,31,35,47,48,49) is easily explained.

The metabolism of sulphur compounds by thiobacilli has been reviewed by Trudinger (50). In elemental sulphur oxidation, available evidence indicates that the initial reaction is between the sulphur surface and a cellular component at the bacterial surface. Participation of an extracellular sulphur solubilizing enzyme appears doubtful. If this is also true for sulphides, then a diffusion resistance to mass transfer could

not exist between the bacterium and the surface, and shculd not appear in the model. The nature cf the initial reaction for sulphur attack is not known, but may invclve formation of polysulphides. Attack at solid sulphide surfaces is not discussed.

4. Bacterial Leaching Rates

Rate data for bacterial leaching systems has been presented in at least three ways. Bacterial growth rates are normally reported as doubling times or specific growth rates. Investigators performing manometric experiments report oxygen uptake values ($Q_{O_2}(N)$) in microlitres of S.T.P. oxygen per milligram of cell nitrogen per hour. This quantity is closely related to the specific growth rate (51). Leaching rates are usually reported as milligrams of metal icn released per litre per hour. This quantity may be nearly proportional to the bacterial growth rate.

Tuovinen and Kelly (33) have summarized the ranges cf cell doubling times usually encountered on various media. For oxidation of elemental sulphur they report doubling times of 10 to 25 hours, for a ferrous iron substrate, 6.5 to 15 hcurs, and for a thiosulphate substrate, 36 hours. McGcran *et al.* (40) reported a doubling time of 7-8 days for sulphur oxidation by *T. ferrooxidans*. Their data for doubling times on chalcopyrite

are suspect, since precipitation of ammonic-jarosite probably invalidated the bacterial nitrogen values (41).

Lacey and Lawson (52) fit Monod's model to their batch data for *T. ferrooxidans* growing on ferrous iron and determined μ_m values of 0.12 hr^{-1} at 20°C and 0.2 hr^{-1} at 31°C. They found that the saturation constant K was in the range of 1 to 2 g/l. MacDonald and Clark (36) determined μ_m to be 0.145 hr^{-1} at 32°C in batch culture and 0.161 hr^{-1} at 28°C in continuous culture. Their continuous experiments yielded a K value of 0.402 g/l.

Many oxygen uptake values have been reported in the literature as a result of manometric experiments with *T. ferrooxidans* but the highest values reported appear to be those by Landesman *et al.* (53,54). For ferrous iron oxidation they reported values in the range of 19,000 to 22,500 $\mu l\ O_2$ per mg N per hour, for chalcopyrite oxidation, 3200, for bornite, 450, and for pyrite, 1600.

Representative maximum release rates for bacterial leaching have been reported by Bruynesteyn and Duncan (1). They reported a copper release rate of 725 mg/l-hr on a chalcopyrite concentrate and 1300 mg/l-hr on a zinc sulphide concentrate.

5. Yield of Bacteria

Yield data for T. ferrooxidans have been reported as the ratio of carbon dioxide fixed to oxygen consumed, the yield of cell number or dry weight per mole of substrate consumed, and as the free energy efficiency. Interpretation of yield data is complicated by the fact that the bacteria may have a high maintenance energy requirement in order to maintain low intracellular hydrogen and metal ion concentrations which occur in excessive levels in its environment (33). As a result, one expects higher yield values at higher growth rates, when the maintenance energy requirement is a small fraction of the total energy requirement (10,51).

Beck (55) reported carbon dioxide fixation efficiencies of 2.1 to 3.0 μ moles CO_2 per 100 μmoles C_2 for growth on ferrous iron. Beck and Brown (38) reported 22 μ moles CO_2 per 100 μ moles O_2 for growth on sulphur. Nielsen and Beck (56) reported 1.5 μmoles CO_2 fixed per 100 μ moles O_2 for oxidation of chalcocite to covellite.

Temple and Colmer (26) reported that T. ferrooxidans fixed 16.05 mg of carbon while oxidizing 120 g of $FeSO_4 \cdot 7H_2O$. Silverman and Lundgren (57) reported fixation of 0.97 μ moles of CO_2 per 50 μ moles ferrous iron. Tuovinen et al. (58) grew the bacteria on a medium containing 2 g/l ferrous iron and measured

a resultant bacterial concentration of 10^8 cells per ml. MacDonald and Clark (36), growing the bacteria in continuous culture measured a cell yield of 4.7×10^{10} cells per g of ferrous iron oxidized.

Free energy efficiency is the ratio of the minimum chemical work required to create the biomass to the maximum amount of chemical work which could be obtained from the substrate that was used. The minimum chemical work required to synthesize the biomass is usually taken to be the free energy change for the fixation of carbon dioxide into glucose as given by Baas-Becking and Parks (59):

$$6\ CO_2\ (0.0003\ atm) + 6\ H_2O\ (1.) \rightarrow 6\ O_2\ (0.2\ atm) + C_6H_{12}O_6\ (s.) \qquad (45)$$

$$\Delta F = 708.9\ kcal/mole$$

The maximum amount of chemical work which is available by oxidizing a substrate is the free energy change for the oxidation reaction for the conditions under which the reaction is taking place. Tuovinen and Kelly (33) have summarized some of the values which have been used for the free energy of ferrous iron oxidation and accept the calculation of Lees et al. (60) as being the most representative value for the conditions under which bacteria will mediate the reaction. We believe that Lees' calculation is incomplete and present the following one in its stead:

We begin by assuming that the ferric iron produced precipitates as ferric hydroxide, for which the sclubility product given by Latimer (61) is 10^{-38}. Using the ion product of water as 10^{-14}, we can express the activity of ferric ion as a function of hydrogen ion activity:

$$a_{Fe^{+++}} = 10^4 \, a_{H^+}^3 \tag{46}$$

The oxidation of ferrous ion is given by the following equation:

$$Fe^{++} + {}^1/_4 \, O_2 + H^+ \rightarrow {}^1/_2 \, H_2O + Fe^{+++} \tag{47}$$

for which the electrode potential at 25°C can be calculated from

$$E = 0.458 - 0.059 \log_{10} \left(\frac{a_{Fe^{+++}}}{a_{Fe^{++}} \, a_{O_2}^{1/4} \, a_{H^+}} \right) \tag{48}$$

Substituting for ferric ion activity, and assuming the activity of atmospheric oxygen tc be .2,

$$E = 0.212 + 0.059 \, [2 \, pH + \log_{10} a_{Fe^{++}}] \tag{49}$$

which is easily converted to the free energy change per mole of ferrous iron oxidized by multiplying by -23,060. This expression shows an increase in absolute value of molar free energy change with pH due to decreased solubility of ferric icn as pH

increases, as opposed to the expression derived by Lees et al.

The value of -11.3 kcal/mole used by Temple and Colmer (26) and subsequent workers (33) for the free energy change for reaction 47 appears to have been taken from Bichowsky and Rossini (62) as the difference of the heats of formation of aqueous ferric ion and aqueous ferrous ion, and as such is a standard enthalpy change, not a free energy change.

It has been observed that the majority of the ferric iron generated in bacterial cultures precipitates as the basic ferric sulphate mineral, jarosite, $AFe_3(SO_4)_2(OH)_6$, where A can be Na, K, Rb, NH_4, Ag, Pb/2, or H_3O (16,42,65). Duncan and Walden (39) show curves suggesting that NH_4, K, and H_3O are the most probable candidates. In view of the uncertainty of the form in which the ferric iron precipitates in bacterial cultures and the fact that equilibrium precipitation is slow to be obtained, it seems best to simply use the standard free energy change at 298°K for the oxidation of aqueous ferrous ion. This can be calculated from the standard electrode potentials given by Latimer (61) to be -10.6 kcal/mole.

Assuming a free energy change of -11.3 kcal/mole for ferrous iron oxidation, Temple and Colmer (26) reported a free energy efficiency of 3.2%, Silverman and Lundgren (57) reported 20.5%, and Lyalikova (79) reported 30%. Lyalikova noted a

decrease in efficiency with age of culture.

6. Review of Torma's Work

Torma (16,63,64) optimized a number of variables in batch leaching of a zinc sulphide concentrate. Optimum conditions were defined as those which gave maximum rates of zinc release and minimum lag times. Zinc release rates were calculated from the linear portion of zinc extraction vs. time curves. No attempt was made to explain why this portion of the curve should be linear instead of showing the exponential increase usually associated with batch bacterial growth.

A constant rate of zinc release is suggestive of a mass transfer limited process, but the rate change with temperature suggests that a chemical or biological reaction was limiting. Two other possibilities arise. The surface available for leaching may remain relatively constant for most of the batch experiment, decreasing rather sharply near the end of the leach. Alternatively, the increase in bacterial population may balance the decrease in surface area until near the end of the leach. Some support for the former hypothesis is provided by Levenspiel (17) who has modelled the case of a single shrinking sphere where the reaction rate for dissolution of the sphere is proportional to the surface of the sphere only. His plot of fraction of the original sphere undissolved vs. dimensionless

time shows an approximately linear decrease in the fraction undissolved up to about 60% of the time for complete dissolution of the particle, after which the dissolution rate decreases markedly. If either of these hypotheses is true, then it is likely that under all conditions where linear leach curves were encountered, either surface area or mass transfer rates were limiting the observed release rates. If surface area was limiting the release rates, the effects of the other variables investigated would still be felt; the release rate per unit surface area could still be sensitive to temperature, pH, nutrient concentrations, etc.

Torma determined the optimum temperature to be 36-37°C, the optimum pH to be 2.3. The absence of added potassium chloride, magnesium sulphate, or calcium nitrate from the basal salts medium did not affect the final zinc concentrations achieved or the zinc release rates. Ammonium ion and phosphate ion were required; levels in the medium 9K of Silverman and Lundgren (66) were sufficient for maximum release rates and zinc concentrations. 1% carbon dioxide in the air supplied to the leaching vessels was sufficient to achieve maximum rates. The release rates were linear in initial concentrate pulp density. Initial concentration of surface area of mineral was shown to be the fundamental variable for correlating the release rates measured on both varying pulp densities and varying particle sizes.

The highest release rate measured in this study was 1150 mg/l-hr, measured in a shake flask for the fraction of the concentrate having the highest specific surface area. The highest zinc concentration achieved was about 120 g/l, measured in a baffled stirred batch tank containing 12 l of concentrate slurry at a pulp density of 24%. It was concluded that after suitable pretreatment the product solution would be suitable for recovery of zinc by electrolysis.

One attempt was made to measure the effect of the bacteria on the substrate. Three samples were taken from a batch leach at appropriate time intervals, the solids were recovered by filtration and washing with distilled water, and then fractionated by size. The zinc content of representative size fractions was determined. The results indicated that the smallest fractions leached faster than the largest fraction, while particles in the large fraction shrank to become part of the smaller fractions. The smallest particles should not disappear completely due to the inert material initially present in the concentrate. No attempt was made to measure the surface area concentration while a leach was in progress, and to correlate it with the observed leach rates.

From the data presented, it would appear that the surface area concentration in a slurry that was actively leaching could

be substantially different than that in the slurry initially. In particular, the weight of the finest fraction, which would contribute a great deal of the total surface concentration, becomes a small fraction of initial value as leaching progresses. This is one of several instances where Torma has estimated the effect of the environment on the bacteria, but failed to estimate the reciprocal effect of the bacteria on the environment.

Two other examples of this occur in the determination of ammonium and phosphate requirements. As the bacterial population grows, the concentration of ammonium ion drops (39) and the phosphate concentration probably drops as well. Therefore, although there was enough of these nutrients in the basal salts medium for the conditions under which the experiments were performed, for very high bacterial populations (and as a result, high zinc concentrations), it may prove necessary to make additions of these nutrients.

The bacteria are responsive to the concentration of carbon dioxide in the medium, not that in the air supply. For a given concentration in the air supply under constant conditions for mass transfer, the concentration of carbon dioxide in the medium will be a function of how fast it is being consumed by the bacteria; i.e., it will be a function of the growth rate. Torma's measurements are therefore specific to the type of

leaching vessel he used (shake flasks), and the maximum release rate achieved in his carbon dioxide experiments (650 mg/l-hr). Higher growth rates may require higher gas phase CO_2 concentrations, or increased provisions for mass transfer of CO_2 into solution.

As noted by Torma, his use of the Monod equation to fit his data is empirical. Its conventional use is to fit specific growth rate data as a function of substrate concentration in the culture. Torma used it to fit zinc release rates as a function of initial substrate concentration in batch leaches. Under these conditions it fails to take into account the reciprocal effects of bacteria on substrate and substrate on bacteria, making it impractical for predicting continuous culture results. Torma also points out that the usual requirement for one substrate to be limiting when this equation is used is not always met by his data. Some of Torma's data would appear to have been fit better by Blackman kinetics (9).

Torma modelled his leach curves with a generalized logistic equation proposed by Edwards and Wilke (67):

$$[Zn] = [Zn]_m / \{1 + \exp (f(t))\} \qquad (50)$$

where f(t) is a fifth order polynomial. Torma did not give F values for each power of t included in the model, but his use of

all five suggests that he felt each was significant. With so many constants in the model, it is doubtful if physical significance could be assigned to them all. There is nc obvious way in which this model takes into account bacterium-environment interaction.

III. DERIVATION OF MODEL

Despite its ability to account only for the log and stationary phases, Monod's model is most often used in discussions of continuous culture theory. It has been used in analyses of continuous culture in several reactor systems besides the single stage continuous perfectly stirred tank reactor which we have discussed. Examples are: multiple stage continuous stirred fermentors (68,69), single fermentors with feedback (68), tubular reactors (68), and biological film and floc reactors (70,71).

It is desired to derive a model which will predict the growth rate of the bacteria and the release rate of zinc when the sulphide surface is the limiting substrate. Since one cannot reliably estimate cell numbers, and will have to measure some quantity proportional to cell mass, a distributed model should be chosen. Structure should not be needed since the prediction of steady-state results in a continuous culture is the major concern. For simplicity of fitting, it should be deterministic.

Attachment to the mineral surface appears to be prerequisite to zinc release and bacterial growth; thus consideration must be given to the manner in which the bacteria become attached to the mineral. This in turn establishes how much biomass is attached to the surface. If it is assumed that

growth is not limited by any other component of the system, the bacteria which are attached should grow at their maximum specific growth rate, which is constant. The bacteria which are not attached to sulphide mineral have no access to substrate and can be assumed not to grow.

Because it considers the adsorption and desorption of bacteria at a dispersed phase surface, the model of Erickson et al. (23) offers the most promise for describing bacterial leaching kinetics. It can be simplified to account for the constant substrate concentration in a sulphide mineral particle. It will be necessary to account for the change in surface area as substrate is consumed, and to adapt the model to continuous culture.

Following Erickson et al. (23) we assume the bacterial concentration is X, and σ of these are attached to the surface. If a dynamic equilibrium between those bacteria attached and those in solution is postulated, and if one assumes that the rates of attachment and release follow first order kinetics, then

$$k_1 (s - \sigma f) (X - \sigma) = k_{-1}\sigma \qquad (51)$$

where f is the surface area occupied per unit of bacterial concentration. This says that the rate of attachment is

proportional to the concentration of bacteria-free surface and the bacterial concentration in solution; the rate of release is proportional to the bacterial concentration attached.

Solve for σ :

$$\sigma^2 f - (s + fX + \{\frac{k_{-1}}{k_1}\})\ \sigma + sX = 0 \qquad (52)$$

$$\sigma = \frac{(s + fX + \kappa) \pm \sqrt{(s + fX + \kappa)^2 - 4\ fsX}}{2f} \qquad (53)$$

For $s=0$, $\sigma=0$, therefore take only the negative radical. Assume that growth rate is proportional to the number attached:

$$r_X = \nu\sigma = \nu \left(\frac{(s + fX + \kappa) - \sqrt{(s + fX + \kappa)^2 - 4\ fsX}}{2f}\right) \qquad (54)$$

ν is thus the maximum specific growth rate for the bacteria which are attached.

Equation 54 is quite similar in form to equation 24 obtained by Dabes *et al.* (9), but differs in that equation 54 does not give μ uniquely in terms of substrate concentration.

To calculate the steady-state conditions in a continuous backmix reactor, the kinetic model will have to be solved together with the mass balance on bacteria over the reactor. At steady state the mass balance on bacteria (equation 1) gives the

relation

$$\frac{r_X}{X} = \mu = D \tag{55}$$

Solving the model with the bacterial mass balance gives

$$D = \frac{\nu}{X}\left[\frac{(s + fX + \kappa) - \sqrt{(s + fX + \kappa)^2 - 4\,fsX}}{2f}\right] \tag{56}$$

To see how X depends on s and D we square equation 56 to get

$$\left(\frac{2DfX}{\nu}\right)^2 - \frac{4\,DfX}{\nu}(s + fX + \kappa) + 4\,fXs = 0 \tag{57}$$

Divide through by X and discard the zero root:

$$4\left(\frac{Df}{\nu}\right)^2 X - 4\,\frac{Dfs}{\nu} - 4\,\frac{Df^2X}{\nu} - 4\,\frac{Df\kappa}{\nu} + 4\,fs = 0 \tag{58}$$

Solve for x:

$$X = \frac{\kappa}{f\,(D/\nu - 1)} + \frac{\nu}{Df}\,s \tag{59}$$

To fit the model, we have to determine three constants, ν, κ, and f. We have three variables any two of which determine the third. We can vary the dilution rate; or we can vary X and s for a constant dilution rate by changing the pulp density or

grinding for a different length of time. Equation 59 shows that for a constant D, a plot of X versus s should be a straight line with slope ν/Df and intercept $\kappa/f(D/\nu - 1)$. Several of these plots can be made for other dilution rates. If we now plot the reciprocal of the slope versus dilution rate, we should get a straight line having zero intercept and slope (f/ν). The reciprocal of the intercept should be a linear function of the dilution rate:

$$\frac{1}{\text{Intercept}} = \frac{f}{\nu\kappa} D - \frac{f}{\kappa} \qquad (60)$$

The line should give $f/\nu\kappa$ as the slope, and $(-f/\kappa)$ as the intercept. We now have estimates of (f/ν), $(f/\nu\kappa)$, and (f/κ) from which the three constants may be calculated.

The relation which has been derived gives the steady-state bacterial concentration as a function of dilution rate and steady-state surface concentration. The steady-state zinc concentration can be determined from the bacterial concentration by measuring the yield of bacteria as a function of zinc released. Prediction of performance for a given dilution rate and feed will require that the steady-state surface concentration be calculated from the size distribution of the feed in conjunction with the determined kinetics, the residence time distribution in the reactor, and some simplifying assumptions regarding the geometry of the particles. A prototype

for this calculation is given by Levenspiel (17).

IV. APPARATUS AND MATERIALS

A. Apparatus

A schematic diagram of the leaching apparatus is given in Figure 2. The stirred tank reactor was made of lucite plastic, and had an inside diameter of 11.25 inches. A schematic drawing of the tank is given in Figure 3. The ratios of the dimensions are given in Table I.

The tank had four baffles, and the agitation was provided by a six-bladed turbine. The turbine was driven by a Graham N30MR2.4 variable speed transmission.

Air was sparged into the tank through a 1/4 inch stainless steel pipe nipple. To avoid plugging, no air distributor was used in the tank. To avoid excessive evaporation in the tank, the air was humidified by bubbling through water before entering the tank. Carbon dioxide was added to the air stream at a rate adequate to increase its concentration in the air to 1% by volume.

Solids were fed to the tank using a B. I. F. Volumetric Disc Feeder, Model 22-01.

Product was removed intermittently by suction into a

Figure 2

SCHEMATIC DIAGRAM OF THE CONTINUOUS LEACHING APPARATUS

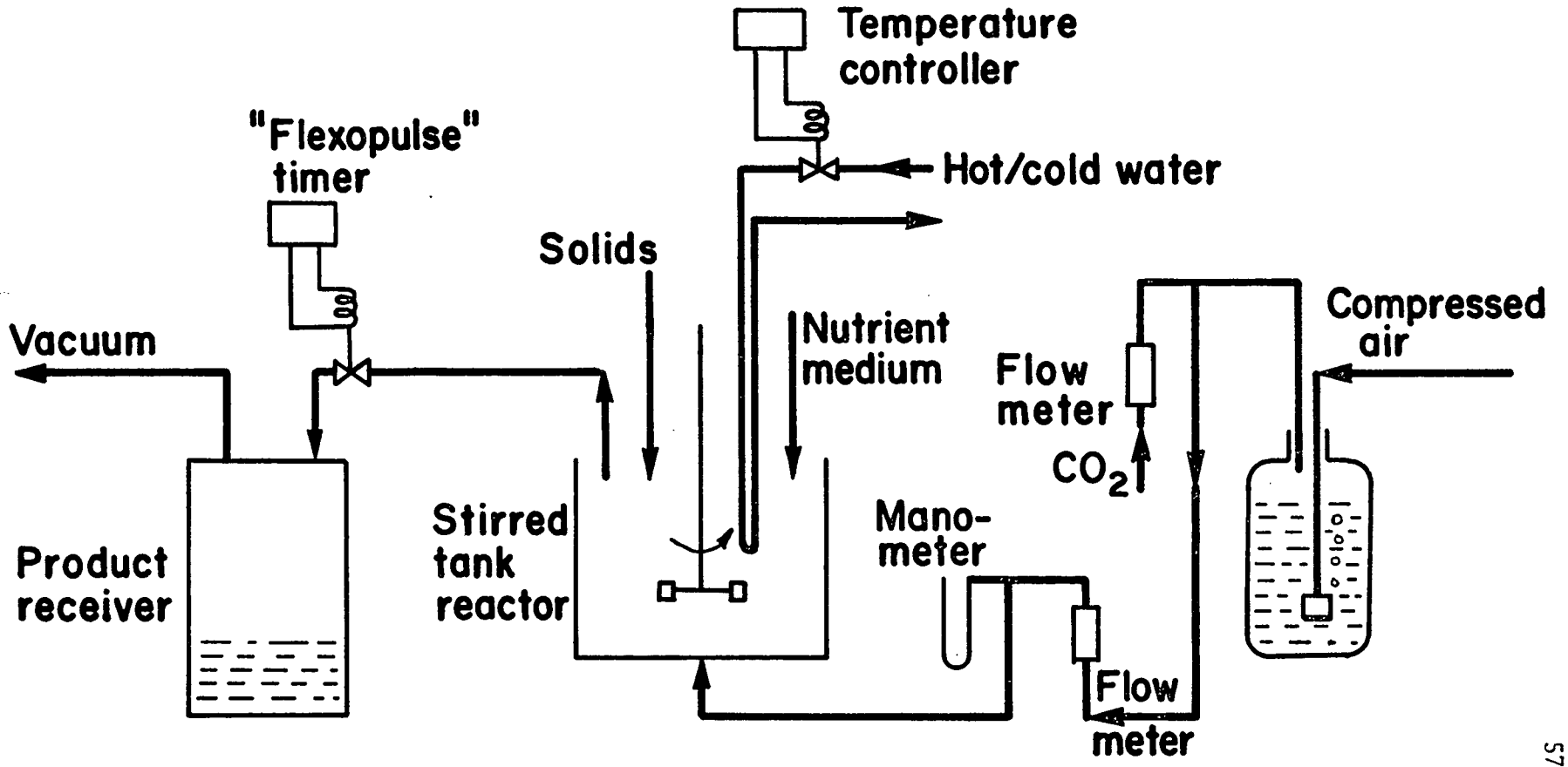

Table I. Geometric Ratios For Stirred Tank Reactor (Refer to Figure 3).

D_t/D_i	= 3
H_L/D_i	= 3
H_i/D_i	= 1
W_b/D_t	= 0.10
L_i/D_i	= 0.25
W_i/D_i	= 0.20

Figure 3

SCHEMATIC DIAGRAM OF STIRRED TANK REACTOR SHOWING DIMENSIONS

(Refer to Table I)

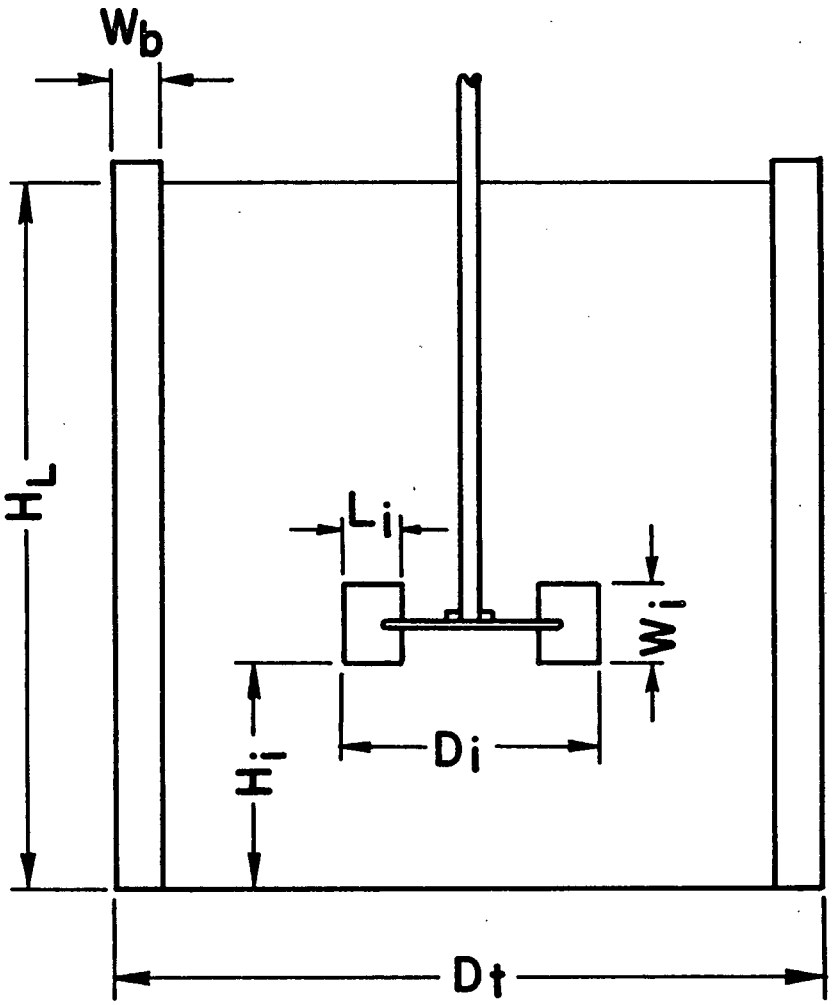

stainless steel product receiver. The interval of sampling was controlled by a Flexopulse Interval Timer (Eagle Signal Division of E. W. Bliss Company) which opened a solenoid valve periodically. Level control was achieved by positioning the suction tube at the desired level, and arranging to remove more material than was fed. When the level dropped below the end of the tube, air was taken into the product receiver instead of product. Vacuum was maintained by a water aspirator.

Temperature in the tank was controlled by a Yellow Springs Instrument Company Thermistemp Model 63 temperature controller. This controller operated a solenoid valve which permitted hot (or cold) water to flow through a stainless steel coil in the tank.

A schematic diagram of the nutrient medium flow circuit is given in Figure 4. The medium was recirculated through the constant head tank by a Cole-Parmer No. 85-07 magnetic drive centrifugal pump. The constant head was maintained by allowing the medium to flow over a weir in the constant head tank, and return to the reservoir. Some medium was taken from the head tank and passed through a needle valve to the reactor.

B. Materials.

The concentrate was a single 1000 lb. lot of Sullivan Mine

Figure 4

SCHEMATIC DIAGRAM OF NUTRIENT MEDIUM FEED CIRCUIT

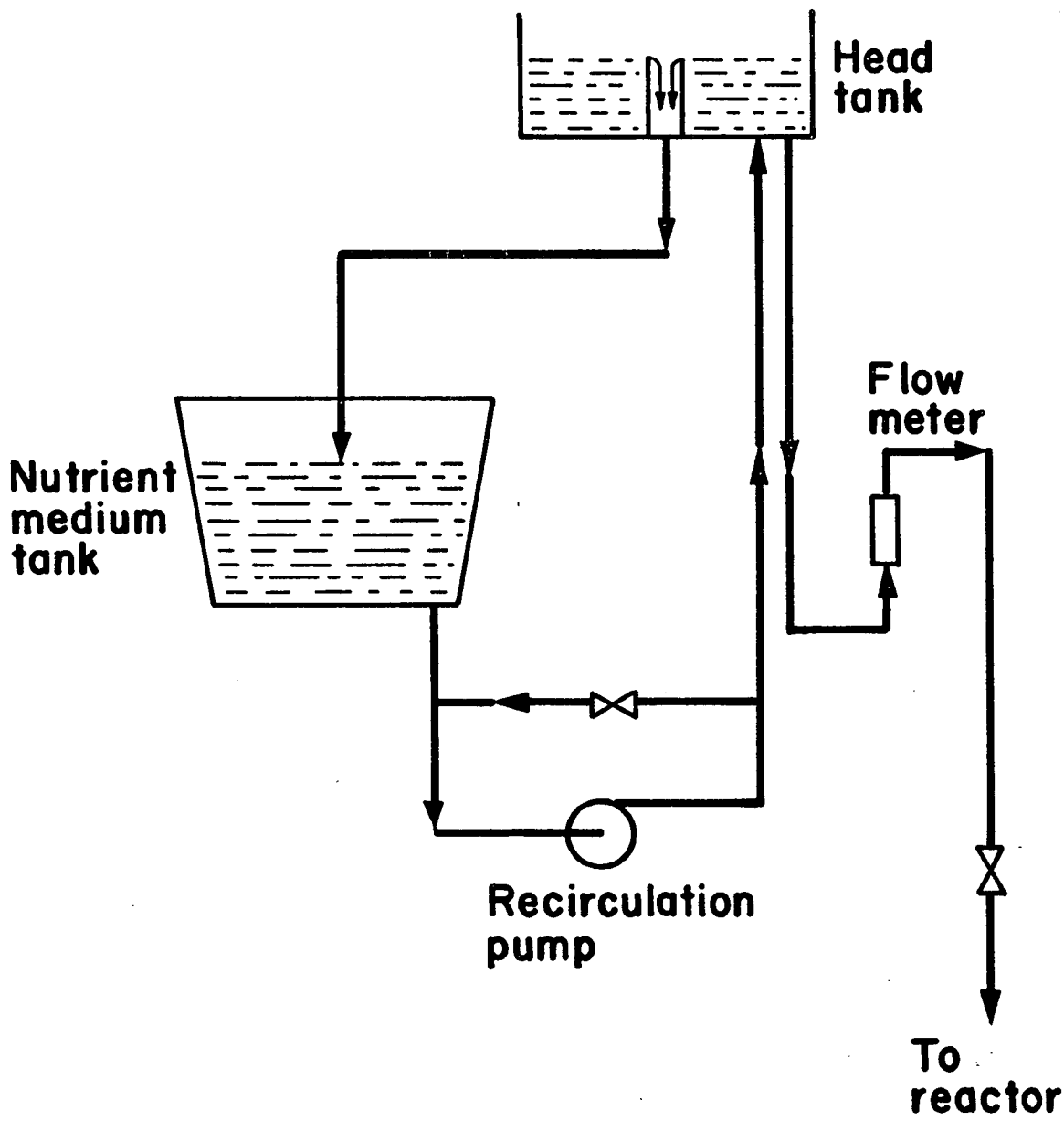

zinc concentrate supplied by Cominco Limited.

The inoculum for the tank was a pure strain of Thiobacillus ferrooxidans (N.C.I.B. 9490) obtained from B.C. Research (48). It was grown in shake flask cultures on the test concentrate to acclimatize the bacteria to the new substrate.

The liquid medium fed to the tank was the medium 9K described by Silverman and Lundgren (66) with water added in place of the ferrous iron solution. The proportion of sulphuric acid was varied to maintain the tank pH between 2.0 and 2.5.

Antifoam, when used, was Dow Polyglycol 15-200.

V. PROCEDURES

A. Ball Milling

For the preliminary experiments a 0.5 pound portion of concentrate was placed in a No. 2 U.S. Stoneware porcelain ball-mill along with 0.25 pound of water and 5.0 pounds of 1/2 inch steel balls. Successive batches were milled at 65 rpm for 15, 30, 45, 60, and 90 minutes. The resulting slurries were dried at 60°C overnight and the dry cakes were homogenized with a mortar and pestle and stored in plastic bags.

Concentrate for the continuous experiments was milled in a 20 inch diameter steel ball mill containing 350 pounds of 1/2 inch steel balls. A 35 pound batch of concentrate was milled with 8 litres of water at 46 rpm for 1.5 hours. The concentrate was dried at 60°C and pulverized in a rotating disc pulverizer (Cave & Co.).

B. Surface Area Determination

The specific surface area of a mineral sample was determined by fitting the Brunauer, Emmett and Teller equation (72) to an adsorption isotherm for the material. The adsorption isotherm was determined by a dynamic method, using equipment designed and built by Orr (73). A schematic diagram of the

apparatus is given in Figure 5.

About half a gram of the mineral sample was placed in a tared U-tube made of 5 mm O.D. glass tubing. The sample was dried in the tube at 110°C for 12 hours. After cooling, three tubes of concentrate were weighed and mounted in the apparatus. A mixture of 5 volume % nitrogen in helium was passed through the tubes at 20 ml/min and the power to the thermal conductivity cell was turned on. After about one half hour warm up time, the first sample tube was immersed in liquid nitrogen.

After the adsorption peak had been recorded, the instrument was calibrated with known volumes of nitrogen. Atmospheric pressure and temperature were noted for each calibration peak. While the calibration peaks were being taken, the probe of the nitrogen thermometer was immersed in the liquid nitrogen bath. The pressure on the manometer was noted just before desorption, and the probe was removed. The liquid nitrogen bath was removed and a desorption peak was recorded. The procedure was repeated on the other two samples. The gas mixture was changed to 15 and 25 volume % nitrogen in helium to complete the data for the three samples.

Figure 5

SCHEMATIC DIAGRAM OF
THE DYNAMIC NITROGEN ADSORPTION APPARATUS

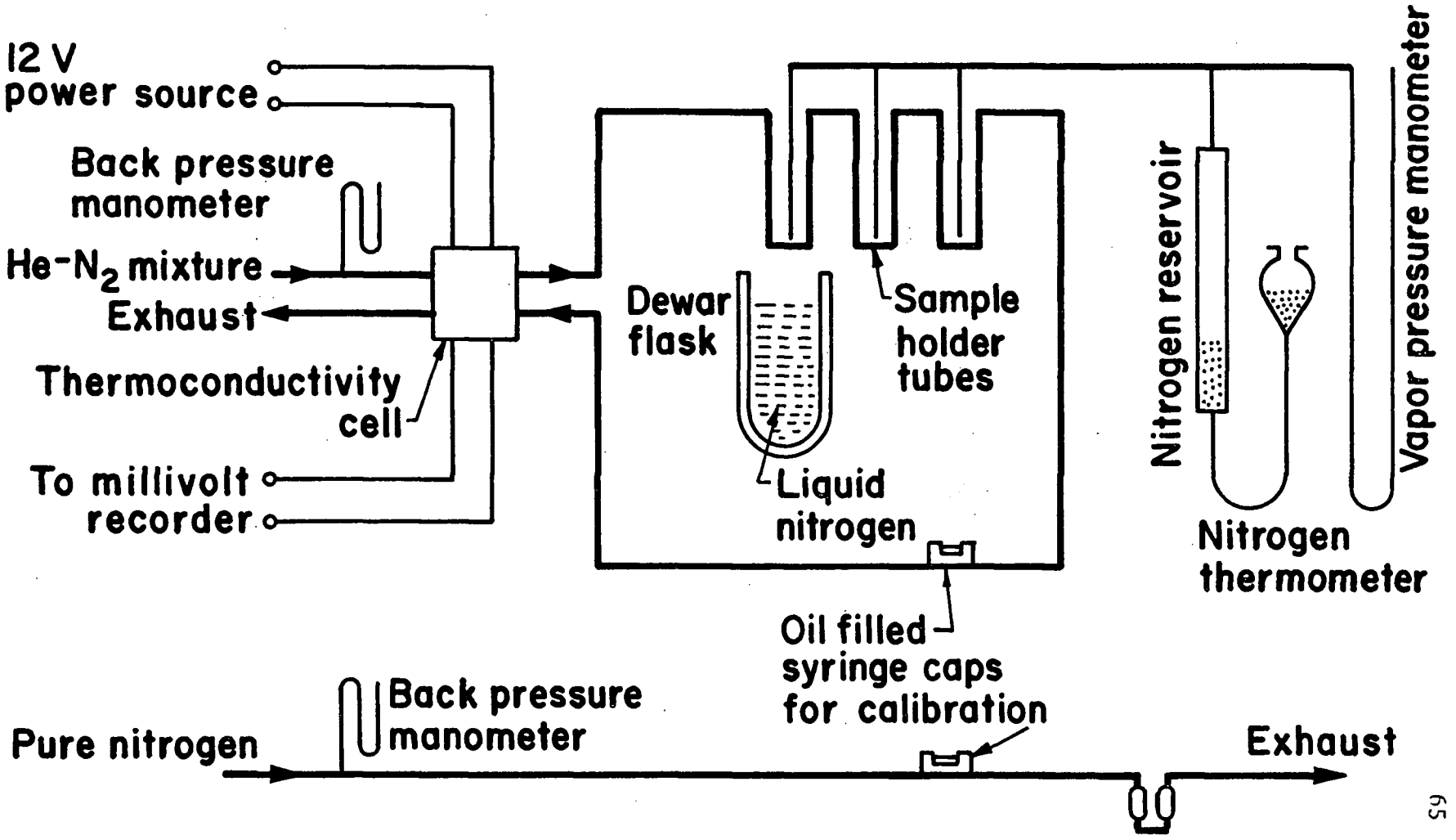

C. Shake Flask Leaches

For shake flask studies, 5 g portions of concentrate and 70 ml of iron free medium 9K were placed in baffled 250 ml Erlenmeyer flasks and 3 ml of 12N H_2SC_4 were added. One day was allowed for the pH to stabilize due to acid consumption by the concentrate, and additional acid was added as required to bring the flask contents to pH 2.5. The flasks were then inoculated with 5 ml of bacteria previously grown on this concentrate. Sterile control flasks were carried in which 5 ml of the nutrient medium were added in place of inoculum, and a crystal of thymol was added to maintain sterility. The flasks were incubated at 35°C on a gyratory shaker, and the pH and dissolved zinc and iron concentrations were determined at convenient intervals.

The final extraction was determined after removing the leached out solids by filtration on a Buchner funnel with Whatman No. 5 filter paper. The residue was washed several times with pH 2 water (water acidified to pH 2 with sulphuric acid), the filtrate was made to volume and analyzed for zinc. The calculation was corrected for the zinc removed in sampling, and for the zinc added with the inoculum.

D. Analysis Of The Zinc Concentrate

The concentrate was delivered in five barrels containing about 200 pounds each. In addition, there had been delivered earlier two smaller cans totalling about 300 pounds of concentrate. The following procedure (known as coning and quartering) was adopted to mix the concentrate.

All the concentrate was placed in one pile. This cone shaped pile was flattened, roughly quartered, and each quarter piled into its own separate cone. Shovelsful of concentrate were then taken sequentially from each of the smaller cones until all of the material had been recombined into a single cone. This procedure was repeated for a total of three times. The thoroughly mixed concentrate was then replaced in the five barrels.

The samples for analysis were dried for about one week at 60°C and then each sample was homogenized with a Cave & Co. pulverizer. Duplicate aliquots of each sample (about 0.5 g) were weighed out for analysis.

The 0.5 g portion was placed in a 250 ml beaker with 10 ml of concentrated nitric acid and 5 ml of concentrated hydrochloric acid. The mixture was evaporated to dryness on a hot plate and then 5 ml of concentrated nitric acid and 5 ml of

concentrated sulphuric acid were added to the residue, which was again evaporated to dryness. The residue was dissolved in about 30 ml of pH 2 water, made to volume, and analyzed for zinc and iron.

For the sulphur analysis, the concentrate was first washed with pyridine to remove any flotation chemical which might contribute sulphur to the analysis (41). The pyridine was displaced with ethanol followed by distilled water. The concentrate was dried at 100°C for 16 hours.

The concentrate was combusted in a stream of oxygen gas using a Leco Model 521 induction furnace. Vanadium pentoxide was added as a catalyst (74), and powdered iron was added as an accelerator. The sulphur dioxide produced was absorbed in a solution containing 30 ml of concentrated hydrochloric acid, 5 ml of 10% potassium iodide solution, and 1 ml of 2% starch solution per litre. Iodine was generated by titrating 0.025 N potassium iodate into the reaction vessel:

$$KIO_3 + 5\ KI + 6\ HCl \rightarrow 3\ I_2 + 6\ KCl + 3\ H_2O \qquad (61)$$

Sulphur dioxide absorbed in the solution reduced the iodine to iodide:

$$SO_2 + I_2 + 2\ H_2O \rightarrow H_2SO_4 + 2\ HI \qquad (62)$$

Iodine in the solution was detected as a dark blue colour by the starch. Two blanks and six standards using reagent grade zinc sulphide were run with the concentrate samples.

E. Monitoring The Continuous Stirred Tank

1. Total Organic Carbon

Bacterial concentration was estimated as total organic carbon concentration using a Beckman No. 915 Total Organic Carbon Analyzer. Total organic carbon concentration is the difference between total carbon concentration and inorganic carbon concentration in a sample.

Total carbon was determined by injecting a 20 µl sample into a bed of cobalt nitrate catalyst at 800°C. An oxygen stream passing through the bed picked up the carbon dioxide generated by incineration of the organic carbon and decomposition of the carbonates in the sample. The carbon dioxide was detected by its absorption of infra-red light. Each sample injected generated a peak on a chart recorder. The height of the peak was proportional to the amount of carbon injected.

A separate low temperature (150°C) furnace containing a phosphoric acid wetted packing liberated any inorganic carbon from another 20 µl sample as carbon dioxide. The oxygen stream from this furnace could be fed into the same detector yielding a peak on the recorder whose height was proportional to the amount of inorganic carbon in the sample. In practice, the inorganic carbon in the tank slurry was about 2 mg/l, negligible when compared to the total carbon readings. Therefore, inorganic carbon readings were done only infrequently.

2. Non-distillable Ammonium Ion

Bacterial concentration was also estimated by the "non-distillable" or "net" ammonium ion concentration. This is the difference between the total ammonium ion concentration after Kjeldahl digestion and the steam distillable ammonium ion concentration, and is thus an estimate of bacterial nitrogen concentration in the sample. To determine the total ammonium ion, the sample was digested in a Kjeldahl flask with concentrated sulphuric acid and a Hengar selenized boiling granule. The digestion was carried out over a Bunsen flame for about two hours. This digestion converted the organic nitrogen to ammonium ion. After the digestion, the sample was washed into a micro-Kjeldahl steam still (W. Buchi, Switzerland) with sufficient sodium hydroxide to make the mixture strongly

alkaline. The mixture was steam distilled, and the distillate was collected in a flask containing 5 ml of saturated boric acid and 3 drops of an indicator solution. The indicator was made up of one part 0.2% methyl red and five parts 0.2% bromocresol green in ethanol. After about 50 ml of distillate had been collected, the flask contents were titrated to a colourless end point with 0.01 N HCl. The ammonium ion equivalent of the hydrochloric acid was calculated.

The distillable ammonium ion is an estimate of the inorganic ammonium ion in the slurry. It was determined by placing the tank slurry in the still without digesting it, and repeating the above procedure.

3. Pulp Density

The pulp density was determined by pipetting a known quantity of slurry into a glass centrifuge bottle. The slurry was centrifuged at low speed to settle the solids but leave the bacteria suspended. The centrifugate was decanted and 10% HCl was added to the solids. The bottle was stoppered and shaken to dissolve precipitated iron compounds. The slurry was centrifuged and decanted as before. The procedure was repeated for a total of two HCl washes and one distilled water wash. The solids were then resuspended in distilled water and filtered on a Buchner funnel using Whatman number 5 filter paper. The filter cake was

dried over night at 105°C. It was cooled, weighed, and stored for surface area analysis and digestion for zinc and iron analyses.

4. Miscellaneous

Zinc and iron concentrations were determined on a Perkin Elmer Model 303 atomic absorption spectrophotometer. Daily samples of tank slurry were centrifuged in a clinical centrifuge and the clear centrifugate was sampled for zinc and iron analysis. Whenever the product receiver was being emptied, a sample of the slurry was taken for dissolved zinc and dissolved iron analysis. In doing a mass balance on zinc over the tank, the concentration of zinc in the product was used to determine the amount of soluble zinc removed from the tank.

To complete the mass balance on zinc over the tank, the solid residues from the tank were analyzed for zinc content by the procedure given in section V.D.

10 ml of slurry and 10 ml of centrifugate from the tank were weighed for determination of densities. From these two densities and the pulp density, it was possible to estimate the volume fraction of liquid in the slurry. This was essential in order to determine true extraction rates. It was also possible to correlate the centrifugate density with dissolved zinc

ccncentration, and to correlate the difference in the two densities with the pulp density of the slurry. These correlations provided a quick check cn the tank conditicn.

The amount of concentrate collected over a measured interval of about 20 minutes was weighed to give an estimate of solid feed rate.

The tank depth was measured with the air flow and agitation on and again with the air and agitation switched off. The measurement with the agitaticn and air switched off allowed determination of the volume of slurry in the tank, and the difference between the two readings provided a measure of the gas holdup in the tank.

The stainless steel product receiver was calibrated to a centimeter dipstick so that the volume of the product could be ncted as a function of time. This allowed calculaticn of the product flow rate, from which the dilutien rate was calculated.

The air flow was maintained at about 10 l/min, the CO_2 flow at about 95 ml/min, measured at the conditions of flow. The agitator turned at about 450 rpm. The flcw of liquid medium was checked on a rotameter.

The temperature and pH of the tank slurry were noted daily.

The mean temperature was controlled to 36°C.

One size distribution analysis was performed on a feed sample using a Bahco 6000 Microparticle Classifier. Six fractions were produced, and the representative maximum particle diameter for each fraction was calculated by averaging the maximum and minimum diameter of ten particles as determined with an ocular micrometer.

Cell numbers were estimated in a Petroff-Hausser counting chamber. The number of bacteria in nine of the smallest squares was counted in ten fields from each of two slides. From the average number per smallest square, the cell number concentration could be calculated.

VI. RESULTS AND DISCUSSION

A. Preliminary Experiments

1. Analysis of the Zinc Concentrate

To characterize the zinc concentrate used in these studies, it was assayed for zinc, iron, and total sulphur.

It was important that the feed concentrate be as uniform in composition as possible, so that upsets in the continuous process would not be traceable to changes in the feed composition. The concentrate was sampled in such a way that a statistical measure of the variance of the assays could be made. Two samples (a and b) were removed from each of the five barrels. An effort was made to take one sample near the bottom of the barrel and the other near the top.

The results of the chemical analysis of the zinc concentrate are presented in Table II. These data were analyzed by the hierarchical classification, a statistical design permitting the testing of the significance of heterogeneity in the concentrate (75). In these experiments, each observation was broken down into the general mean, the barrel effect, the effect of the samples a and b within each barrel, and the error effect of the duplicates:

Table II. Zinc, Iron, And Sulphur Analysis Of Zinc Concentrate (As Received).

Sample	Percent Zinc	Percent Iron	Percent Sulphur
1a1	56.44	4.872	31.77
1a2	55.99	4.770	33.27
1b1	55.76	4.852	31.26
1b2	55.54	4.817	31.05
2a1	55.69	4.554	31.16
2a2	55.03	4.552	30.96
2b1	54.78	4.964	31.37
2b2	54.95	4.869	-----
3a1	54.67	4.713	32.61
3a2	55.53	4.801	31.25
3b1	56.16	4.536	30.82
3b2	56.21	4.647	32.52
4a1	56.19	4.491	31.86
4a2	56.09	4.546	31.11
4b1	55.96	5.774	32.28
4b2	54.90	4.971	31.93
5a1	55.69	4.726	30.42
5a2	56.10	4.613	31.33
5b1	56.15	5.704	31.35
5b2	56.02	4.451	32.18

$$y = \bar{\bar{y}} + (\bar{y}_B - \bar{\bar{y}}) + (\bar{y} - \bar{y}_B) + (y - \bar{y}) \qquad (63)$$

where

y = an observation

$\bar{\bar{y}}$ = the general mean

$\bar{y}_B$ = the mean of four observations from a barrel

$\bar{y}$ = the mean of two duplicates

The analyses of variance for zinc, iron, and sulphur analyses are given in Tables III, IV, and V. They show that neither the variance contributed by the barrels, nor the variance contributed by the samples a and b within each barrel is significantly different from zero at the 95% level. We may therefore conclude that there should not be significant variation of the concentrate composition from barrel to barrel, or from sample to sample within each barrel, when compared to the variance of the analytical method (the variance contributed by the duplicates).

The assay values used in these experiments were 55.69% zinc, 4.812% iron, and 31.61% sulphur.

Table III. Analysis Of Variance For Zinc Content Of Zinc Concentrate.

Source	S.S.	d.f.	M.S.	F
Barrels	1.974	4	0.4935	1.08
Samples	2.282	5	0.4564	3.29
Error	1.388	10	0.1388	
Total	5.644	19	0.2971	

$F(4,5,.95) = 5.1922$

$F(5,10,.95) = 3.3258$

Neither Barrel Nor Sample Effect Significant At The 95% Level.

Average Zinc Composition Of Concentrate Is 55.69%.

95% Confidence Limits: Upper: 55.44%
Lower: 55.95%

Table IV. Analysis Of Variance For Iron Content Of Zinc Concentrate.

Source	S.S.	d.f.	M.S.	F
Barrels	0.1872	4	0.04679	0.222
Samples	1.0555	5	0.2111	1.859
Error	1.1357	10	0.1136	
Total	2.3783	19	0.1252	

$F(4,5,.95) = 5.1922$

$F(5,10,.95) = 3.3258$

Neither Barrel Nor Sample Effect Significant At The 95% Level.

Average Iron Composition Of Concentrate Is 4.812%

95% Confidence Limits: Upper: 4.978%
Lower: 4.647%

Table V. Analysis Of Variance For Sulphur Content Of Zinc Concentrate.

Source	S.S.	d.f.	M.S.	F
Barrels	1.422	4	0.3555	0.5605
Samples	3.171	5	0.6342	1.231
Error	4.639	9	0.5154	
Total	9.232	18		

$F(4,5,.95) = 5.1922$
$F(5,9,.95) = 3.4817$

Neither Barrel Nor Sample Effect Significant At The 95% Level.

Average Sulphur Composition Of The Concentrate Is 31.61%.

95% Confidence Limits: Upper: 31.96%
Lower: 31.26%

2. Percentage Extraction - Milling Time Experiment

A portion of the concentrate used is not zinc sulphide, and this gangue material may prevent bacterial contact with otherwise leachable material. Grinding should overcome this by exposing more sulphide mineral to the bacteria. In addition, the sulphide mineral may have to be stressed in order to render it susceptible to bacterial attack. More grinding should subject the crystal structure to more stress. Finally, the surface to volume ratio for the coarser sulphide material may be so small that after the fines have been dissolved, the leach rate drops to a negligible value. The extraction would then appear to be less than the true potential of the concentrate.

To determine the ball milling time required to produce maximum extraction, portions of the zinc concentrate were ball milled for various lengths of time and then leached in shake flasks (duplicate batch tests). Determining the specific surface area provided a measure of the effectiveness of the milling. A sample calculation of percentage extraction is given in Appendix I.

The results in Table VI show that milling for 45 minutes was sufficient to obtain the maximum extraction. Values for 60 and 90 minutes were not significantly higher. Maximum extraction was obtained with a specific surface area of about 1.7 m^2/g.

Table VI. Percentage Extraction - Milling Time Results

Washed	Dried	Milled	Bacteria	% Extraction	Average % Extraction	Specific Surface Area (m^2/g)
-	-	-	+	41.3, 44.6	43.0	0.820
-	+	-	+	46.4, 63.5	55.0	-----
+	+	-	+	40.3, ----	40.3	-----
+	+	15 min	+	69.5, 71.5	70.5	1.116
+	+	30 min	+	71.8, 78.5	75.2	1.569
+	+	45 min	+	80.6, 84.1	82.4	1.676
+	+	60 min	+	80.9, 79.8	80.4	2.026
+	+	90 min	+	80.9, 84.5	82.7	2.373
+	+	90 min	-	12.1, ----	12.1	2.373

Milling for the continuous experiments was done in a larger mill. After 90 minutes in the larger mill, the specific surface area of the material typically was of the order of 3 m^2/g; after 90 minutes milling in the smaller test mill, it was 2.373 m^2/g, indicating that the larger mill was more effective than the small mill. Batch shake flask tests on concentrate from the large mill had an average percentage extraction of 88.6%, slightly higher than predicted from the data in Table VI.

Washing and drying the unmilled concentrate had no effect on extraction.

3. Development of the Non-Distillable (Net) Ammonium Ion Method

To determine how much of the nitrogen associated with the bacteria could be distilled as ammonium ion without digestion, the following experiment was performed. Duplicate aliquots of a washed cell suspension were digested by the Kjeldahl procedure and distilled. The average total ammonium ion content of these aliquots was 0.5484 mg. Duplicate aliquots of the suspension were distilled without digestion, and the average distillable ammonium ion content was found to be 0.02346 mg, or 4.28% of the total. Thus, less than 5% of the bacterial nitrogen will report as distillable ammonium ion.

A second experiment was performed to determine if the ammonium ion trapped as jarosite would be released by the caustic distillation without digestion, and thus not report as bacterial nitrogen. A sample of jarosite was obtained from B.C. Research. Duplicate portions were weighed out and completely dissolved in 35% HCl solution. Aliquots of these solutions were distilled with caustic. The ammonium ion content of the jarosite determined by this method was 0.677%. When samples of the jarosite were distilled with caustic without any prior treatment to dissolve the solids, the ammonium ion content averaged 0.693%.

The results show that ammonium ion trapped as jarosite will report as distillable ammonium ion, and not as net ammonium ion. Thus, formation of ammonio-jarosite should not affect the estimation of bacterial nitrogen.

4. Development of the Pulp Density Determination Procedure

In these studies we are interested in the pulp density and surface area of the sulphide mineral, excluding any precipitated iron salts. Therefore, a procedure was necessary to dissolve the iron salts before the solids were weighed and their specific surface area determined. Another potential problem was that the bacteria attached to the surface of the mineral might affect the measurement of surface area by the B. E. T. method, either by

altering the actual surface area presented to the adsorbing nitrogen, or by altering the effective surface area covered by a nitrogen molecule. A procedure was therefore necessary to remove the attached bacteria from the mineral surface.

Four procedures to achieve these two objectives were evaluated:

(a.) Wash with 10% HCl, filter.
(b.) Wash with 10% HCl and acetone, filter.
(c.) Wash with 10% HCl, centrifuge.
(d.) Wash with pH 2 water, centrifuge.

In these procedures, the HCl wash was intended to dissolve precipitated iron compounds and cause the bacteria to leave the surface due to the unfavourable environment.

Two 20 ml samples were removed from the leach tank, and made to 10% HCl with concentrated acid. They were stoppered, shaken well, and allowed to stand for 13 hours. The solids were recovered by filtration on Whatman No. 5 paper, and dried at 105°C. One filter cake was digested by the Kjeldahl procedure and the total ammonium ion was determined. The other filter cake was resuspended in pH 2 water, and analyzed for distillable ammonium ion and total carbon. All washings and filtrates were

collected and made to volume. Dissolved zinc and iron, non-distillable ammonium ion, and total carbon were determined in the original slurry and in these filtrates. The results are summarized in Table VII, where all the concentrations have been corrected to the basis of the concentrations in the original sample. (Note that the determinations on the resuspended cake are of low accuracy due to the difficulty of resuspending the cake homogeneously.)

Table VII shows that the HCl treatment increased the dissolved iron level substantially while the dissolved zinc level decreased slightly. 35% of the net ammonium ion remained associated with the solids.

It was concluded that the 10% HCl wash procedure dissolved some of the iron precipitate, but was not successful in removing the bacteria from the solids. To improve the removal of bacteria from the solids it was decided to include an acetone washing step. Acetone might be able to dissolve the bond between the bacteria and the mineral and should lyse the cells. To this end, the HCl washing procedure was repeated on two 50 ml samples from the leach tank. Following filtration, the filter cakes were washed with acetone, then distilled water. The results are presented in Table VIII.

The data in Table VIII support the conclusion that the 10%

Table VII. Distribution Of Organic Material Between Solids And Filtrate: 10% HCl Wash.

Original Tank Product

15-07-71

Two Samples, 20 ml

Zn = 20100 mg/l

Fe = 890 mg/l

Net NH_4^+ = 131 mg/l

Total C = 435 mg/l

Wash With 10% HCl, Filter.

Filter Cakes:

I (digest)	II (resuspend)
Total NH_4^+ = 47 mg/l	Distillable NH_4^+ = 1 mg/l
Net NH_4^+ = 46 mg/l	Total C = 295 mg/l

Filtrate:

Zn =	19475 mg/l
Fe =	1275 mg/l
Net NH_4^+ =	69 mg/l
Total C =	217 mg/l

Table VIII. Distribution Of Organic Material Between Solids And Filtrate: Acetone Wash

Original Tank Product

22-09-71

2 Samples, 50 ml

Zn = 38100 mg/l

Fe = 1086 mg/l

Net NH_4^+ = 196 mg/l

Total C = 750 mg/l

Wash With 10% HCl, Acetone, Filter.

Filter Cakes:

I (digest)	II (resuspend)
Total NH_4^+ = 124 mg/l	Distillable NH_4^+ = 7 mg/l
Net NH_4^+ = 117 mg/l	Total C = 252 mg/l

Filtrates:

I	II
Zn = 37720 mg/l	Precipitation Of Zinc Sulphate Due To Acetone Addition Invalidates Analysis.
Fe = 3422 mg/l	
Net NH_4^+ = 69 mg/l	
Total Carbon Not Possible Due To Acetone Wash	

HCl dissolves a substantial amount of iron precipitate while dissolving very little of the zinc in the mineral. The acetone wash was unsuccessful in removing bacteria from the solids; 60% of the net ammonium ion remained associated with the solids. When acetone was added to filtrate II a white precipitate was formed. This precipitate was found to contain 25% zinc, and was tentatively identified as a hydrated zinc sulphate.

It was possible that the bacteria were successfully removed from the surface by the 10% HCl treatment, but that the suspended bacteria were partially removed from the filtrate with the solids during filtration. This would account for the high net ammonium ion and total carbon levels in the filter cake. The washing procedure was therefore modified as follows:

50 ml of slurry were pipetted into a centrifuge bottle and centrifuged at low speed to settle the solids but leave the bacteria suspended. The centrifugate was decanted and 10% HCl was added to the solids. The bottle was stoppered and shaken, and then centrifuged and decanted as before. The procedure was repeated for a total of two HCl washes and one distilled water wash. The solids were resuspended in distilled water and filtered. The results of this experiment are presented in Table IX.

The data in Table IX show that the zinc concentrations in

Table IX. Distribution Of Organic Material Between Solids And Centrifugate: 10% HCl Wash.

Original Tank Product

18-11-71

Two Samples, 50 ml

Zn = 46350 mg/l

Fe = 1565 mg/l

Net NH_4^+ = 360 mg/l

Total C = 1400 mg/l

Wash With 10% HCl, Centrifuge.

Solids:

I (digest)	II (resuspend)
Total NH_4^+ = 69 mg/l	Distillable NH_4^+ = 4 mg/l
Net NH_4^+ = 65 mg/l	Total C = 252 mg/l

Centrifugates:

	I	II
Zn =	48050 mg/l	47500 mg/l
Fe =	4545 mg/l	4548 mg/l
Net NH_4^+ =	296 mg/l	304 mg/l
Total C =	1104 mg/l	1144 mg/l

the filtrates were slightly higher than in the original sample; the iron concentrations were about three times that in the original sample. The zinc dissolved represents dissolution of about 5% of the filter cake weight. The ratio of zinc to iron dissolved is 0.48; the ratio of zinc to iron in the zinc concentrate is about 10. It was concluded that the increase in dissolved iron was due to dissolution of iron precipitate, not due to dissolution of zinc concentrate. 18% of the net ammonium ion remained in the filter cake, a marked improvement over the previous procedures.

To show the effect of the 10% HCl in these procedures, an experiment was performed where pH 2 water was substituted for 10% HCl, and the solids were recovered by centrifugation. The results in Table X show that there was some increase in the iron levels in the filtrates, no increase in the zinc levels, and 65% of the net ammonium ion remained in the cake. The distillable ammonium ion in the resuspended cake was substantially higher than in the HCl washed cakes, suggesting that some ammoniojarosite had not been dissolved by the pH 2 water wash.

These four experiments are not strictly comparable, since the conditions in the tank were not identical in each case. However, they indicate that the objectives of removing bacteria and iron precipitate from the solids were most nearly achieved by a 10% HCl wash and centrifugation. This method is summarized

Table X. Distribution Of Organic Material Between Solids And Centrifugate: pH 2 Wash.

Original Tank Product

18-03-72

2 Samples, 50 ml

Zn = 34500 mg/l

Fe = 671 mg/l

Net NH_4^+ = 384 mg/l

Total C = 1416 mg/l

Wash With pH 2 Water, Centrifuge.

Solids:

I (digest)	II (resuspend)
Total NH_4^+ = 285 mg/l	Distillable NH_4^+ = 34 mg/l
Net NH_4^+ = 251 mg/l	Total C = 447 mg/l

Centrifugates:

	I	II
Zn =	34975 mg/l	33850 mg/l
Fe =	838 mg/l	813 mg/l
Net NH_4^+ =	144 mg/l	135 mg/l
Total C =	470 mg/l	452 mg/l

in the Procedures section (page 71).

In an attempt to evaluate the effect of bacteria attached to the mineral surface on the specific surface area determination, a washed cell suspension was incubated with a slurry of silica spheres of diameter one micron (76). A slurry of the same spheres was incubated with pH 2 water as a control. After three days incubation the spheres were recovered by low speed centrifugation and washed twice with pH 2 water. They were resuspended in pH 2 water and filtered. The filter cakes were digested for total ammonium ion. The test spheres and the control spheres analyzed 0.093% and 0.0035% ammonium ion respectively; thus, some bacteria had attached to the test spheres. The specific surface of the test spheres and the control spheres was found to be 4.14 m^2/g and 4.55 m^2/g respectively. Therefore, bacteria on the surface may reduce the specific surface area determined by the B. E. T. method by about 10%.

5. Non-Ideal Product Removal from the Tank

It was suspected that removing product by slurping it from the surface of the tank to control the liquid level might result in removal of material not representative of the contents of the bulk of the tank. Accordingly, experiments were performed on several occasions to determine the difference, if any, in

composition between material removed directly from the tank, and material removed through the product removal line.

Table XI shows the distribution of zinc in samples taken at the same time, one directly from the tank, and one from the product removal line. The undissolved zinc was determined by measuring the pulp density of each sample and analyzing the solid cake for zinc content.

The data for 17-06-72 and 24-06-72 show a higher level of undissolved zinc in the product sample than in the tank sample. This is not due to the HCl washing of the tank solids; the discrepancy is larger than the maximum of 5% dissolved by HCl washing. It is likely due to the fact that the product removal slurper removed some of the foam along with the material from the bulk of the tank. The material in the foam had a higher undissolved zinc level than the material in either the tank or product samples.

The data for 19-07-72 and 29-07-72 show that careful adjustment of the removal slurper cycle so that mostly tank material was removed could eliminate this problem. Since the product was removed in pulses, the duration of the pulse and the length of time between pulses could be adjusted so that the slurp tube was submerged for most of the pulse, minimizing sampling of the foam.

Table XI. Distribution Of Zinc In Tank And Product Samples

		Dissolved Zinc (g/l)	Undissolved Zinc (g/l)	Total Zinc (g/l)
17-06-72	Tank	6.40	8.18	14.57
	Product	-----	10.07	-----
	Foam	-----	-----	-----
24-06-72	Tank	14.22	18.34	32.56
	Product	13.89	21.04	34.93
	Foam	14.09	75.00	89.09
19-07-72	Tank	7.62	16.13	23.75
	Product	7.78	16.33	24.11
	Foam	8.10	31.32	39.42
29-07-72	Tank	12.68	27.68	40.36
	Product	12.35	27.24	39.59
	Foam	13.33	68.10	81.43

As further proof that this adjustment was successful, the data in Table XII are presented. This summarizes the net ammonium ion, total carbon and dissolved iron values in the tank and product samples for the steady state of 28-07-72 ---- 29-07-72. The potential for different values in the product was there: a sample of the foam taken during this period had a net ammonium ion level of 200 mg/l, a total carbon level of 798 mg/l, and an iron concentration of 0.531 g/l, all substantially different from the levels in the tank or in the product.

The high levels of undissolved zinc in the foam may be due to the production by the bacteria of a surfactant with a collector action, or presence of flotation reagents on the concentrate. The tank then acted as a flotation cell, concentrating the hydrophobic mineral in the foam. The organic material which concentrated in the foam may have been surface active products of the cells' metabolism, cells themselves, antifoam, flotation reagents, or cells attached to the hydrophobic mineral.

Although there is no data specifically demonstrating it, it is quite probable that when the product material contained higher levels of undissolved zinc than the tank material (indicating sampling of the foam), it also contained higher levels of organic matter, since organic matter concentrated in

Table XII. Comparison Of Tank And Product Sample Concentrations For Steady State 28-07-72 ---- 29-07-72.

Sample		Net Ammonium Ion (mg/l)	Total Carbon (mg/l)	[Fe] (g/l)
28-07-72 1	Tank	146	506	0.681
	Product	148	503	0.702
28-07-72 2	Tank	145	498	0.699
	Product	149	502	0.708
28-07-72 3	Tank	154	506	0.662
	Product	153	511	0.699
29-07-72 1	Tank	151	516	0.715
	Product	151	499	0.741
29-07-72 2	Tank	153	516	0.717
	Product	152	504	0.716

the foam.

The lowered iron concentration in the foam may be due to dilution of the foam by nutrient medium falling through it as it entered into the tank.

Levels of dissolved zinc for the steady states obtained between 22-06-72 and 29-07-72 were not significantly different in the tank and product samples. A least squares line was fit to product dissolved zinc concentrations as a function of tank dissolved zinc concentrations, and it was impossible to reject the hypotheses that the slope was one and the intercept was zero at the 90% level (Appendix II).

Unfortunately, there are not enough data to indicate what percentage of the time the non-ideal product removal was a problem. It is likely that it was a greater problem at higher dilution rates when the foaming was greatest. The data in Table XI suggest that once the problem was discovered it could be eliminated, so that the data for the dilution rate of 0.1038 hr^{-1} are probably not affected. The data for the dilution rate of 0.0595 hr^{-1} probably have been biased, but they correlate quite well with the data from the other three dilution rates, so the non-ideality was not too great.

When non-ideal product removal was occurring, the bacterial

growth rates were actually higher than those calculated, since the rate at which bacteria were removed from the tank was actually greater than that calculated. Higher levels of undissolved zinc in the product stream than in the tank make the residence time of the concentrate particles in the tank less than that calculated from the dilution rate due to a higher throughput rate of concentrate.

B. Continuous Leaching Experiments

1. Introduction

Because the proposed applications of concentrate leaching are in continuous processing, a kinetic study was done in continuous culture. To make the study as easy to analyze as possible, an ideal reactor had to be chosen. Two ideal continuous reactor types are the plug flow reactor, and the perfectly stirred tank reactor. The plug flow reactor was ruled out because of the difficulty of maintaining true plug flow of a three phase mixture for the high residence times required. As well, most of the biokinetic models that had been developed to describe continuous fermentations had considered the fermentation to be taking place in a chemostat, a continuous stirred tank reactor.

The variables of pH and temperature were studied in batch

culture by Torma (16), and it was felt that the optima determined in batch culture should apply to continuous culture as well. Other variables such as levels of dissolved oxygen, carbon dioxide, and nutrient in the nutrient medium could be important limiting factors in the continuous process, but were not studied because of the desire to measure the effect of the concentration of substrate surface area. To this end, it was decided to maintain oxygen, carbon dioxide, and nutrients at levels which would not limit the bacterial growth rate.

2. "Sterile" Run

To evaluate the contribution of the bacteria to the continuous leaching results, one run was made where no bacteria were intentionally introduced. Since it was not possible to sterilize the tank and keep it sterile, the added precaution of eliminating ammonium sulphate from the nutrient medium was taken. Thus the only sources of nitrogen for any stray bacteria in the system would be that entering with the concentrate, or nitrogen in the air supplied to the tank. The results for this run are tabulated in Appendix III.

Although the occasional bacterium was evident under a microscope, the correction factors calculated were slightly less than those which had been previously calculated by determining directly the net ammonium ion and total carbon content of the

concentrate. Therefore the contribution of the observed bacteria to these measurements was probably very small, and the level of bacteria during the sterile run was a very small fraction of the levels observed during the continuous leaching runs. Further evidence of the low level of bacterial activity during this run is the low level of ferric iron. Duncan and Walden (39) indicated that there is seldom any ferrous iron present when the leaching bacteria are active. The low level of ferric iron was indicated by a low Eh value of +290 mv (measured relative to a Ag/AgCl reference electrode) as compared to values of about +440 mv measured when active bacteria were present. There was no evidence of the usual yellow-orange ferric iron precipitate, and the centrifugate from the leach slurry was a pale green colour, indicative of ferrous rather than ferric ion in solution. The dissolved iron values were relatively high in comparison with the dissolved zinc values, indicating that little iron was being removed from the solution by precipitation. As a result of the failure of iron to precipitate with accompanying generation of acid, the requirement for acid to maintain the low pH was higher for this run than for any other run. From all these observations, we may conclude that the level of bacterial activity was very low, and the sterile run did measure chemical leaching of zinc.

Two objections may be raised to this method of estimating the contribution of chemical leaching to the total amount of

leaching observed. One is that the level of ferric iron in solution during the sterile run was quite low, while in the continuous leaching runs all the iron in solution was probably in the ferric form. Insofar as the ferric iron can contribute to the overall leaching observed with a zinc concentrate (Duncan and Walden (39)), the sterile run should give a low estimate for the chemical leaching contribution. However, the levels of dissolved iron observed in our continuous leaching runs were considerably lower than the 22.4 g/l used by Duncan and Walden in their experiments.

The other objection is that it is conceivable that one may have either chemical leaching or bacterial leaching but not both simultaneously. If the surface of the leachable mineral is completely covered with bacteria, then the access of the chemical leaching agents to the surface may be restricted. If this objection is valid, the estimates of chemical leaching given by the sterile run should be too high.

Ignoring these two objections, the chemical leaching kinetics have been assumed to involve a fast dissolution of acid labile zinc compounds (e.g. zinc oxide, zinc sulphate), followed by a slow, steady leaching of the sulphide. It has been assumed that the latter process would exhibit a rate proportional to the exposed surface area.

For the present purposes, the amount of readily soluble zinc was defined to be the amount which dissolves in pH 2 water in 15 minutes. By washing 5 g of feed concentrate in pH 2 water for 15 minutes, this was determined to be 2.06% of the feed weight. The release rate attributable to this mechanism may be calculated by

$$r_{OX} = (0.0206)\ (\text{feed pd, g/l})\ D \qquad (64)$$

For the sterile run, this was 0.0750 g/l-hr. The average release rate for the sterile run was 0.2185 g/l-hr, so the rate attributable to the slow chemical leaching of the concentrate is 0.1435 g/l-hr.

Assuming that the slow chemical leaching component may be described by

$$r_{CH} = ks \qquad (65)$$

the constant k may be calculated from the release rate of 0.1435 g/l-hr and the average steady-state surface area concentration of 107.7 m^2/l to be 1.33×10^{-3} g/hr-m^2. The baseline chemical leaching rate may now be determined as the sum of the two contributions:

$$r_b = r_{OX} + r_{CH} = 0.001333s + 0.0206 \text{ (feed pd, g/l)} \quad (66)$$

This may be converted to a concentration by dividing by the dilution rate.

The sterile run data also were used to provide a baseline correction to the net ammonium ion and total carbon concentrations measured in the other continuous runs. It was assumed that the net ammonium ion and total carbon concentrations measured in the sterile run were contributed by the incoming concentrate. The baseline correction was therefore calculated as mg/l net ammonium ion or total carbon per percent feed pulp density.

3. Kinetic Data

a. Correlation of Data

All the data for the continuous leaching runs are tabulated in Appendix IV. A sample calculation for one steady-state run is given in Appendix V.

The theory (page 53) suggests that the steady-state data should be plotted as bacterial concentration versus substrate

surface area concentration, with dilution rate as a parameter. These plots are given in Figures 6 and 7. In addition, in Figures 8 and 9 the data are plotted as a function of pulp density, so that the effects of substrate concentration and substrate surface area concentration may be compared. The lines which have been drawn through the data are the lines of least squares fit. A summary of the slopes and intercepts of these lines is given in Table XIII.

In Figures 6 and 8 bacterial concentration is estimated by net ammonium ion concentration; in Figures 7 and 9 it is estimated by total carbon concentration. The data show a good correlation between the two measures of bacterial concentration, and accordingly they are discussed interchangeably.

The most important single feature about Figures 6 - 9 from the point of view of bacterial kinetics is that there is a range of substrate concentrations or substrate surface area concentrations for a given dilution rate for which valid steady-states may be obtained. This is because, unlike homogeneous fermentations, the specific growth rate is not a unique function of the substrate concentration. If there were only one specific growth rate which would be supported by a given steady-state substrate concentration (e.g. as in the Monod model), then there could be only one substrate concentration for steady-state at a given dilution rate, since at steady-state the specific growth

Figure 6

STEADY-STATE NET AMMONIUM ION CONCENTRATION Vs SURFACE AREA CONCENTRATION

X D = 0.0171 hr^{-1}

○ D = 0.0284 hr^{-1}

□ D = 0.0595 hr^{-1}

Δ D = 0.1038 hr^{-1}

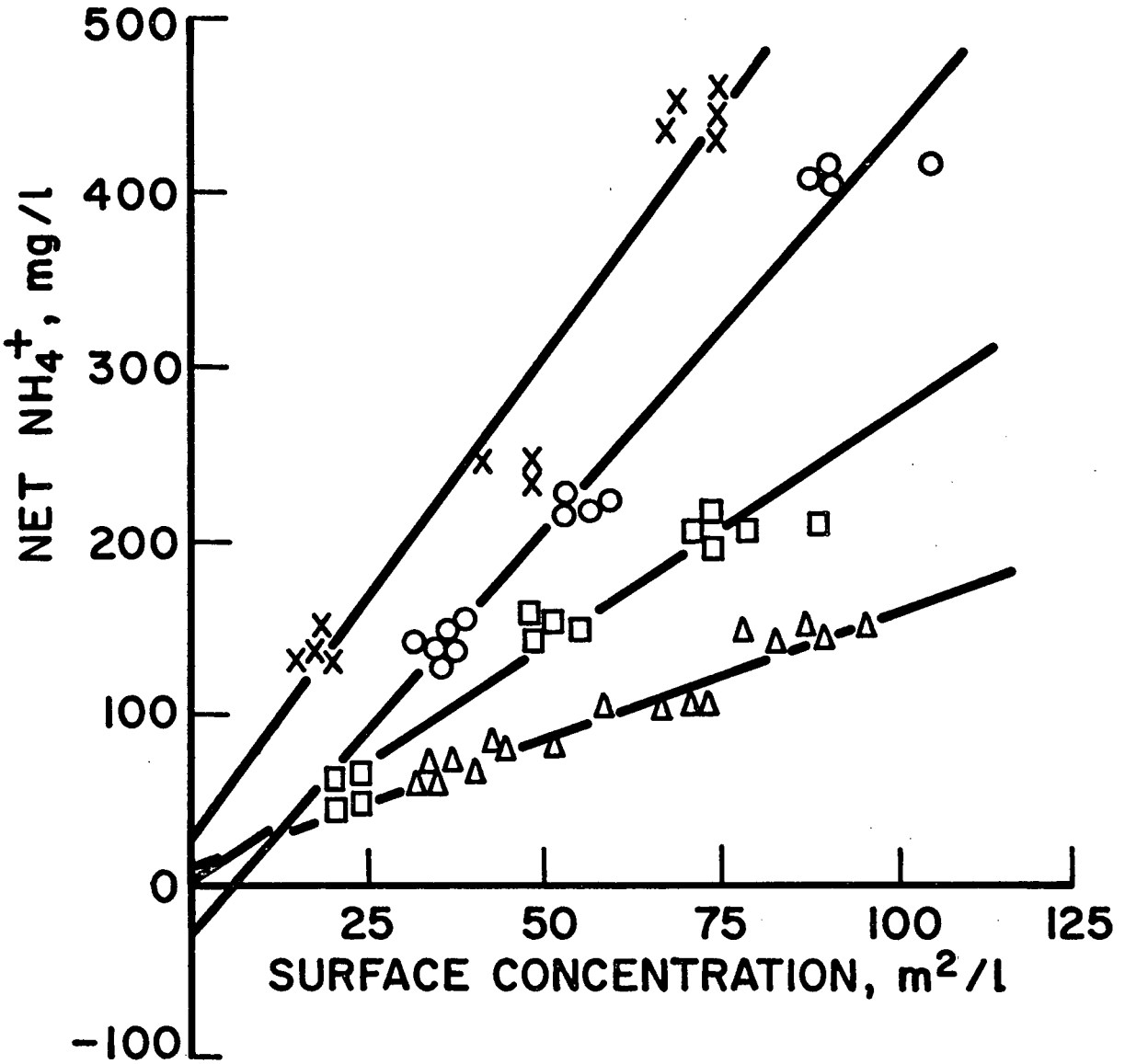

Figure 7

STEADY-STATE TOTAL CARBON CONCENTRATION Vs SURFACE AREA CONCENTRATION

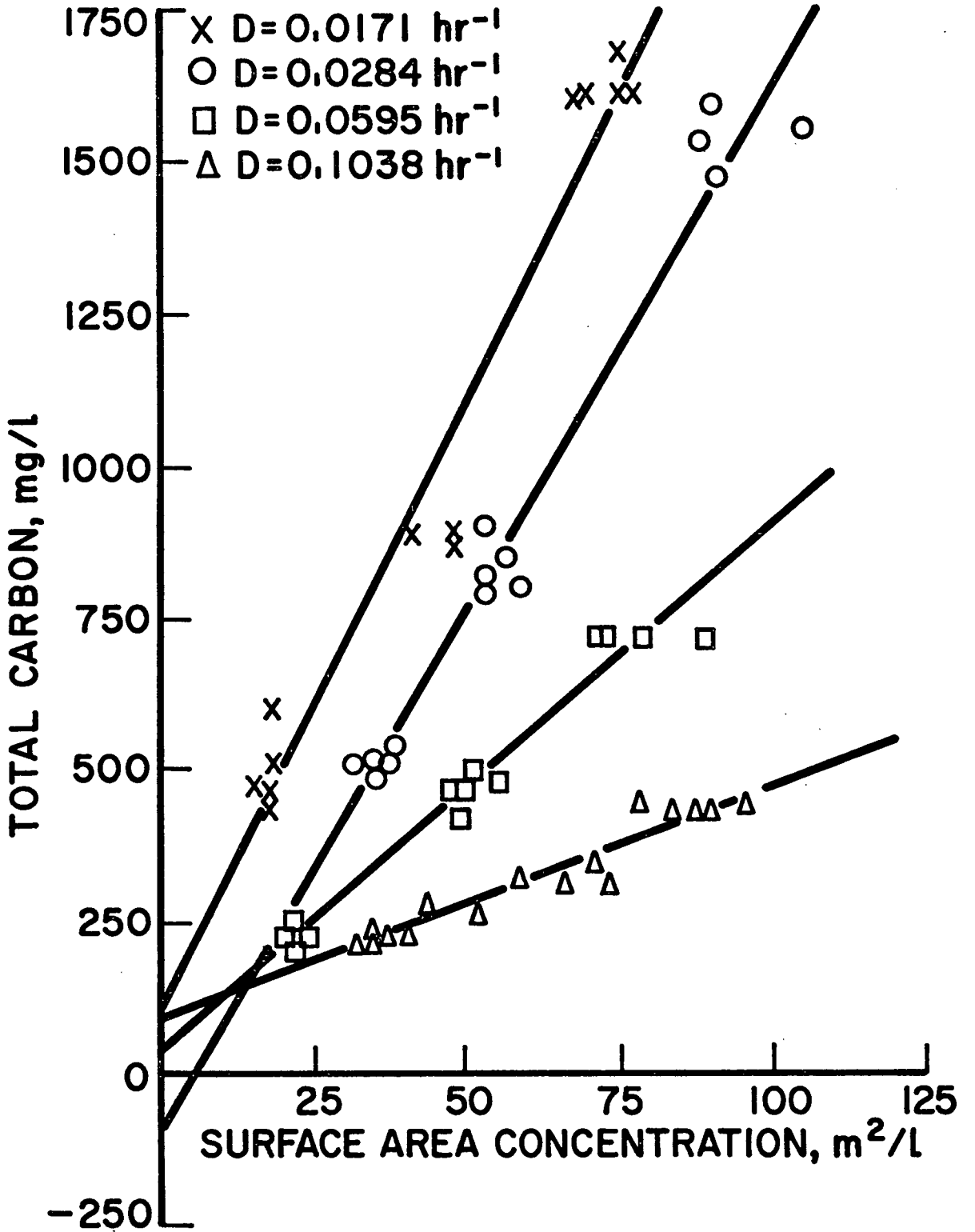

Figure 8
STEADY-STATE NET AMMONIUM ION CONCENTRATION Vs PULP DENSITY

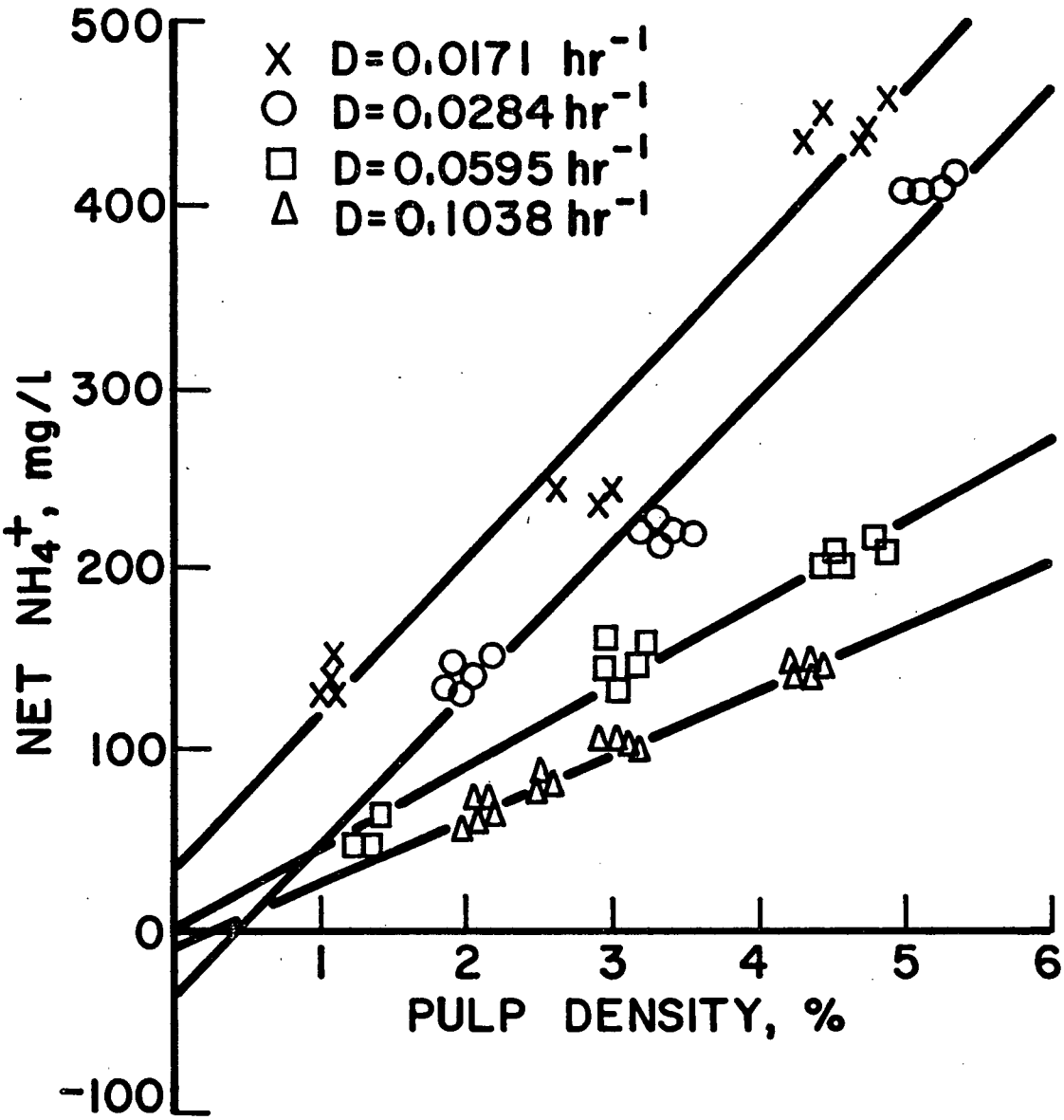

Figure 9

STEADY-STATE TOTAL CARBON CONCENTRATION Vs PULP DENSITY

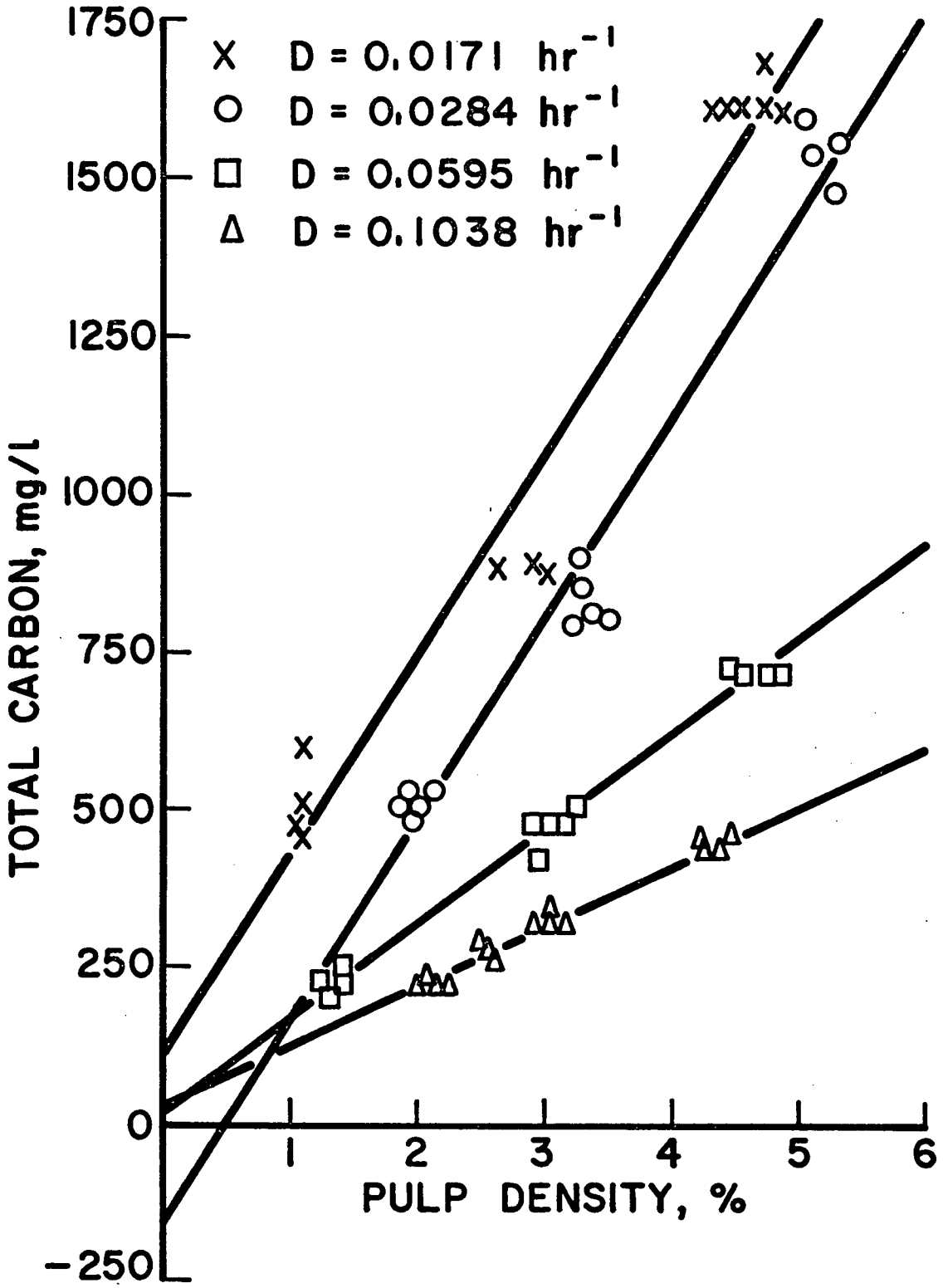

Table XIII. Summary Of Slopes And Intercepts For Steady-State Results

Figure	Variables Ordinate	Abscissa	Dilution Rate	Slope	Intercept
6	X_N	s	0.0171	5.50	29.5
			0.0284	4.55	-24.2
			0.0595	2.61	6.75
			0.1038	1.44	13.7
7	X_C	s	0.0171	20.1	104
			0.0284	17.2	-104
			0.0595	8.58	42.4
			0.1038	3.82	88.2
8	X_N	pd	0.0171	86.2	33.4
			0.0284	83.5	-36.2
			0.0595	45.4	0.134
			0.1038	35.4	-7.68
9	X_C	pd	0.0171	319	113
			0.0284	316	-151
			0.0595	149	21.5
			0.1038	94.7	28.1
16	Uncorrected [Zn]	s	0.0171	0.629	2.66
			0.0284	0.426	-1.23
			0.0595	0.244	1.20
			0.1038	0.103	2.97
18	Uncorrected [Zn]	pd	0.0171	10.0	2.90
			0.0284	7.82	-2.33
			0.0595	4.24	0.560
			0.1038	2.57	1.30
20	Corrected [Zn]	s	0.0171	0.517	2.45
			0.0284	0.350	-1.14
			0.0595	0.202	0.977
			0.1038	0.0770	2.75
22	Corrected [Zn]	pd	0.0171	8.22	2.63
			0.0284	6.42	-2.01
			0.0595	3.52	0.434
			0.1038	1.94	1.45

rate equals the dilution rate (equation 55). In this case, the lines on our plots would all be vertical.

Our model (equation 54) predicts that specific growth rate should depend not only on substrate surface area, but also on the bacterial concentration:

$$\mu = \frac{r_X}{X} = \frac{\nu}{X}\left(\frac{(s + fX + \kappa) - \sqrt{(s + fX + \kappa)^2 - 4\,fsX}}{2f}\right) \qquad (67)$$

The dependence of specific growth rate on substrate surface concentration is thus not unique. In this important respect our model is therefore borne out by the experimental data.

Our model predicts that the lines for each dilution rate should have no curvature (equation 59), and this prediction appears to be borne out by the experimental data.

Our model predicts that the slopes of the lines when plotted against the reciprocal of the dilution rates should define a straight line passing through the origin. Figures 10 and 11 plot the data in this manner with surface area concentration as the independent variable; in Figures 12 and 13, pulp density is the independent variable. Since only four dilution rates were used, there are only four points to define the line. It would appear, however, that if the line is to go through the origin, the line must curve downward at higher

Figure 10

SLOPE Vs RECIPROCAL DILUTION RATE FOR NET AMMONIUM ION -SURFACE CONCENTRATION PLOT (Figure 6)

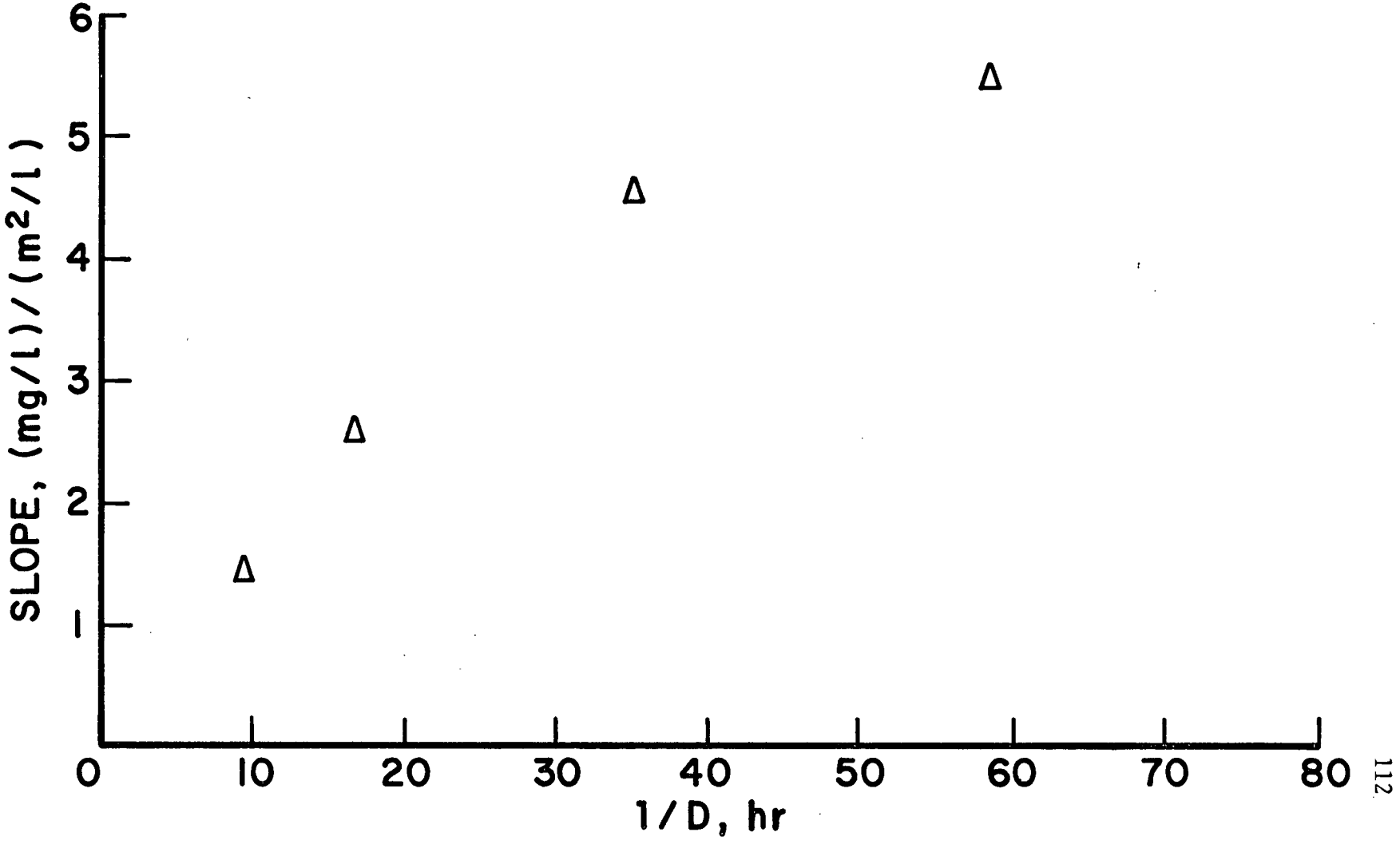

Figure 11

SLOPE Vs RECIPROCAL DILUTION RATE FOR TOTAL CARBON -SURFACE CONCENTRATION PLOT (Figure 7)

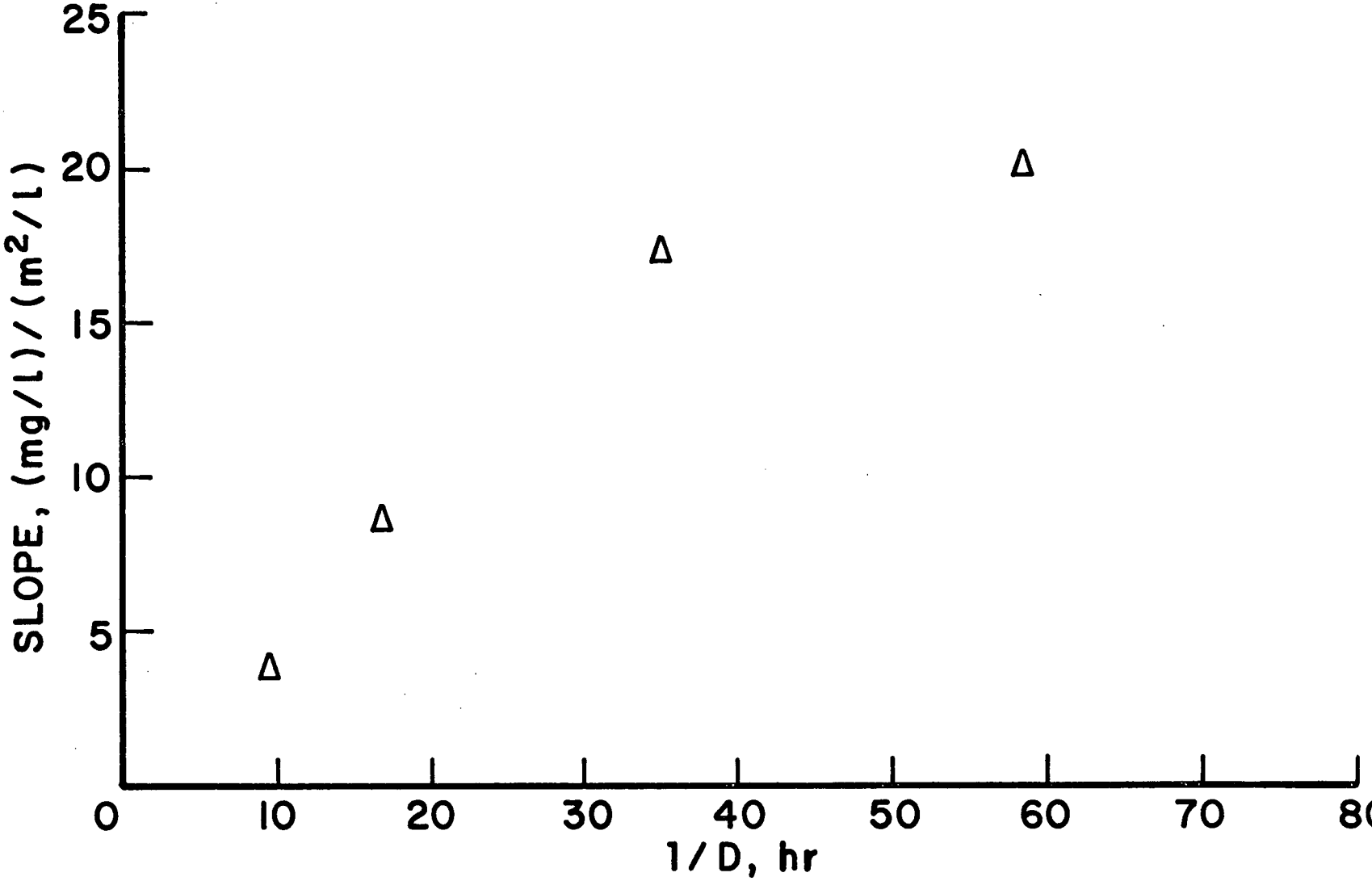

Figure 12

SLOPE Vs RECIPROCAL DILUTION RATE FOR NET AMMONIUM ION - PULP DENSITY PLOT (Figure 8)

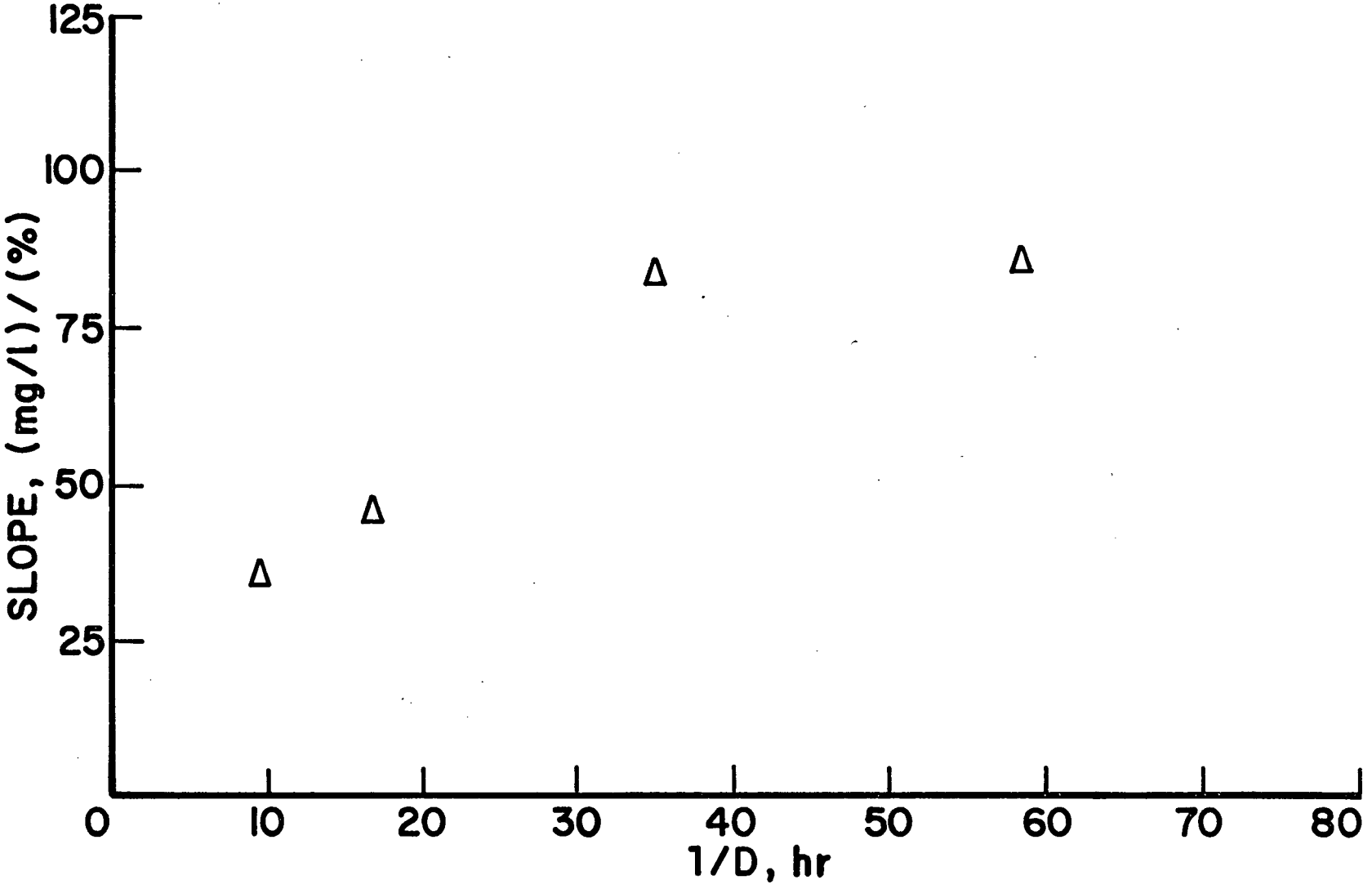

Figure 13

SLOPE Vs RECIPROCAL DILUTION RATE FOR TOTAL CARBON - PULP DENSITY PLOT (Figure 9)

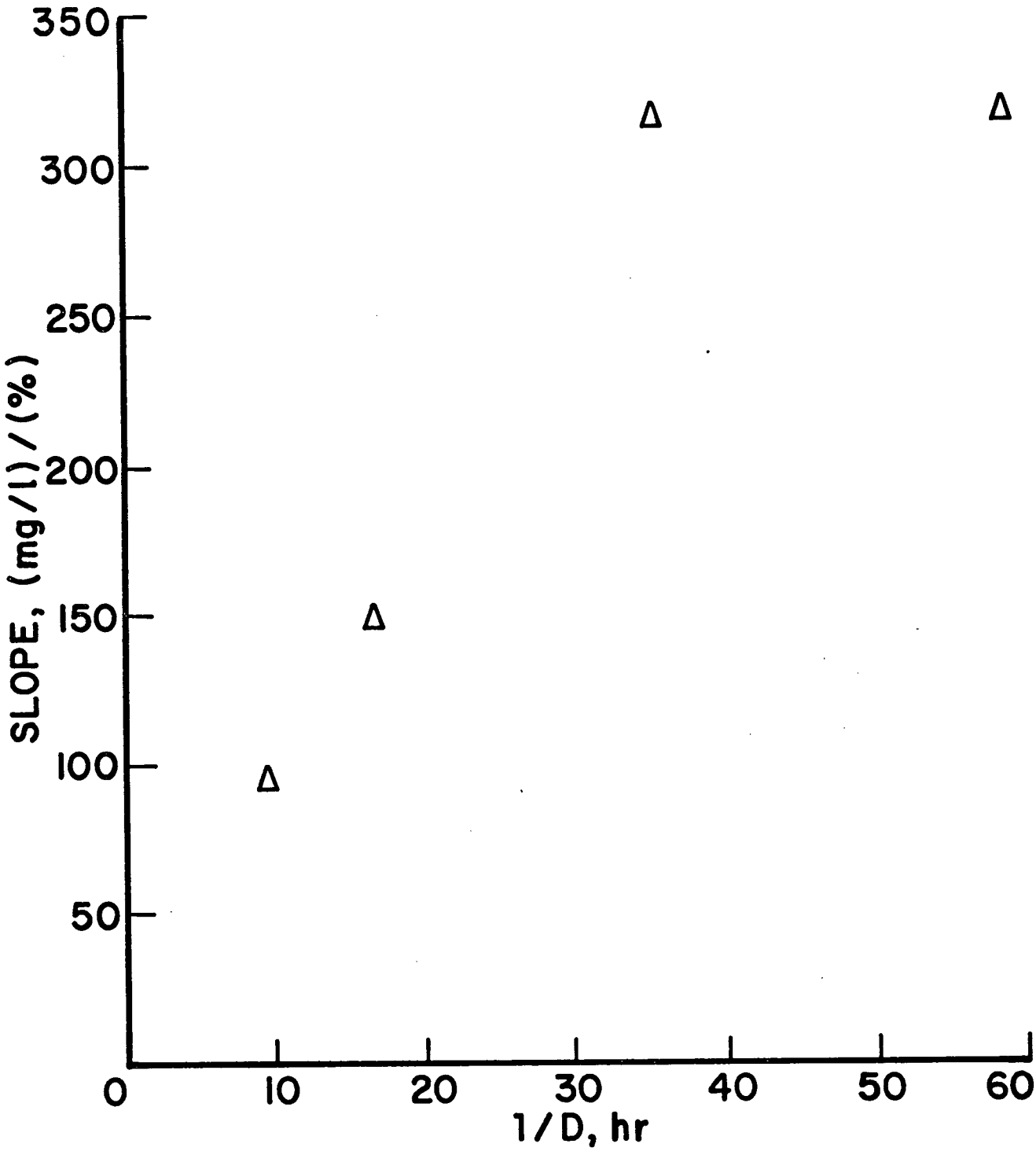

values of reciprocal dilution rate. In addition, when pulp density is the independent variable, the lines appear to have a positive intercept.

The downward curvature at high reciprocal dilution rates (residence times) may be explained by noting that not all the concentrate fed is leachable. At higher residence times, the percentage extraction increases, and the fraction of the surface area exposed that is "active" becomes smaller. For any given dilution rate, the percentage extraction is approximately constant (Table XIV), so that the fraction of active surface will be a constant which will decrease with decreasing dilution rate. The effect of applying such a correction factor to the measured surface concentrations is to increase the slope of the line for a given dilution rate. Since the correction factor would become smaller as the dilution rate became smaller, the greatest increase in slope should occur for the smallest dilution rate. The effect would be to help straighten out the line in these plots.

All the leach residue analyses fell in the range 54.2% to 58.5% zinc, independent of percentage extraction. This range includes residues that were both HCl and pH 2 water washed. These data indicate that the explanation for the curvatures in Figures 10 - 13 may not be valid, as all the residues probably contained a high percentage of leachable zinc.

Table XIV. Summary Of Percentage Zinc Extractions.

Dates	Dilution Rate	Total Output	Soluble Output	% Zinc Extracted
	(hr^{-1})	(g)	(g)	
22-11-71 ---- 27-11-71	0.0171	5005	3312	66.2
15-12-71 ---- 17-12-71	0.0167	850.4	514.0	60.4
24-02-72 ---- 28-02-72	0.0284	2101	1087	51.7
11-04-72 ---- 14-04-72	0.0273	3298	1832	55.5
4-05-72 ---- 9-05-72	0.0294	2002	1117	55.8
16-05-72 ---- 18-05-72	0.0603	2490	1111	44.6
14-06-72 ---- 17-06-72	0.0595	1194	517.0	43.3
21-06-72 ---- 23-06-72	0.0588	857.0	344.6	40.2
12-07-72 ---- 13-07-72	0.1040	1370	467.0	34.1
16-07-72 ---- 19-07-72	0.1034	1364	439.2	32.2
21-07-72 ---- 23-07-72	0.1040	2360	785.1	33.3
28-07-72 ---- 29-07-72	0.1038	2307	748.3	32.4
10-09-72 ---- 12-09-72	0.0588	1904	204.8	10.8
17-12-72 ---- 21-12-72	0.0171	514.0	369.6	71.9

The theory predicts that the intercepts of the lines in Figures 6 and 7 should become more negative as dilution rate increases. None of the intercepts appears to be significantly different from zero. Positive intercepts are not possible in terms of the theory presented. With no substrate fed to the tank, the only possible steady-state should be with no bacteria in the tank. The intercepts show no clear trend with dilution rate.

How can we reconcile these results with the predicted model? The steady-state results are predicted by equation 59:

$$X = \frac{\kappa}{f\,(D/\nu - 1)} + \frac{\nu}{Df}\,s \qquad (59)$$

Zero intercepts suggest that the constant κ is negligibly small. If this is so, k_{-1} is much smaller than k_1. Consideration of equation 51 shows that in this case the equilibrium between the bacteria attached and the free swimming bacteria is such that the surface is virtually completely occupied by bacteria. Putting κ equal to zero in equation 54 makes the bacterial growth rate first order in surface concentration, which is expected if the surface is completely occupied by the bacteria.

If the growth rate is first order in surface concentration, then all the growth rate data should be correlated by plotting

growth rate as a function of surface concentration. Figures 14 and 15 show that the growth rate data for net ammonium ion and total carbon are well correlated by this type of plot, giving a straight line intercepting near the origin. The slope of this line is an estimate of ν/f, and this is a better estimate than would be obtained from the slope of the plot of slopes versus reciprocal dilution rate (Figure 10 or 11) since all the data are used directly.

There appears to be an effect due to dilution rate on these plots, with higher dilution rates giving a higher growth rate for a given surface concentration. This may possibly be explained by the observation that at lower dilution rates and higher percentage extractions a lower fraction of the surface is active.

Because the intercept plot suggested by the theory could not be made, it was not possible to make estimates of the three constants in the model. We have an estimate of ν/f, and we know that κ is much smaller than $f(D/\nu - 1)$ for the range of dilution rates investigated. According to the model, if the dilution rate were made high enough, the intercept term should become significant as D/ν approaches unity. We may therefore conclude that ν is somewhat larger than the greatest value of dilution rate used in this study, 0.1038 hr^{-1}. The upper limit on dilution rate at which a steady-state bacterial population can

Figure 14

GROWTH RATE EXPRESSED AS NET AMMONIUM ION Vs SURFACE AREA CONCENTRATIONS

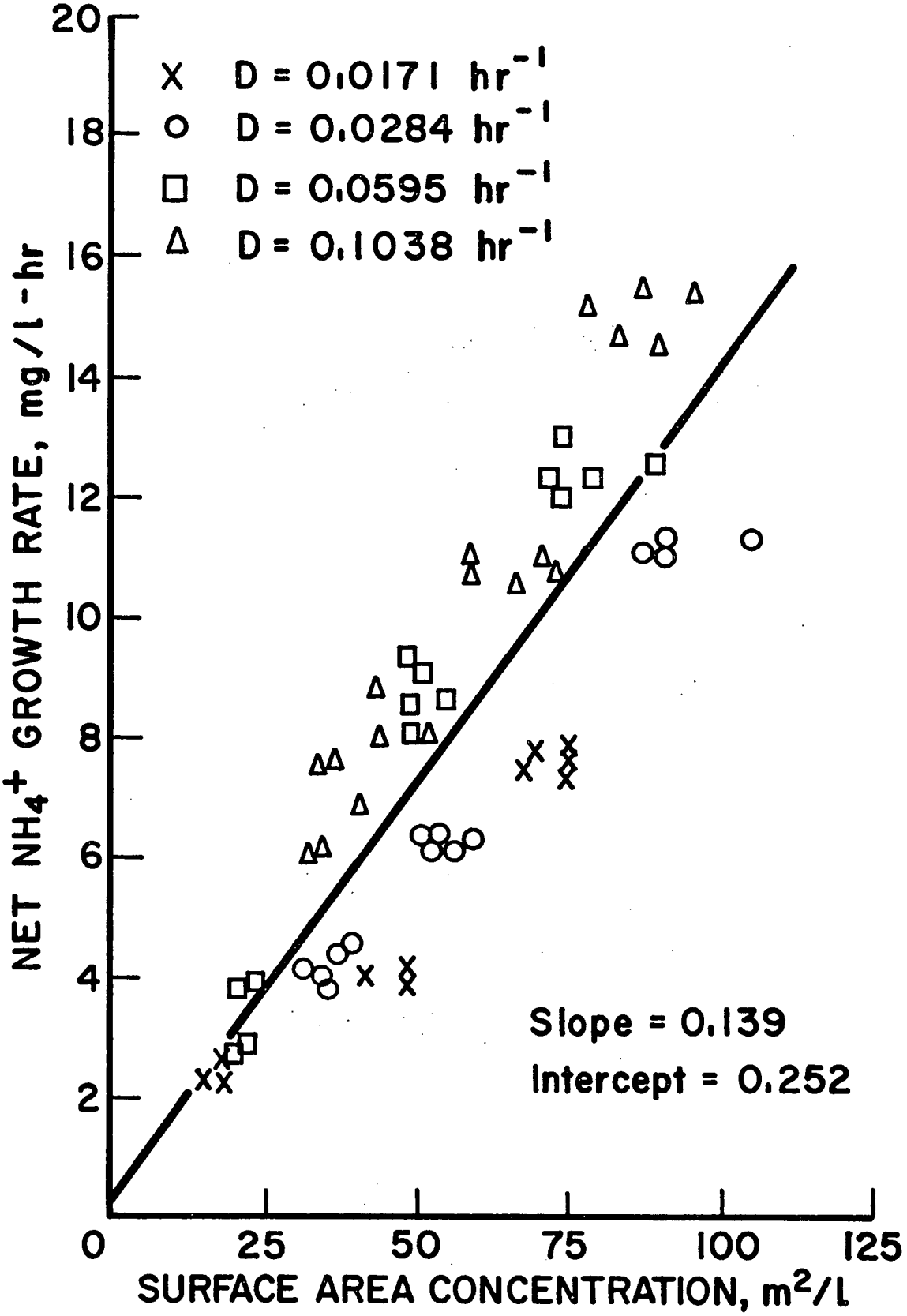

Figure 15

GROWTH RATE EXPRESSED AS TOTAL CARBON Vs SURFACE AREA CONCENTRATIONS

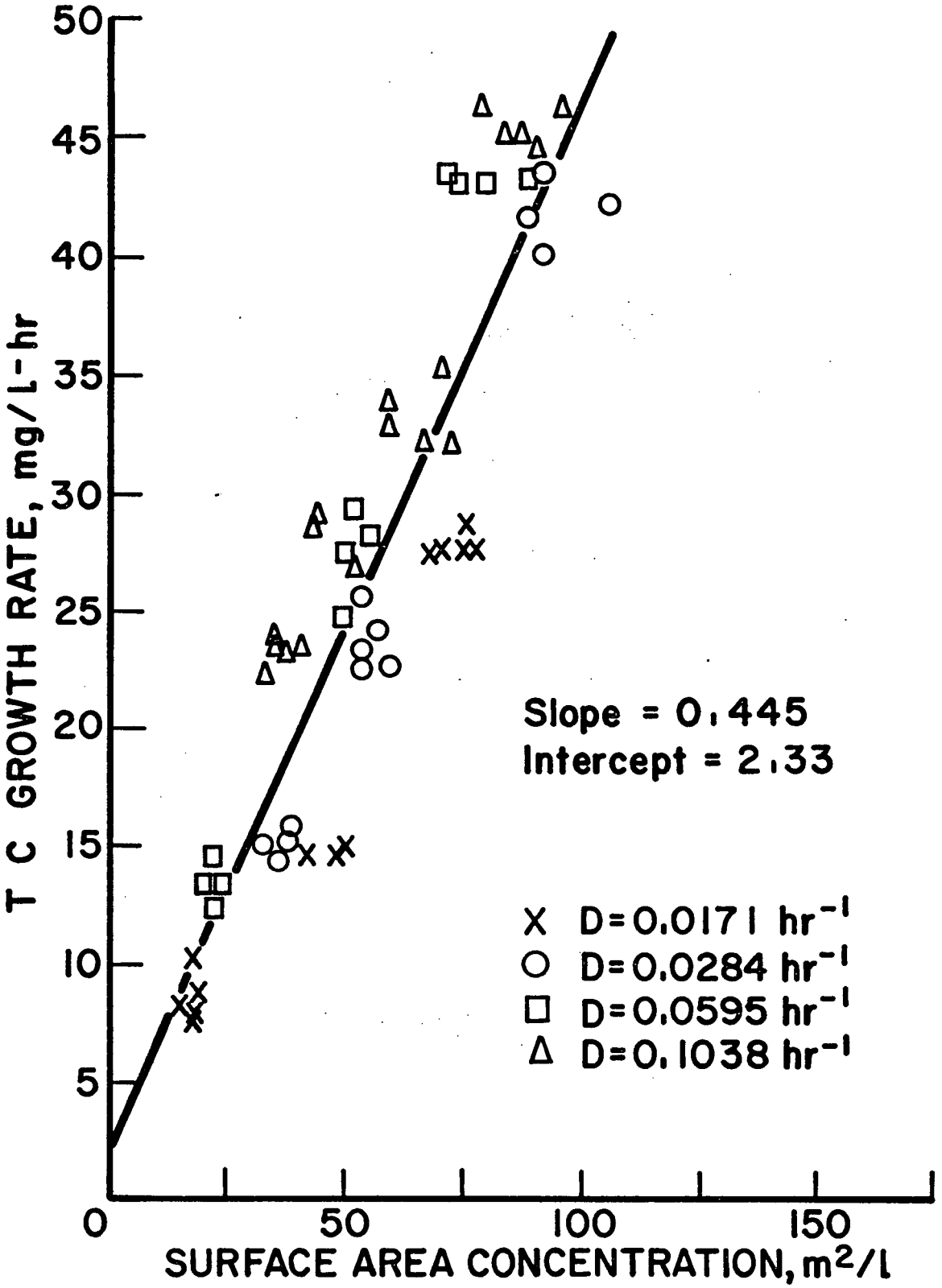

be maintained in the reactor is ν , the maximum specific growth rate for the bacteria which are attached. Evidently this work has not covered the full range of possible dilution rates. For comparison, Hempfling and Vishniac (77) have grown T. neapolitanus in continuous culture on a thiosulphate medium and determined a maximum specific growth rate of about 0.45 hr^{-1}.

b. Wall Growth

It may be argued that wall growth is responsible for the lack of appearance of a critical dilution rate (36,71). Two observations suggest that this is unlikely:

The total mineral surface area in the tank was usually greater than 300 m^2. The surface of the walls of the tank in contact with the slurry was only 3.2 m^2. Thus growth on the walls of the tank is unlikely to make a significant contribution to the total growth measured.

While it is likely that bacteria were associated with the scale which formed on the tank sides, these bacteria would not be able to grow at a significant rate, since the only substrate available was the zinc concentrate. Bacteria attached to the walls would be dependent on soluble substrate for growth. Dissolved iron in bacterial leaching systems is normally in the

ferric form (39), and thus is not a substrate. There did not appear to be any dead areas in the tank where concentrate could accumulate and support bacterial growth above the critical dilution rate.

c. Generation Time

The generation time corresponding to the highest dilution rate used in this work is about 6.7 hr and is the shortest generation time which has been reported for T. ferrooxidans when growing on a solid substrate. We may conclude from the above argument that this does not represent the minimum generation time for the organism.

d. Zinc Concentrations and Release Rates

Similar plots for zinc concentrations and release rates, both corrected and uncorrected for chemical leaching are given in Figures 16 - 25. They show the same general features as the bacterial concentration and growth rate plots, a consequence of the close association of bacterial growth with sulphide oxidation. The chemical leaching correction does not appear to have much effect on the degree of correlation of the data. Like the bacterial concentration data, the zinc concentrations show a better correlation with surface concentrations than with pulp densities.

Figure 16

STEADY-STATE ZINC CONCENTRATION Vs SURFACE AREA CONCENTRATION (NOT CORRECTED FOR CHEMICAL LEACHING)

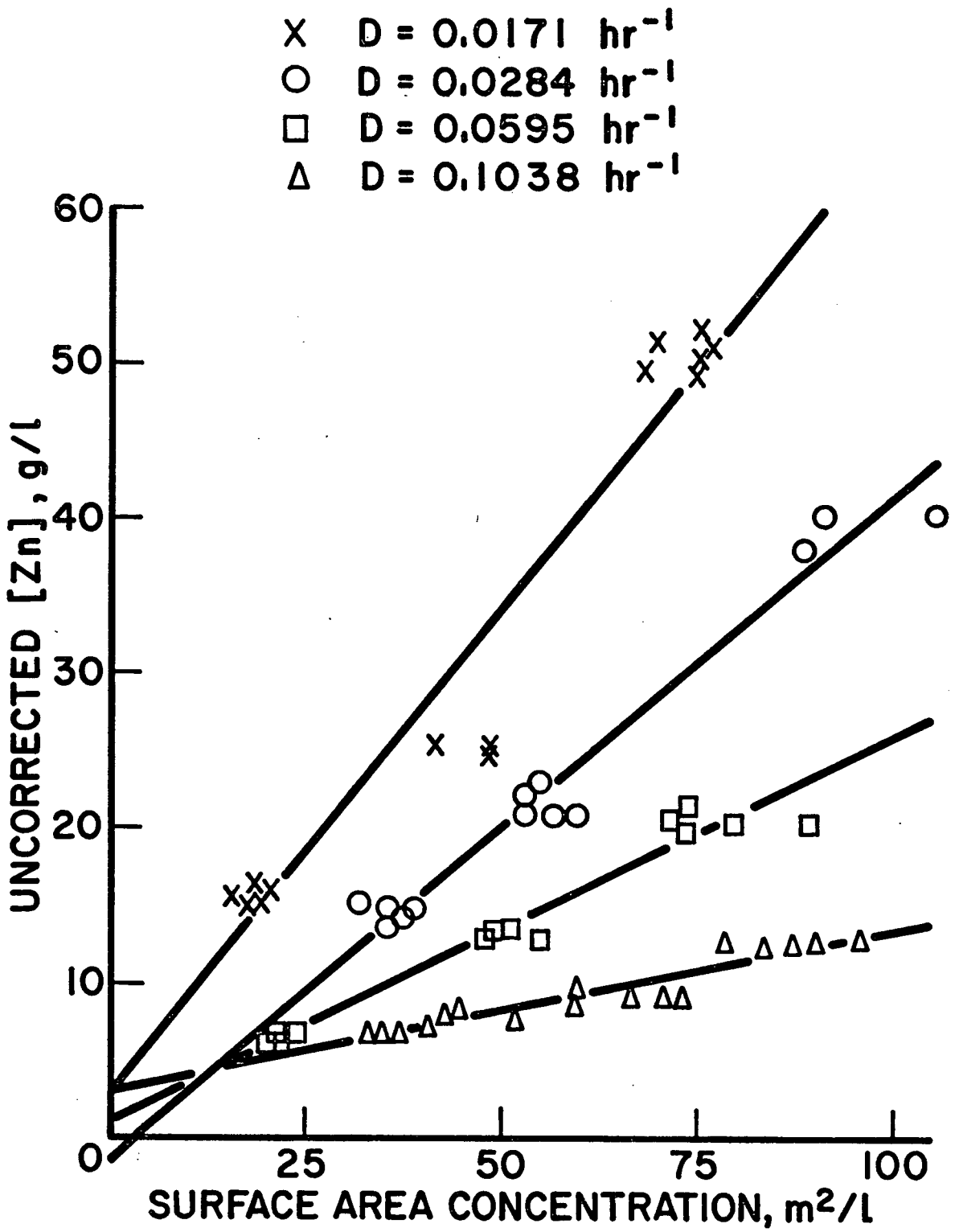

Figure 17

SLOPE Vs RECIPROCAL DILUTION RATE FOR UNCORRECTED ZINC - SURFACE AREA CONCENTRATION PLOT (Figure 16)

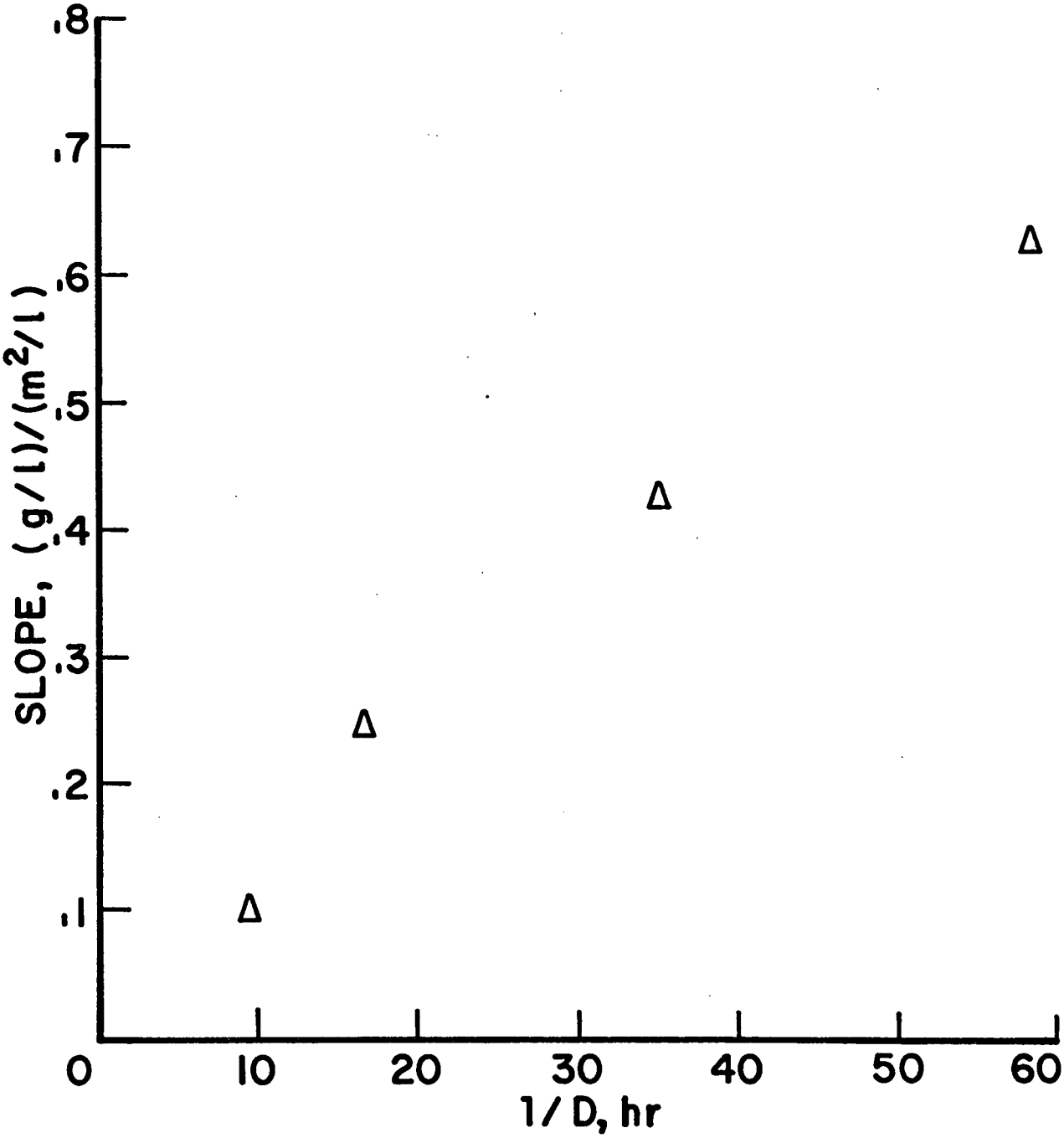

Figure 18

STEADY-STATE ZINC CONCENTRATION Vs PULP DENSITY (NOT CORRECTED FOR CHEMICAL LEACHING)

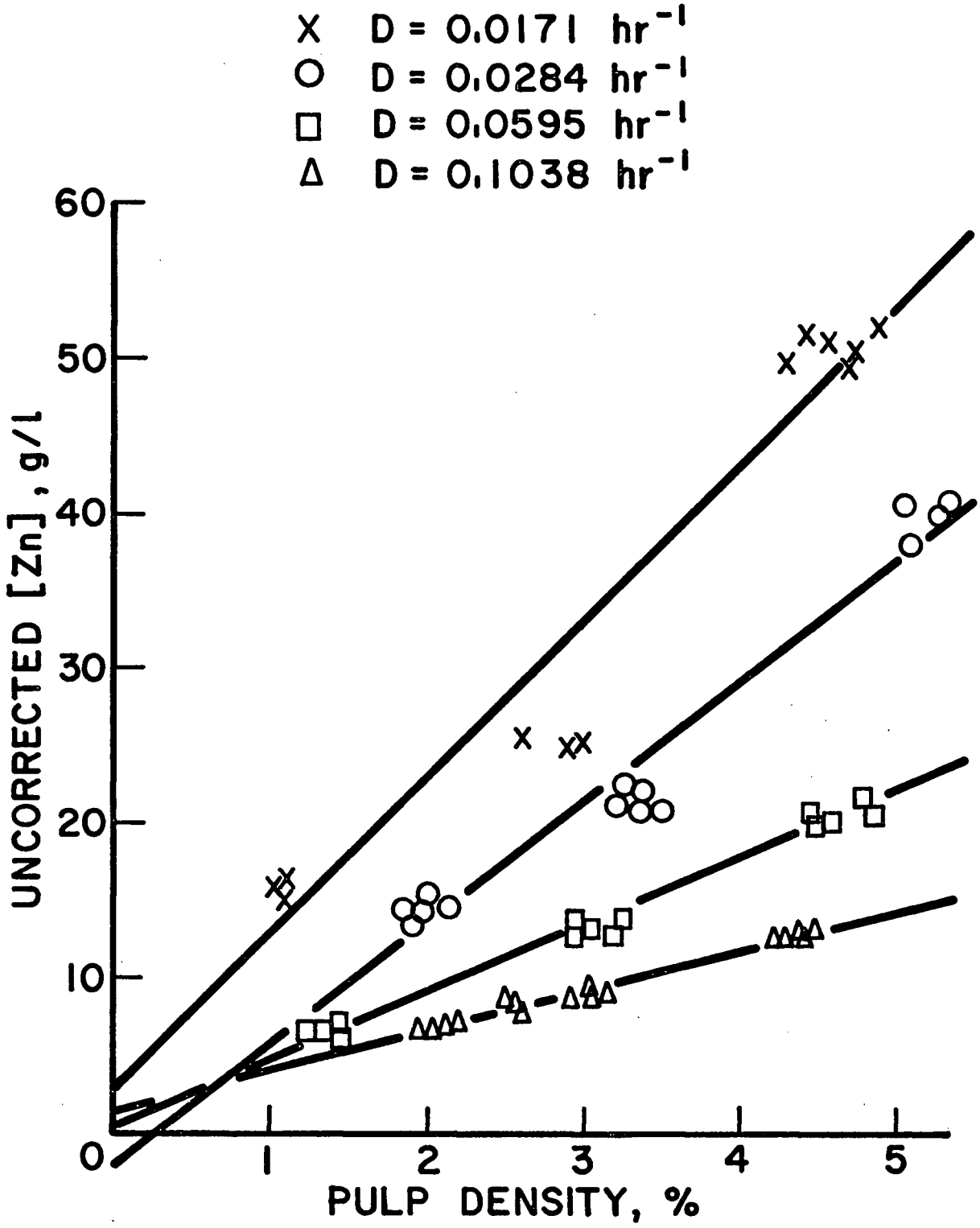

Figure 19

SLOPE Vs RECIPROCAL DILUTION RATE FOR UNCORRECTED ZINC-PULP DENSITY PLOT (Figure 18)

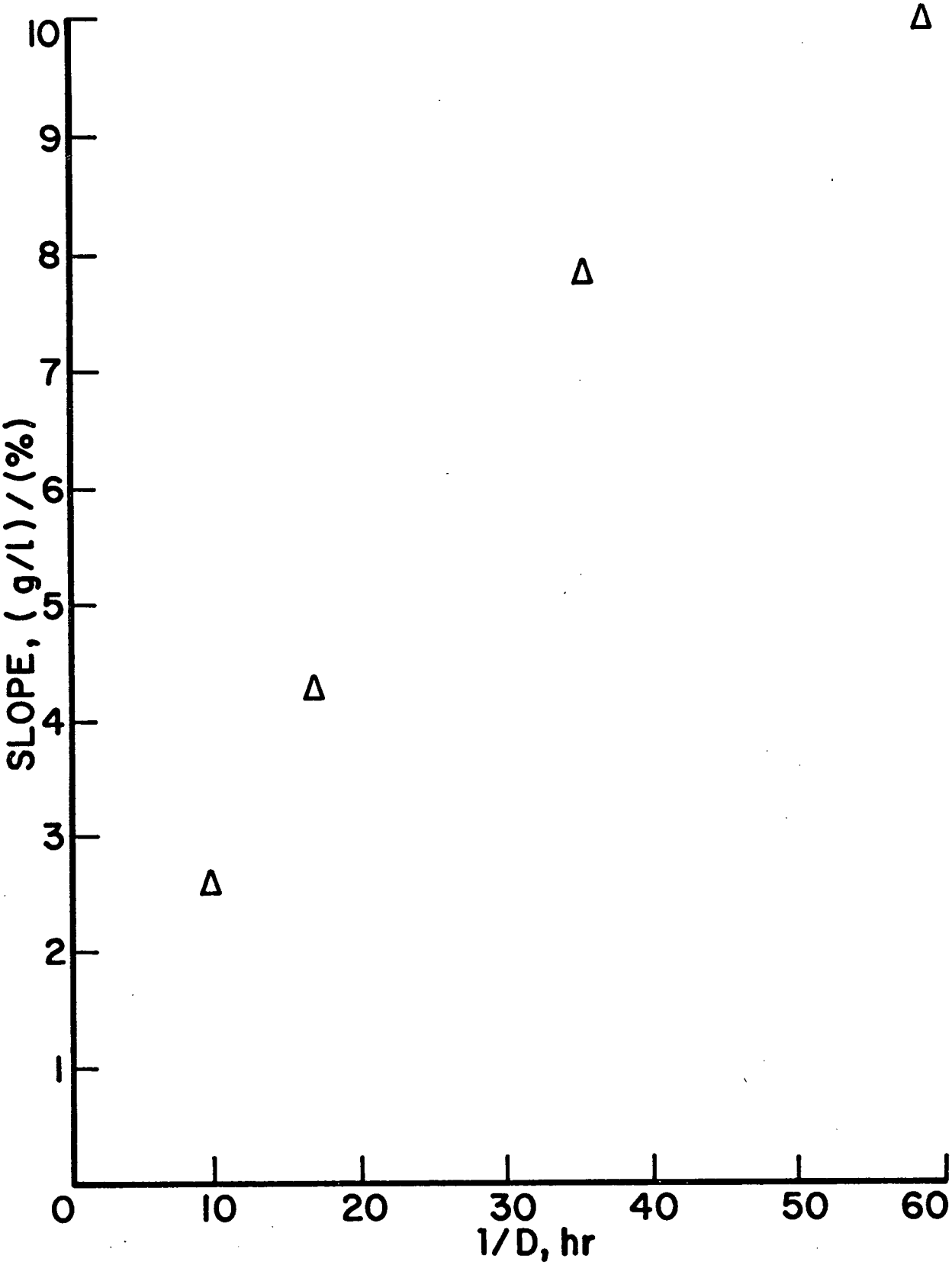

Figure 20

STEADY-STATE ZINC CONCENTRATION Vs SURFACE AREA CONCENTRATION (CORRECTED FOR CHEMICAL LEACHING)

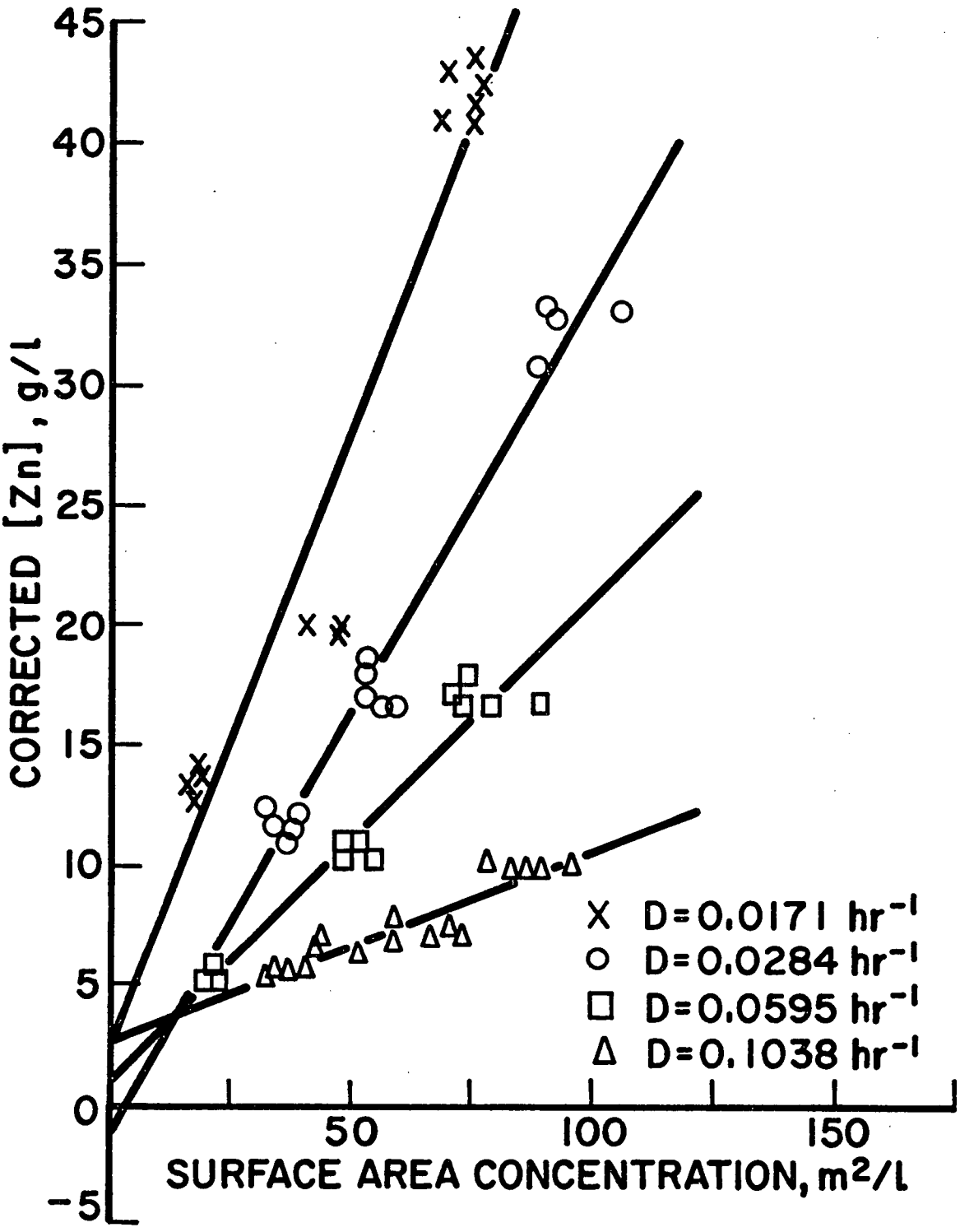

Figure 21

SLOPE Vs RECIPROCAL DILUTION RATE FOR CORRECTED ZINC - SURFACE AREA CONCENTRATION PLOT (Figure 20)

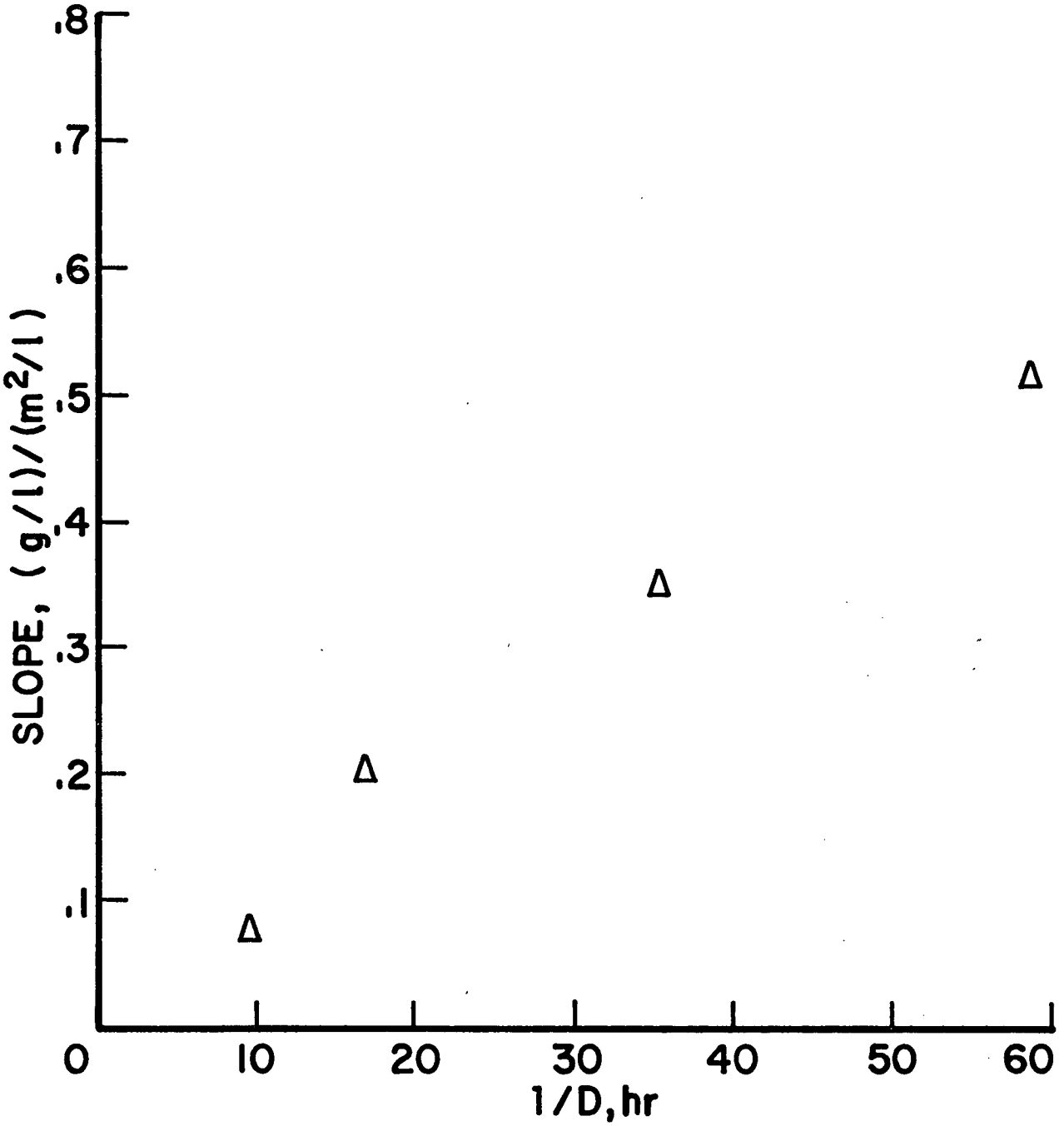

Figure 22

STEADY-STATE ZINC CONCENTRATION Vs PULP DENSITY (CORRECTED FOR CHEMICAL LEACHING)

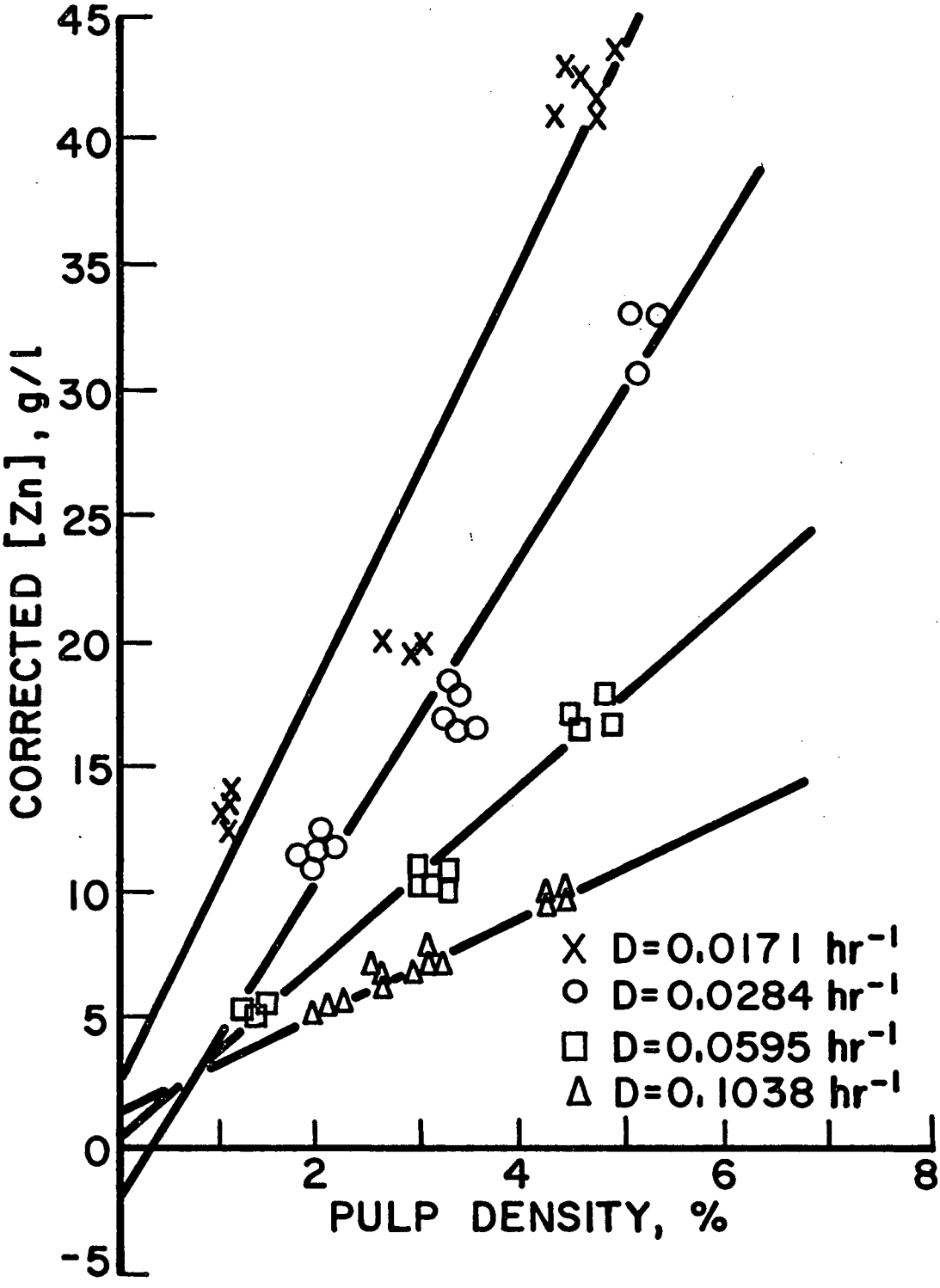

Figure 23

SLOPE Vs RECIPROCAL DILUTION RATE FOR CORRECTED ZINC-PULP DENSITY PLOT (Figure 22)

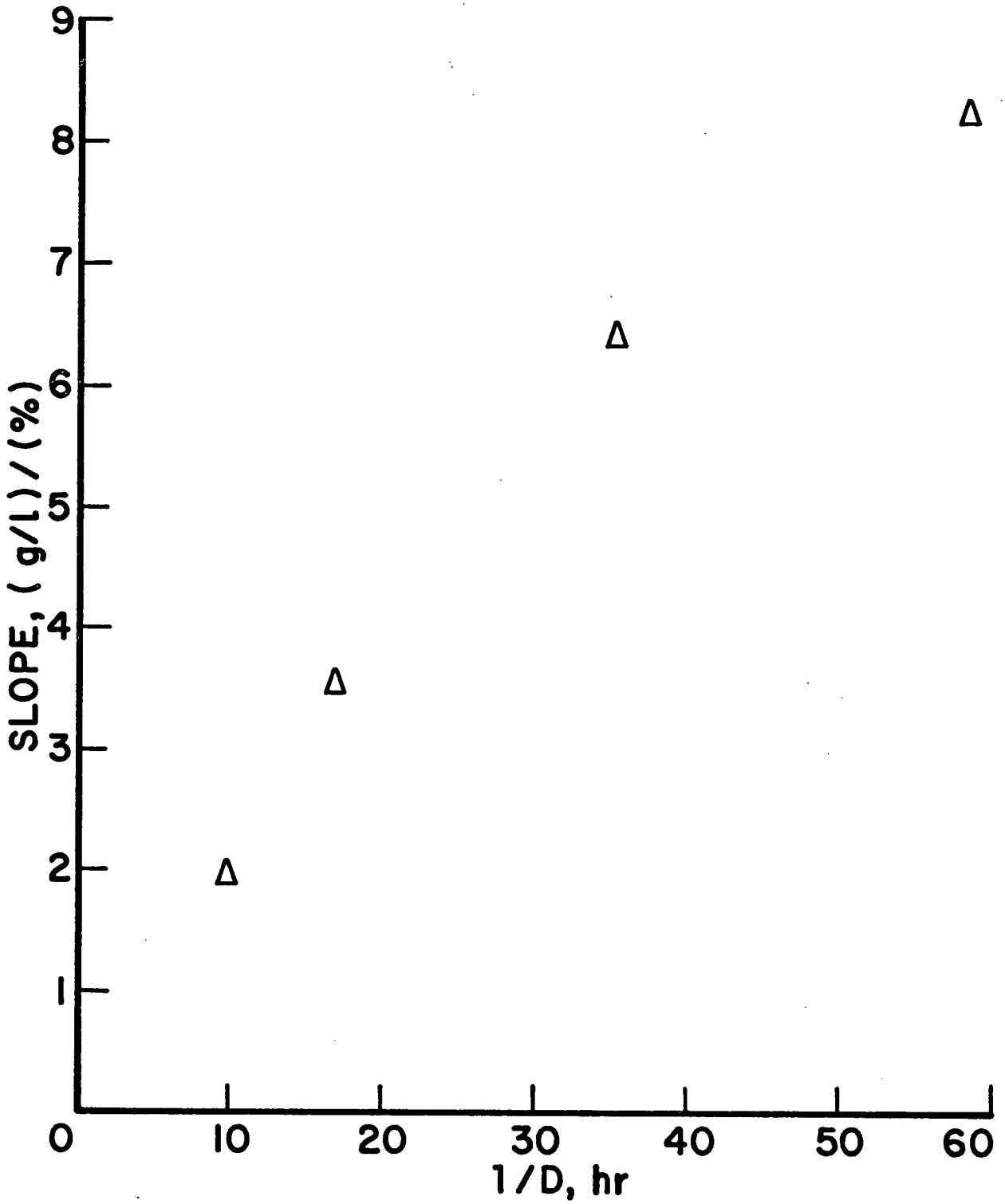

Figure 24

ZINC RELEASE RATE Vs
SURFACE AREA CONCENTRATION
(NOT CORRECTED FOR CHEMICAL LEACHING)

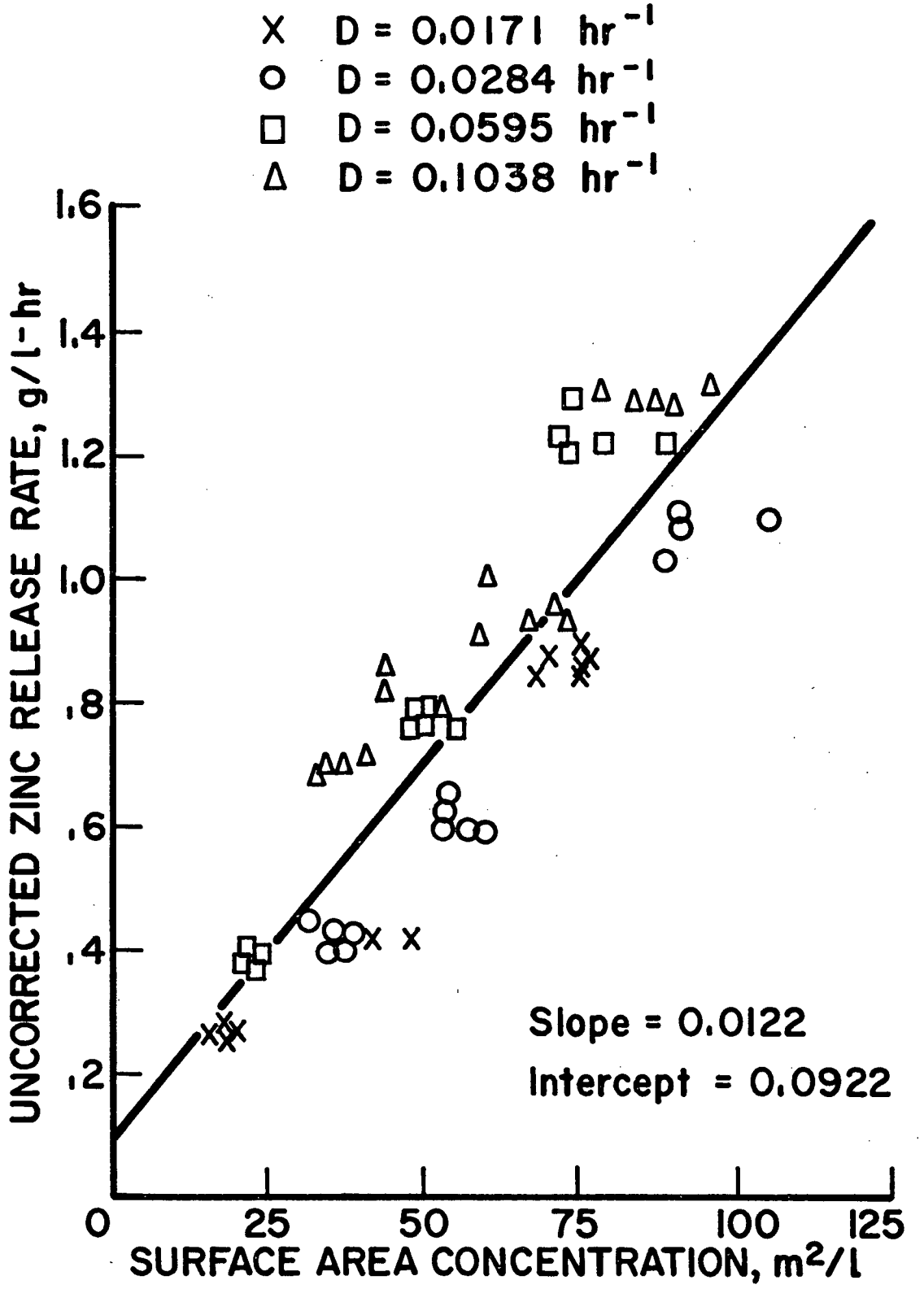

Figure 25

ZINC RELEASE RATE Vs SURFACE AREA CONCENTRATION (CORRECTED FOR CHEMICAL LEACHING)

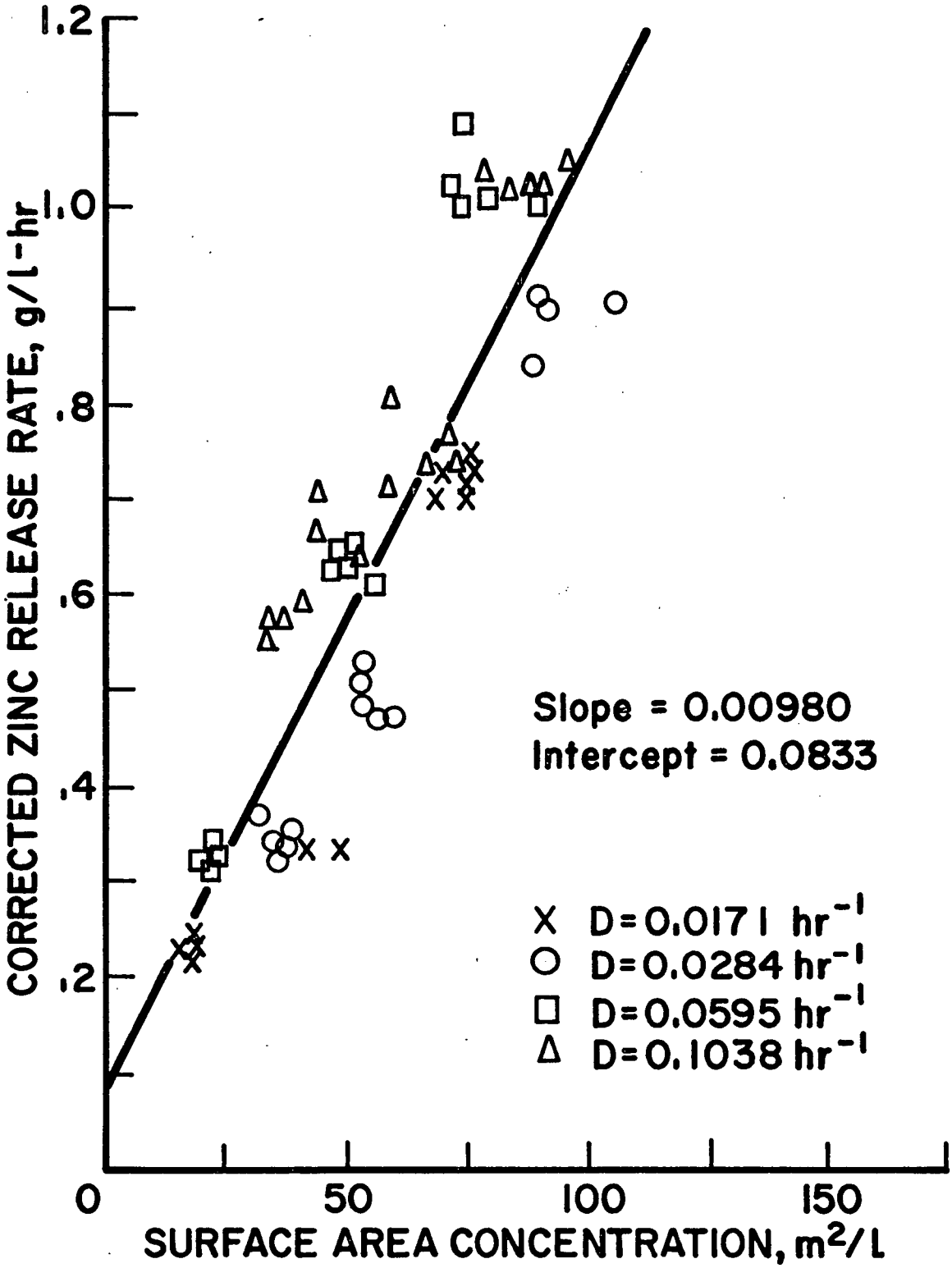

e. Batch Run

The maximum zinc release rate observed in this study was about 1.3 g/l-hr, which agrees well with the value reported for batch leaching of a zinc sulphide concentrate by Bruynesteyn and Duncan (1). Figure 26 presents the leaching curve for a batch run in the apparatus used for the continuous experiments. The slope of the linear portion of the leaching curve gives a rate of 1.2 g/l-hr. Concentrate was fed continuously to this batch experiment, so that the rate was probably limited to this value by mass-transfer of oxygen or carbon dioxide into the slurry. The continuous experiments have thus demonstrated the highest rate that the combination of agitator speed and air flow would permit.

Since the release rate is first order in surface area, there would appear to be no limit to the rate which can be achieved by increasing the surface area. Practical limitations might be the ability to transfer sufficient oxygen or carbon dioxide to the bacteria, or generation of high concentrations of toxic products, e.g. zinc ions.

f. Oxygen Uptake Rates

In order to compare our rates with values of $Q_{O_2}(N)$ which

Figure 26

DISSOLVED ZINC Vs TIME CURVE FOR BATCH LEACHING IN THE STIRRED TANK REACTOR

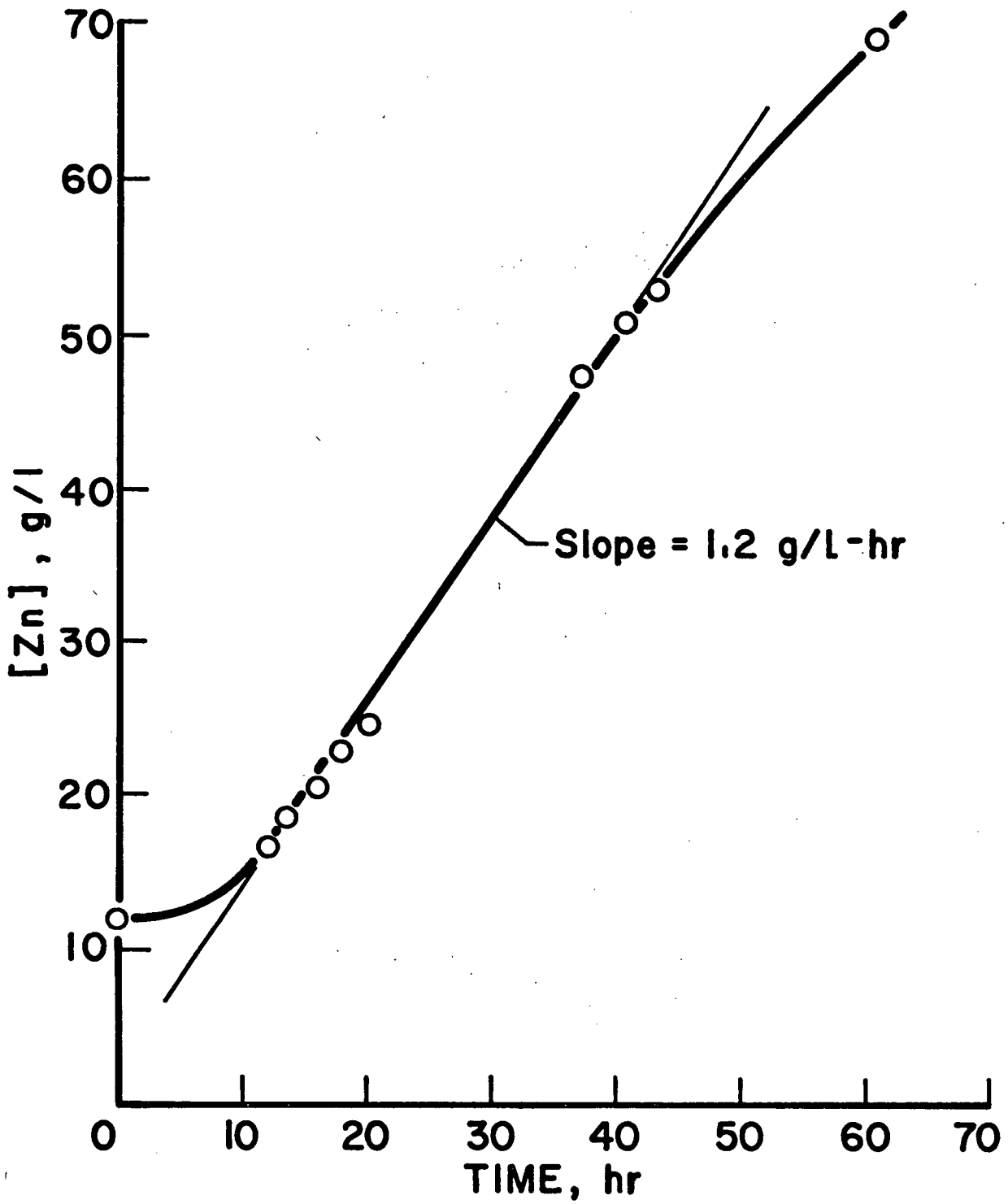

have been reported in the literature, we have calculated such a value from the net ammonium ion yield coefficient and the dilution rate. The net ammonium ion yield coefficient represents the ratio of net ammonium ion concentration to zinc concentration in the tank at any steady-state. If we define a $Q_{Zn}(NH_4^+)$ analogously to $Q_{O_2}(N)$ as the rate of zinc release by a unit amount of net ammonium ion in the tank, then

$$Q_{Zn}(NH_4^+) = \frac{r_Z}{X_N} = \frac{D[Zn]}{X_N} = \frac{D}{Y_N} \tag{68}$$

To convert the zinc release rate to an oxygen uptake rate, we can assume that 2 moles of oxygen are required to release one mole of zinc, and we can correct the net ammonium ion level to an organic nitrogen level by the ratio of the molecular weights. Since the uptake rate is usually expressed volumetrically, we assume that the oxygen is a perfect gas at STP:

$$Q_{O_2}(N) = \frac{(18)(2)(22.4)\ 10^6}{(14)\quad 65.4}\frac{D}{Y_N} = \frac{0.882 \times 10^6\ D}{Y_N}\ \frac{\mu l\ O_2\ (STP)}{mgN - hr} \tag{69}$$

Our highest $Q_{O_2}(N)$ is then

$$Q_{O_2}(N) = \frac{(0.882)(10^6)(.1038)}{12} = 7650\ \frac{\mu l\ O_2\ (STP)}{mgN - hr} \tag{70}$$

which is significantly higher than any value reported previously for this organism growing on a solid substrate.

g. Production of Heat

Whenever the release rate of zinc was greater than about 0.8 g/l-hr, it was necessary to cool the tank in order to control the temperature. The heat being removed under these circumstances was produced by the leaching reaction as shown by the following calculation:

If it is assumed that all the carbon dioxide is fixed as glucose, the reactions taking place in the tank may be approximated by the following coupled reactions:

$$ZnS + 2O_2 \rightarrow ZnSO_4 \qquad \Delta H = -208.4 \text{ kcal/mole} \qquad (71)$$

$$6CO_2 + 6H_2O \rightarrow C_6H_{12}O_6 + 6O_2 \qquad \Delta H = +673.0 \text{ kcal/mole} \qquad (72)$$

A representative value of the yield constant Y_c is 43 milligrams total carbon per gram of zinc released (Figure 28). Therefore release of one mole of zinc results in fixation of

$$\frac{(65.4)(43)}{(72)(1000)} = 0.0391 \text{ moles glucose} \qquad (73)$$

The net change in enthalpy for the two reactions is then

$$-208.4 + (.0391)(673.0) = -182.1 \text{ kcal/mole Zn} \quad (74)$$

which is removed as heat.

4. Yields

The yield constants for all the continuous runs are plotted versus dilution rate in Figures 27 and 28.

There is no clear trend in the data when plotted as a function of dilution rate. If there were a large maintenance energy requirement, the yield constants should be lower at lower dilution rates (51). Our data suggest that the maintenance requirements for this organism were quite low, and it may be concluded that T. ferrooxidans probably does not use energy to maintain low intracellular concentrations of hydrogen and metal ions (33). This conclusion is supported by the observations of Beck (55) and Landesman et al. (53) that endogenous activity was not detectable in Warburg respirometer experiments. However, an investigation covering a wider range of dilution rates might reveal a stronger trend in the values of the yield constants.

The ratio of total carbon to net ammonium ion remained constant at about 3.6 mg total carbon per mg net ammonium ion for the range of dilution rates investigated (Figure 29).

Figure 27

NET AMMONIUM ION YIELD CONSTANT Vs DILUTION RATE

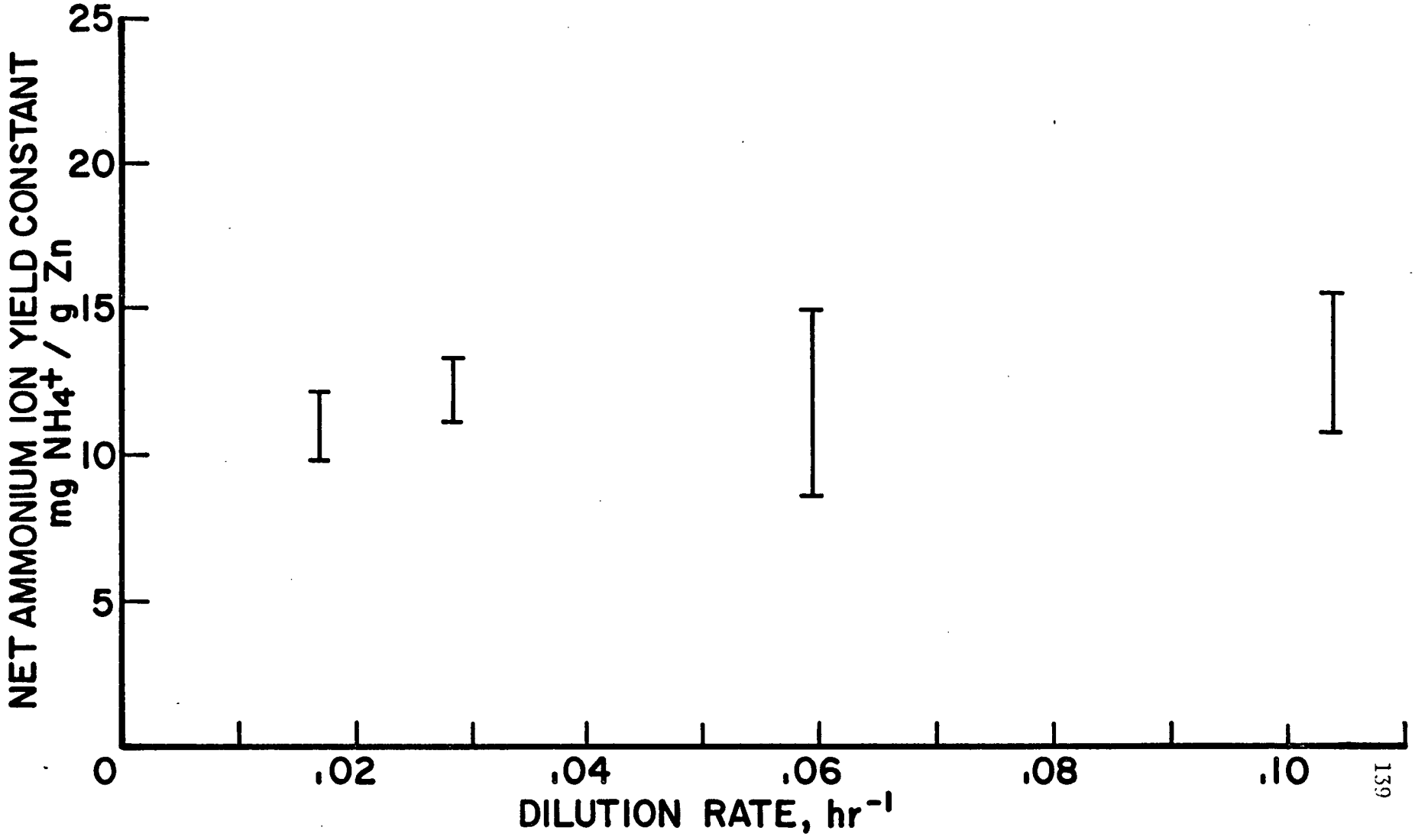

Figure 28

TOTAL CARBON YIELD CONSTANT Vs DILUTION RATE

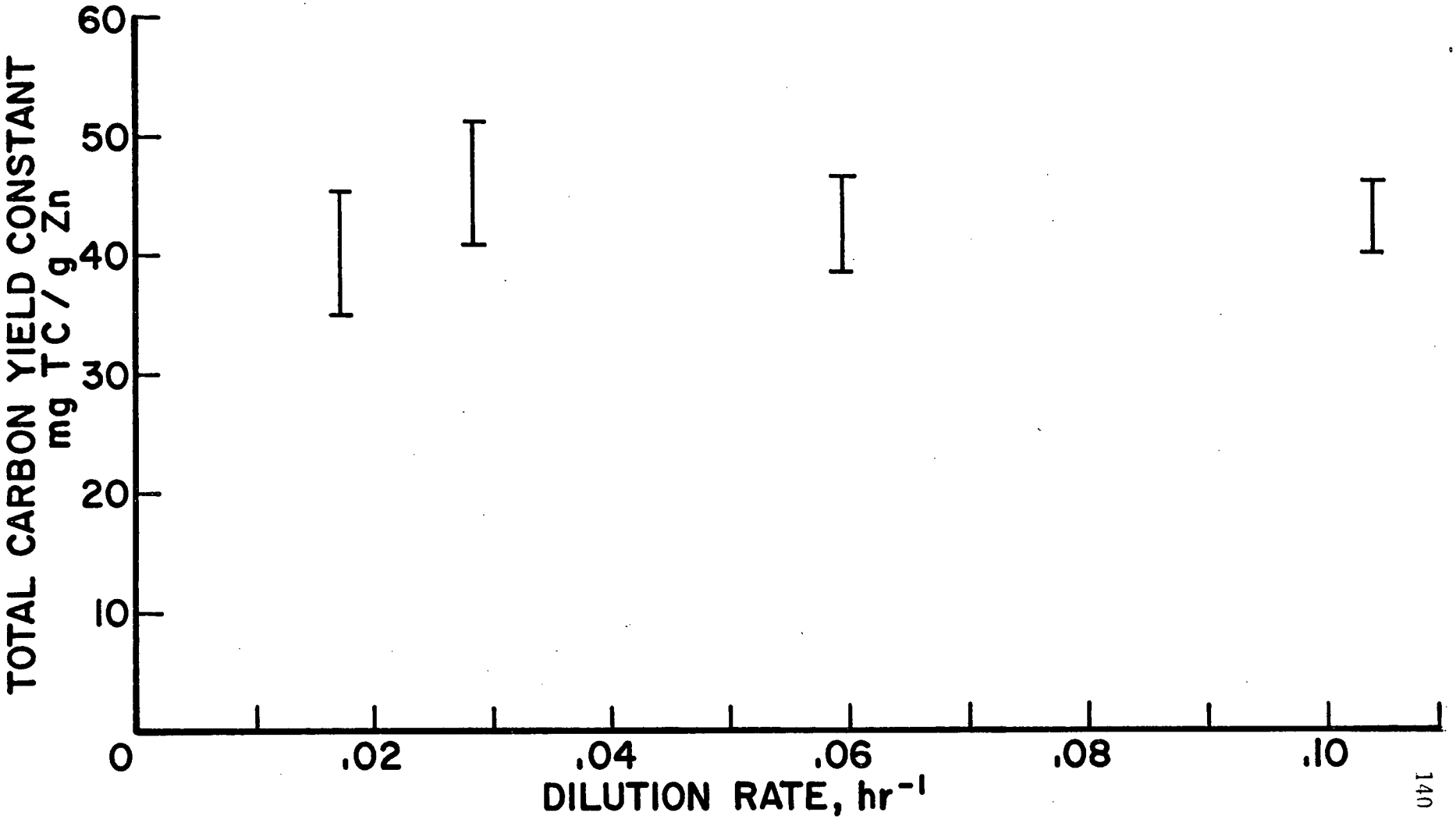

Figure 29

RATIO OF TOTAL CARBON YIELD TO NET AMMONIUM ION YIELD
Vs DILUTION RATE

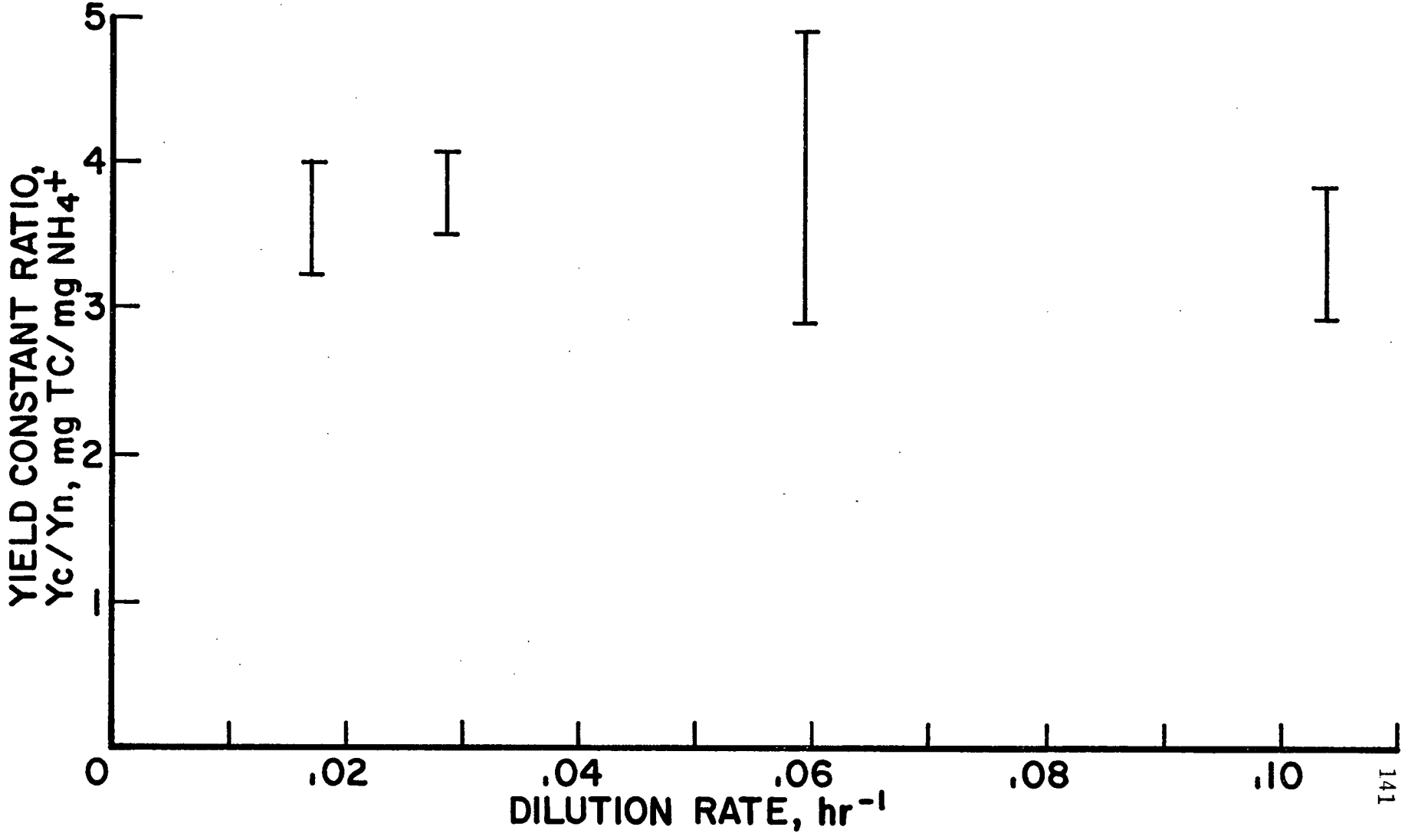

An attempt was made to correlate the total carbon and net ammonium ion measurements with cell numbers. Total carbon, net ammonium ion, and cell numbers were determined on a washed cell suspension prepared from the product from a continuous run. The total carbon was 7240 mg/l, the net ammonium ion was 1904 mg/l, and the concentration of cell numbers was 9.44×10^{13} cells per litre. From these results we may calculate that there should be 0.779×10^{-10} mg TC/cell, and 0.202×10^{-10} mg net ammonium ion/cell. The ratio of TC to net ammonium ion is 3.80 which agrees fairly well with the values measured in the continuous runs (Figure 29). The cell equivalent of net ammonium ion agrees fairly well with the results of Silverman and Lundgren (66) who reported 10^{10} cells to contain 0.191 mg nitrogen.

There is no yield data in the literature for T. ferrooxidans growing on a zinc sulphide substrate. To compare our data with literature values, we should express it in a form which is independent of the substrate used. Two ways of doing this are to convert the data to ratios of carbon dioxide fixed for oxygen consumed and to calculate free energy efficiencies.

The yield constant Y_c may be converted to a carbon dioxide fixation efficiency by assuming that when one mole of zinc was released, two moles of oxygen were consumed (equation 71). Assuming that Y_c is 43 mg TC/g Zn the efficiency can be

calculated to be 11.7 μ moles of CO_2 fixed per 100 μ moles of O_2 taken up. This is larger than the value of 2.1-3.0 reported by Beck (55) for growth on ferrous iron, but less than the value of 22 reported by Beck and Brown (38) for growth on sulphur.

Calculation of the free energy efficiency for the reaction requires a value for the free energy change for the oxidation of zinc sulphide to zinc sulphate in aqueous solution. We shall use -163.9 kcal/mole, the standard free energy change for the reaction at 25°C as evaluated from the free energies of formation of the reactants and products (61). Correction for the effect of the concentrations of the reactants and product was not thought to be warranted in this case since the corrections are not very large and are difficult to evaluate in a system having so many ionic species. For the free energy change for fixation of carbon dioxide as glucose we shall use the value of +118.2 kcal/mole of CO_2 given by Baas-Becking and Parks (59).

Taking Y_C as 43 mg carbon fixed per g of zinc released, the free energy efficiency (FEE) is

$$FEE = \frac{(43)(118.2)(65.4)(100\%)}{(1000)(163.9)(12)} = 16.9\% \qquad (75)$$

This value lies between the values of 3.1% of Temple and Colmer (26) and 30% of Lyalikova (79), and is close to the value of 17.8% which may be calculated from the cell numbers yield coefficient of McDonald and Clark (36). The above three values are all for growth on ferrous iron.

If the net ammonium ion yield constant stayed constant at about 12 mg net ammonium ion/g Zn released, the 820 mg/l ammonium ion in the medium 9K would be exhausted at a dissolved zinc concentration of about 68 g/l. The maximum level obtained by Torma (16) was 120 g/l, so that the yield constant must have been different for his concentrate, or the yield constant may have become smaller as ammonium ion became a limiting substrate. This points to the possibility of increasing the maximum concentrations attainable by addition of ammonium ion to the medium.

5. Percentage Extractions

The percentage extractions for all the runs are summarized in Table XIV. The percentage extraction increases with decreasing dilution rate as expected. The maximum percentage extraction achieved was 71.9% which is insufficient to make this process competitive with the conventional electrolytic zinc process. It will be necessary either to use tanks in series or recycle of unleached residues to bring the percentage

extraction above the maximum batch extraction of 88.6%.

The percentage extractions should be a function of the initial particle size and the dilution rate (17). Therefore any variations within a given dilution rate may be in part attributable to variation in the quality of the grinding from run to run.

An attempt was made in Appendix VI to calculate the percentage extraction from a knowledge of the leaching kinetics, the dilution rate, and the feed particle size distribution. This procedure failed, predicting low by a factor of ten. Possible reasons for this discrepancy are presented in Appendix VI.

Once one knows the percentage extraction at an intermediate dilution rate, one can make simplifying assumptions and predict the percentage extractions at other dilution rates with fair accuracy. The method is included in Appendix VI.

It does not appear to be possible to estimate the time (τ) for complete leaching of a representative concentrate particle from batch data. τ for the concentrate used in these experiments was 65 hours; batch experiments took about 144 hours to go to completion once initiation of growth was obtained. This does not appear to be explainable by the necessity to build up an active population of bacteria in order to achieve the maximum

release rate; the rate reached a maximum soon after initiation of zinc release and the leach curve was linear from that time until the leach was nearly complete. Torma's (16) results were similar.

6. Mass Balance on Zinc

The mass balance results for all the runs are summarized in Table XV. There was a net loss of zinc in every case, ranging from 0.6% to 18.5% of the amount fed into the tank. These losses appear to be attributable to concentrate caking on the sides and top of the reactor above the surface of the leach slurry. Not all the concentrate fed into the tank found its way into the slurry; some stuck to the moist sides of the tank or blew back out the top with the escaping sparging air. The measured feed rates did not take this into account.

This conclusion was tested by attempting to recover the amount of solids which were collected on the tank sides and top after the run for 14-06-72 --- 17-06-72. It was not possible to collect all this material, but 320 g were recovered containing 189 g zinc. This accounts for a substantial portion of the loss for this run. During the run of 28-07-72 --- 29-07-72 care was taken to knock as much material as possible off the sides of the tank into the slurry. This procedure was reflected in sharply reduced losses for the run.

Table XV. Summary Of Mass Balances On Zinc.

Dates	Zinc Input (g)	Zinc Cutput (g)	Zinc Loss (g)	% Loss
22-11-71 ---- 27-11-71	5353	5005	348	6.5
15-12-71 ---- 17-12-71	985.0	850.4	34.6	13.6
24-02-72 ---- 28-02-72	2356	2101	255	10.8
11-04-72 ---- 14-04-72	3538	3298	240	6.8
4-05-72 ---- 9-05-72	2237	2001	235	10.5
16-05-72 ---- 18-05-72	2815	2490	325	11.5
14-06-72 ---- 17-06-72	1470	1197	273	18.5
21-06-72 ---- 23-06-72	933.2	863.3	69.9	7.5
12-07-72 ---- 13-07-72	1465	1377	87	6.0
16-07-72 ---- 19-07-72	1405	1364	41	2.9
21-07-72 ---- 23-07-72	2519	2367	152	6.0
28-07-72 ---- 29-07-72	2333	2318	15	0.6
10-09-72 ---- 12-09-72	2090	1910	180	8.6
17-12-72 ---- 21-12-72	574.7	519.4	55.3	9.6

7. Dissolved Iron Concentration and pH

The dissolved iron concentration and pH data are summarized in Tables XXX - XXXIII in Appendix IV. The iron concentration remained quite low for all the runs, never exceeding 1.8 g/l. The level correlated quite well with the zinc concentration levels in the tank, occasionally modified by the effect of pH (e.g. 15-12-71 --- 17-12-71). The iron level in solution at any time should be determined by the relative rates of release from the mineral by leaching and of precipitation as hydrated ferric compounds. The iron release rate, like the zinc release rate, is determined by the concentration of surface present; the precipitation rate will be a function of the ferric iron concentration and pH.

The much higher ratio of iron to zinc in solution for the sterile run (Table XXI) is due to the fact that the iron was in the ferrous form and so did not precipitate.

8. Acid and Antifoam Requirements

The acid and antifoam requirements for the nutrient medium are summarized in Table XVI. The addition rates of both of these quantities were determined by trial and error in order to achieve the desired process results.

Table XVI. Acid And Antifoam Requirements For Iron-Free 9K Medium.

Date	Solid Feed Rate	Product Rate	Sulphuric Acid	Antifoam
	(g/hr)	(l/hr)	(m/20l)	(drops/20l)
22-11-71 ---- 27-11-71	45.6	0.311	50.	0.
15-12-71 ---- 17-12-71	26.0	0.300	0.	0.
24-02-72 ---- 28-02-72	42.9	0.518	15.	10.
11-04-72 ---- 14-04-72	65.2	0.494	25.	20.
4-05-72 ---- 9-05-72	27.8	0.535	10.	20.
16-05-72 ---- 18-05-72	105.5	1.098	35.	20.
14-06-72 ---- 17-06-72	36.5	1.075	35.	20.
21-06-72 ---- 23-06-72	70.3	1.074	35.	20.
12-07-72 ---- 13-07-72	72.9	1.894	35.	20.
16-07-72 ---- 19-07-72	82.5	1.885	35.	20.
21-07-72 ---- 23-07-72	102.4	1.893	40.	20.
28-07-72 ---- 29-07-72	135.1	1.879	45.	25.
10-09-72 ---- 12-09-72	73.6	1.082	100.	0.
17-12-72 ---- 21-12-72	14.0	0.313	20.	0.

In general, the acid requirement increased with dilution rate and with feed pulp density. The increase in requirement with feed pulp density is due to the acid consuming nature of the concentrate. This property of the concentrate was noted in the preliminary batch experiments, where it was necessary to keep taking the pH down to the optimum level until leaching began. Thereafter, the pH would stay down or even decrease as precipitation of ferric iron generated acid in the medium.

At the higher dilution rates and lower percentage extractions the ratio of acid consumption by concentrate to acid generation by precipitating ferric iron should increase due to the higher ratio of pulp density to ferric iron concentration. This explains why the acid requirement increased with increased dilution rate.

The high acid requirement for the sterile run is due to the lack of acid generation by precipitating ferric compounds in this case.

Antifoam (Dow Polyglycol 15-200) had to be added to keep the slurry from foaming out of the tank at higher dilution rates. The foaming was evidently due to bacterial activity as there was no antifoam requirement for the sterile run which was performed under conditions that otherwise would have required

addition of 20 drops of antifoam to each 20 l of nutrient medium.

9. Concentration of Surface Area in Feed

The feed surface area concentrations and the average product surface area concentrations are summarized in Table XVII. The surface concentration was reduced by about 80% by passage through the tank. Elution of fines as the feed fell into the tank may have been a contributing factor, although the dust accumulation in the laboratory was minimal. The remainder is due to reduction in both pulp density and specific surface area of the concentrate as it was leached.

10. Industrial Applications

Torma (16) has shown that the solutions produced by bacterial leaching of a zinc sulphide concentrate are suitable for zinc recovery by electrowinning. In this study, the technical feasibility of a continuous bacterial leaching process has been demonstrated. Stable steady-states with high leaching rates have been obtained. The data show that there should be no upper limit placed on leach rates by surface area. It should always be possible to provide enough surface area by grinding or increasing the pulp density so that some other factor will limit the rate.

Table XVII. Concentration Of Surface In Feed And Product.

Dates	Dilution Rate	Feed s	Product s
	(hr^{-1})	(m^2/l)	(m^2/l)
22-11-71 ---- 27-11-71	0.0171	437.9	73.3
15-12-71 ---- 17-12-71	0.0167	276.6	46.0
24-02-72 ---- 28-02-72	0.0284	280.4	55.2
11-04-72 ---- 14-04-72	0.0273	406.9	94.0
4-05-72 ---- 9-05-72	0.0294	150.1	35.7
16-05-72 ---- 18-05-72	0.0603	289.0	77.3
14-06-72 ---- 17-06-72	0.0595	89.5	21.8
21-06-72 ---- 23-06-72	0.0588	182.2	50.7
12-07-72 ---- 13-07-72	0.1040	102.3	34.0
16-07-72 ---- 19-07-72	0.1034	118.2	46.6
21-07-72 ---- 23-07-72	0.1040	151.7	65.8
28-07-72 ---- 29-07-72	0.1038	237.3	87.2
10-09-72 ---- 12-09-72	0.0588	188.0	107.7
17-12-72 ---- 21-12-72	0.0171	130.4	17.7

High percentage extractions and high zinc concentrations have not been obtained due to the residence time distribution in the reactor type chosen. To achieve maximum extractions and zinc concentrations, the residence time distribution of a plug flow reactor is necessary. Practically, it would be difficult to maintain plug flow of the three phase mixture for the high residence times required. The desired residence time distribution can be approached by connecting a number of stirred tanks in series. In the limit of an infinite series of stirred tanks, the plug flow residence time distribution would be achieved. Levenspiel (17) shows that the total residence time requirement decreases substantially for a given percentage extraction when two stirred tanks are connected in series.

An alternative would be to separate the leachable solids by flotation or density methods after one stage of leaching in a stirred tank and recycle them through the tank. In this way sufficient residence time in the tank would be provided to achieve the total recovery of all the leachable zinc in the concentrate. Disadvantages of this method would be the cost of making the separation and the losses of leachable mineral in the separation step.

The data which have been taken in this work are representative of reactor performance when the rate of leaching

is limited by the amount of mineral surface area available. Since the major process expense is expected to be the aeration and agitation required to transfer oxygen and carbon dioxide into the slurry (78), it is unlikely that all the tanks in a series would be operated at a surface limiting condition. Sufficient surface would be provided to support a reaction rate capable of using all the oxygen and carbon dioxide that could be transferred. Surface would only be permitted to become limiting at the end of the series, in order to bring the total extraction up to the maximum which could be achieved. Since the concentration of leachable solids leaving the last reactor should be quite low, the leaching rate in this last reactor will be limited by mineral surface area, and the aeration capacity of the earlier reactors will not be needed. The data taken in this work should permit determination of the stage in a series of reactors where the surface area becomes limiting.

This work has not been able to demonstrate the existence of a critical dilution rate. The bacteria used in these studies should have a maximum specific growth rate, and so in the absence of wall growth or non-ideal mixing there should be a critical dilution rate above which the bacteria will wash out of the reactor. Further studies should be undertaken to determine what this is, so that design studies can take into account the full range of potential dilution rates. Although the total residence time requirement will be quite high to ensure high

extractions and dissolved zinc concentrations, this residence time may be divided up among a series of stirred tanks, and so the dilution rate in any given tank may be relatively high. In a series of equal sized stirred tanks, if washout occurs in the first tank, it will progress through the whole series, with consequent process failure. Thus, it may prove necessary to recycle a portion of the leach liquor to ensure a supply of bacteria for the whole reactor train.

Consideration of the net ammonium ion yield constant determined in this work shows that it will probably be necessary to increase the amount of ammonium ion in the nutrient medium. The amount to add will be determined by the zinc concentration required in the feed to the electrowinning plant.

The concentrate tested in this work will require additional grinding in order to achieve extractions in excess of 90%. Foaming may be a problem, but it may be controlled by addition of Dow Polyglycol 15-200 to the leach slurry. This compound does not appear to be inhibitory to the bacteria at levels necessary for successful foam control. There will be a requirement for sulphuric acid addition to control pH; this may be supplied by recycling spent electrowinning solution. Recycle of this solution will minimize losses of dissolved zinc and the nutrients in the medium.

VII. SUMMARY AND CONCLUSIONS

1. Continuous microbiological leaching of the test concentrate is technically feasible. Stable steady-states may be obtained in a continuous stirred tank reactor.
2. The specific growth rate of the bacteria was not a unique function of the substrate concentration or the surface area concentration. Thus conventional continuous culture theory does not apply to this system. There was a range of steady-state substrate concentrations attainable for a given dilution rate. This was a consequence of using a solid substrate.
3. The bacterial concentration did not limit the leaching rates under the conditions of these experiments. The leaching rates and bacterial growth rates were thus first order in surface area.
4. The model which was derived suggested that bacterial concentration should limit leaching rates at higher dilution rates. There should be a maximum dilution rate beyond which washout should occur.
5. The maximum specific growth rate was not approached in these experiments. The highest specific growth rate obtained ($0.1038\ hr^{-1}$) is the highest rate which has been observed for T. ferrooxidans growing on solid substrates.
6. The maximum oxygen uptake coeffecient ($Q_{O_2}(N)$) calculated from these experiments was 7650, about twice as great as

the highest reported for growth of this organism on a solid substrate.

7. Total carbon and net ammonium ion concentrations correlated with each other and were satisfactory measures of the biomass concentration.

8. The bacterial yields remained constant for the range of dilution rates investigated, indicating a low maintenance energy requirement for this organism.

9. The yield coefficient value of 12 mg net ammonium ion per g zinc released suggests that addition of ammonium ion above the levels present in the medium 9K of Silverman and Lundgren (66) should be beneficial when dissolved zinc concentrations exceed 68 g/l.

10. The bacteria fixed about 43 mg carbon per g zinc released.

11. When the percentage extraction for one dilution rate was known, it was possible to use a calculation method given by Levenspiel (17) to predict the results at other dilution rates.

12. It was necessary to grind the concentrate to obtain the maximum batch zinc extraction of 88.6%.

13. The contribution of chemical leaching to the total amount of zinc leached was estimated to be 20 - 25 %.

14. Heat produced at higher release rates necessitated cooling the reactor.

15. At higher dilution rates when bacteria were present, foaming was a problem. Addition of Dow Polyglycol 15-200

to the nutrient medium controlled the foam. When bacterial growth was suppressed by withholding ammonium ion, foaming was not a problem.

16. It was necessary to add sulphuric acid to the nutrient medium to maintain the pH in the optimum range for the bacteria. The requirement for acid increased with increasing dilution rate and increasing pulp density.

17. The best process configuration to achieve high extractions and zinc concentrations in continuous processing will be stirred tanks in series, with or without solids recycle.

VIII. REFERENCES

1. Bruynesteyn, A., and Duncan, D. W., Can. Met. Quart. 10, 57-63 (1971)

2. Tsuchiya, H. M., Fredrickson, A. G., and Aris, R., Advan. Chem. Eng. 6, 125-206 (1966)

3. Fredrickson, A. G., and Tsuchiya, H. M., A. I. Ch. E. J. 9, 459-468 (1963)

4. Eakman, J. M., Fredrickson, A. G., and Tsuchiya, H. M., Chem. Eng. Progr. Symp. Ser. 62, 37-49 (1966)

5. M'Kendrick, A. G., and Pai, M. K., Proc. Roy. Soc. Edinburgh 31, 649-655 (1910-1911)

6. Monod, J., "Recherches Sur la Croissance des Cultures Bacteriennes", Masson Et Cie., Paris (1942), cited in reference 2

7. Monod, J., Ann. Rev. Microbiol. 3, 371-394 (1949)

8. Herbert, D., Elsworth, R., and Telling, R. C., J. Gen. Microbiol. 14, 601-622 (1956)

9. Dabes, J. N., Finn, R. K., and Wilke, C. R., Paper Presented at the 21st C. S. Ch. E. Conference, Montreal, October, 1971

10. Sinclair, C. G., Topiwala, H. H., and Brown, D. E., Chemical Engineer 249, 198-201 (1971)

11. Ware, G. C., J. Theoret. Biol. 17, 91-107 (1967)

12. Andrews, J. F., Biotechnol. Bioeng. 9, 707-723 (1968)

13. Ramkrishna, D., Fredrickson, A. G., and Tsuchiya, H. M., Biotechnol. Bioeng. 9, 129-170 (1967)

14. Luedeking, R., Fermentation Process Kinetics, in "Biological and Biochemical Engineering Science", N. Blakebrough, ed., Vol. 1, pp. 181-243, Academic Press, London, 1967

15. Luedeking, R., and Piret, E. L., J. Biochem. Microbiol. Technol. Eng. 1, 431-459 (1959)

16. Torma, A. E., Ph. D. Thesis, University of B. C. (1970)

17. Levenspiel, O., "Chemical Reaction Engineering", 2nd ed., pp. 349-408, Wiley, 1972

18. Williams, F. M., J. Theoret. Biol. 15, 190-207 (1967)

19. Ramkrishna, D., Fredrickson, A. G., and Tsuchiya, H. M., J. Gen. Appl. Microbiol. 12, 311-327 (1966)

20. Swanson, C. H., Aris, R., Fredrickson, A. G., and Tsuchiya, H. M., J. Theoret. Biol. 12, 228-250 (1966)

21. Chakravarty, M., Amin, P. M., Singh, H. D., Baruah, J. N., and Iyengar, M. S., Biotechnol. Bioeng. 14, 61-73 (1972)

22. Erickson, L. E., and Humphrey, A. E., Biotechnol. Bioeng. 11, 467-487 (1969)

23. Erickson, L. E., Fan, L. T., Shah, P. S., and Chen, M. S. K., Biotechnol. Bioeng. 12, 713-746 (1970)

24. Colmer, A. R., and Hinkle, M. E., Science 106, 253-256 (1947)

25. Colmer, A. R., Temple, K. L., and Hinkle, M. E., J. Bacteriol. 59, 317-328 (1950)

26. Temple, K. L., and Colmer, A. R., J. Bacteriol. 62, 605-611 (1951)

27. Kinsel, N. A., J. Bacteriol. 80, 628-632 (1968)

28. Leathen, W. W., Kinsel, N. A., and Braley, S. A., J. Bacteriol. 72, 700-704 (1956)

29. Unz, R. F., and Lundgren, D. G., Soil Sci. 92, 302-313 (1961)

30. Hutchinson, M., Johnstone, K. I., and White, D., J. Gen. Microbiol. 44, 373-381 (1966)

31. Moss, F. J., and Andersen, J. E., Proc. Australasian Inst. Mining Met. 225, 15-25 (1968)

32. Ehrlich, H. L., in "Biogeochemistry of Sulphur Isotopes", H. L. Jensen, ed., Proceedings of a National Science Foundation Symposium held at Yale University, New Haven, Connecticut, April 12-14, 1962, pp. 153-168

33. Tuovinen, O. H., and Kelly, D. P., Z. Allg. Mikrobiol. 12, 311-346 (1972)

34. Duncan, D. W., Landesman, J., and Walden, C. C., Can. J. Microbiol. 13, 397-403 (1967)

35. Ehrlich, H. L., and Fox, S. I., Biotechnol. Bioeng. 9, 471-485 (1967)

36. MacDonald, D. G., and Clark, R. H., Can. J. Chem. Eng. 48, 669-676 (1970)

37. Bryner, L. C., Beck, J. V., Davis, D. B., and Wilson, D. G., Ind. Eng. Chem. 46, 2587-2592 (1954)

38. Beck, J. V., and Brown, D. G., J. Bacteriol. 96, 1433-1434 (1968)

39. Duncan, D. W., and Walden, C. C., Develop. Ind. Microbiol. 13, 66-75 (1972)

40. McGoran, C. J. M., Duncan, D. W., and Walden, C. C., Can. J. Microbiol. 15, 135-138 (1969)

41. Duncan, D. W., Personal Communication.

42. Wood, J., and Haigh, C., World Mining 25(10), 34-38 (1972)

43. Duncan, D. W., Trussell, P. C., and Walden, C. C., Appl. Microbiol. 12, 122-126 (1964)

44. Jones, G. E., and Benson, A. A., J. Bacteriol. 89, 260-261 (1965)

45. Agate, A. D., Korczynski, M. S., and Lundgren, D. G., Can. J. Microbiol. 15, 259-264 (1969)

46. Schaeffer, W. I., Holbert, P. E., and Umbreit, W. W., J. Bacteriol. 85, 137-140 (1963)

47. Razzell, W. E., and Trussell, P. C., Appl. Microbiol. 11, 105-110 (1963)

48. Razzell, W. E., and Trussell, P. C., J. Bacteriol. 85, 595-603 (1963)

49. Bryner, L. C., and Anderson, R., Ind. Eng. Chem. 49, 1721-1724 (1957)

50. Trudinger, P. A., Rev. Pure Appl. Chem. 17, 1-24 (1967)

51. Pirt, S. J., Proc. Roy. Soc. London , Ser. B 163, 224-231 (1965)

52. Lacey, D. T., and Lawson, F., Biotechnol. Bioeng. 12, 29-50 (1970)

53. Landesman, J., Duncan, D. W., and Walden, C. C., Can. J. Microbiol. 12, 25-33 (1966)

54. Landesman, J., Duncan, D. W., and Walden, C. C., Can. J. Microbiol. 12, 957-964 (1966)

55. Beck, J. V., J. Bacteriol. 79, 502-509 (1960)

56. Nielsen, A. M., and Beck, J. V., Science 175, 1124-1126 (1972)

57. Silverman, M. P., and Lundgren, D. G., J. Bacteriol. 78, 326-331 (1959)

58. Tuovinen, O. H., Niemela, S. I., and Gyllenberg, H. G., Biotechnol. Bioeng. 13, 517-527 (1971)

59. Baas-Becking, L. G. M., and Parks, G. S., Physiol. Rev. 7, 85-106 (1927)

60. Lees, H., Kwok, S. C., and Suzuki, I., Can. J. Microbiol. 15, 43-46 (1969)

61. Latimer, W. M., "The Oxidation States of the Elements and their Potentials in Aqueous Solutions", Prentice-Hall, New York, 1938

62. Bichowsky, F. R., and Rossini, F. D., "The Thermochemistry of the Chemical Substances", p. 89, Reinhold, New York, 1936

63. Torma, A. E., Walden, C. C., and Branion, R. M. R., Biotechnol. Bioeng. 12, 501-517 (1970)

64. Torma, A. E., Walden, C. C., Duncan, D. W., and Branion, R. M. R., Biotechnol. Bioeng. 14, 777-786 (1972)

65. Duncan, D. W., and Bruynesteyn, A., Can. Mining Met. Bull. 64, 32-36 (1971)

66. Silverman, M. P., and Lundgren, D. G., J. Bacteriol. 77, 642-647 (1959)

67. Edwards, V. H., and Wilke, C. R., Biotechnol. Bioeng. 10, 205-232 (1968)

68. Herbert, D., in "Continuous Culture of Micro-Organisms", S. C. I. Monograph No. 12, pp. 21-53, Society of the Chemical Industry, London, 1961

69. Grieves, R. B., and Kao, R., Biotechnol. Bioeng. 10, 497-510 (1968)

70. Atkinson, B., and Dacud, I. S., Trans. Inst. Chem. Engrs. (London) 46, T19-T23 (1968)

71. Atkinson, B., and Davies, I. J., Trans. Inst. Chem. Engrs. (London) 50, 208-216 (1972)

72. Brunauer, S., Emmett, P. H., and Teller, E., J. Amer. Chem. Soc. 60, 309-319 (1938)

73. Orr, R., Ph. D. Thesis, University of B. C. (1969)

74. Burke, K. E., Anal. Chem. 34, 1747-1751 (1962)

75. Li, J. C. R., "Statistical Inference", p. 374, Edwards Bros., Ann Arbor, 1964

76. Stober, W., Fink, A., and Bohn, E., J. Colloid Interface Sci. 26, 62-69 (1968)

77. Hempfling, W. P., and Vishniac, W., J. Bacteriol. 93, 874-878 (1968)

78. McElroy, R. O., Personal Communication.

79. Lyalikova, N. N., Mikrobiolcgia 27, 556-559 (1958)

APPENDIX I

Calculation Cf Percentage Zinc Extracted In Batch Shake Flask Experiments (Table VI)

Appendix I. Calculation Of Percentage Zinc Extracted In Batch Shake Flask Experiments (Table VI).

Estimated Ore Composition Is 55.69 % Zinc.

5. g Ore Contains (.5569) (5.) = 2.785 g Zinc

Total Zinc Extracted = Dissolved Zinc Recovered At The End Of The Leach
+ Dissolved Zinc Removed By Sampling The Flasks (1 ml Samples)
- Dissolved Zinc Introduced With The Inoculum.

= 1.2400 + 0.0016 + 0.0033 + 0.0036 + 0.0044 + 0.0057 + 0.0070 + 0.0112 + 0.0125 + 0.0161 + 0.0151 + 0.0141 - 0.042

= 1.293 g Zinc

Percentage Zinc Extracted = $\frac{(1.293)(100\%)}{(2.785)}$ = 46.4 %

APPENDIX II

Regression Analysis Of Tank And Product Dissolved Zinc Concentrations

Appendix II. Regression Analysis Of Tank And Product Dissolved Zinc Concentrations.

The data for the regression analysis are given in Table XVIII.

Sum Of X = 251.79, Sum Of Y = 249.68, Sum Of XY = 2483.5,
Sum Of Squares X = 2500.3, Sum Of Squares Y = 2468.1,
(Sums Of Squares Uncorrected For The Mean)

Analysis Of Variance

Source	Sum of Squares	d.f.	Mean Square	F
Regression (b_0)	2149.7	1		
Regression ($b_1 \mid b_0$)	317.1	1	317.12	
Residual	1.4	27	0.0506	6272.
Total	2468.1	29		

Hypothesis: Slope = 1.0

$$t = \frac{b_1 - 1.0}{\sqrt{\frac{s^2}{SS_X}}}$$

where SS_X = [Sum Of Squares X] - [Sum Of X]^2/n

$$t = \frac{1.0024 - 1.00}{\sqrt{\frac{0.0506}{2500.3 - [251.70]^2/29}}}$$

$$= 0.190$$

$$t(.05,27) = 1.703$$

The slope is not significantly different from 1.0 at the 90% level.

Hypothesis: Intercept = 0.0

Table XVIII. Regression Analysis Of Tank And Product Dissolved Zinc Concentrations.

Date	Tank Concentration	Product Concentration	Fitted Product Concentration
	(g/l)	(g/l)	(g/l)
12-09-72 2	3.77	3.74	3.69
12-09-72 1	3.78	3.75	3.70
11-09-72 2	3.78	3.70	3.70
11-09-72 1	3.70	3.47	3.62
10-09-72 1	3.35	3.26	3.27
29-07-72 2	12.68	12.35	12.62
29-07-72 1	12.58	12.97	12.52
28-07-72 3	12.41	12.66	12.35
28-07-72 2	12.40	12.66	12.34
28-07-72 1	12.36	12.30	12.30
23-07-72 2	8.98	9.13	8.91
23-07-72 1	8.97	8.86	8.90
22-07-72 2	9.24	8.99	9.17
22-07-72 1	9.62	9.52	9.55
21-07-72 1	8.74	8.90	8.67
19-07-72 1	7.61	7.78	7.54
18-07-72 1	6.80	6.55	6.73
17-07-72 2	7.70	7.90	7.63
17-07-72 1	7.91	7.75	7.84
16-07-72 1	8.31	7.92	8.24
13-07-72 2	6.50	6.38	6.43
13-07-72 1	6.68	6.68	6.61
12-07-72 3	6.87	6.72	6.80
12-07-72 2	6.68	6.52	6.61
12-07-72 1	6.65	6.54	6.58
24-06-72 1	14.22	13.89	14.16
23-06-72 1	13.36	13.08	13.30
22-06-72 2	12.96	13.17	12.90
22-06-72 1	13.06	12.51	13.00

$$t = \frac{b_0}{\sqrt{\left(\frac{[\text{Sum Of X}]^2}{nSS_x}\right) s^2}}$$

Since the intercept cannot be negative (implies a negative concentration in the product sample) this should be a one-tailed test, and only positive values of t should be significant. The calculated b_0 is negative, so t cannot be significant in a one-tailed test. We cannot reject the hypotheses that

$$b_1 = 1.0$$
$$b_0 = 0.0$$

at the 90% significance level.

APPENDIX III

Sterile Run Data

Table XIX. Bacterial Growth Rates For Continuous Leaching At Dilution Rate = 0.0588 Hr^{-1}. (Sterile Run)

Date	Net NH_4^+	Net NH_4^+ Rate	Total Carbon	Total Carbon Rate
	(mg/l)	(mg/l-hr)	(mg/l)	(mg/l-hr)
11-09-72 1	5	0.294	47	2.76
11-09-72 2	4	0.235	55	3.23
12-09-72 1	5	0.294	33	1.94
12-09-72 2	4	0.235	45	2.64

Table XX. Yield Constants For Continuous Leaching At Dilution Rate = 0.0588 Hr^{-1}. (Sterile Run)

Date	Net NH_4^+ Yield	Total Carbon Yield	Ratio
	$(\frac{mg\ NH_4^+}{g\ Zn})$	$(\frac{mg\ TC}{g\ Zn})$	$(\frac{mg\ TC}{mg\ NH_4^+})$
11-09-72 1	1.35	12.7	9.40
11-09-72 2	1.06	14.5	13.76
12-09-72 1	1.32	8.7	6.60
12-09-72 2	1.06	11.9	11.26

Table XXI. Results For Continuous Leaching At Dilution Rate = 0.0588 Hr^{-1}
(Sterile Run)

Date	Pulp Density	Specific Surface Area	s	pH	[Fe]	[Zn]	r_Z	r_Z/s
	(%)	(m^2/g)	(m^2/l)		(g/l)	(g/l)	(g/l-hr)	(g/hr-m^2)
11-09-72 1	5.3760	2.0817	111.91	2.05	1.052	3.70	0.218	0.0019
11-09-72 2	5.2548	2.2425	117.84	2.00	1.121	3.79	0.223	0.0019
12-09-72 1	5.1958	1.8106	94.08	2.10	1.159	3.79	0.223	0.0024
12-09-72 2	5.1816	2.0637	106.93	2.00	1.164	3.77	0.222	0.0021

APPENDIX IV

Ccntinuous Leaching Data

Table XXII. Bacterial Growth Rates For Continuous Leaching At Dilution Rate = 0.0171 Hr^{-1}.

Date	Net NH_4^+	Net NH_4^+ Rate	Total Carbon	Total Carbon Rate
	(mg/l)	(mg/l-hr)	(mg/l)	(mg/l-hr)
22-11-71	440	7.53	1611	27.59
23-11-71	434	7.43	1681	28.79
24-11-71	458	7.84	1601	27.42
25-11-71	---	----	1611	27.60
26-11-71	434	7.43	1601	27.42
27-11-71	451	7.72	1609	27.56
15-12-71	242	4.02	878	14.61
16-12-71	235	3.91	894	14.88
17-12-71	243	4.04	884	14.71
17-12-72	150	2.56	598	10.21
18-12-72	133	2.27	511	8.73
19-12-72	133	2.27	476	8.13
20-12-72	135	2.31	456	7.79
21-12-72	137	2.34	443	7.57

Table XXIII. Bacterial Growth Rates For Continuous Leaching At Dilution Rate = 0.0284 Hr^{-1}.

Date	Net NH_4^+	Net NH_4^+ Rate	Total Carbon	Total Carbon Rate
	(mg/l)	(mg/l-hr)	(mg/l)	(mg/l-hr)
24-02-72	222	6.30	902	25.60
25-02-72	221	6.27	800	22.71
26-02-72	218	6.18	812	23.05
27-02-72	221	6.27	793	22.51
28-02-72	216	6.13	849	24.10
11-04-72	406	11.06	1588	43.28
12-04-72	408	11.12	1532	41.76
13-04-72	413	11.25	1472	40.12
14-04-72	414	11.28	1550	42.25
4-05-72	147	4.32	514	15.13
5-05-72	136	4.00	502	14.77
6-05-72	134	3.94	496	14.60
7-05-72	131	3.85	490	14.42
8-05-72	149	4.38	531	15.63
9-05-72	139	4.09	508	14.95

Table XXIV. Bacterial Growth Rates For Continuous Leaching At Dilution Rate = 0.0595 Hr^{-1}.

Date	Net NH_4^+	Net NH_4^+ Rate	Total Carbon	Total Carbon Rate
	(mg/l)	(mg/l-hr)	(mg/l)	(mg/l-hr)
16-05-72 1	200	12.06	716	43.18
16-05-72 2	203	12.24	722	43.54
17-05-72 1	204	12.30	716	43.18
17-05-72 2	208	12.54	716	43.18
18-05-72 1	216	13.02	716	43.18
14-06-72 2	48	2.85	208	12.36
15-06-72 1	65	3.86	226	13.44
15-06-72 2	64	3.80	246	14.62
17-06-72 1	46	2.73	225	13.38
21-06-72 1	147	8.64	481	28.30
21-06-72 2	154	9.06	500	29.42
22-06-72 1	137	8.06	468	27.53
22-06-72 2	158	9.29	468	27.53
23-06-72 1	145	8.53	421	24.77

Table XXV. Bacterial Growth Rates For Continuous Leaching At Dilution Rate = 0.1038 Hr^{-1}.

Date	Net NH_4^+	Net NH_4^+ Rate	Total Carbon	Total Carbon Rate
	(mg/l)	(mg/l-hr)	(mg/l)	(mg/l-hr)
12-07-72 1	72	7.48	230	23.92
12-07-72 2	59	6.13	226	23.50
12-07-72 3	66	6.86	226	23.50
13-07-72 1	73	7.59	222	23.08
13-07-72 2	58	6.03	215	22.36
16-07-72 1	77	7.96	280	28.95
17-07-72 1	85	8.78	277	28.64
19-07-72 1	79	8.16	259	26.78
21-07-72 1	106	11.02	315	32.76
22-07-72 1	103	10.71	326	33.90
22-07-72 2	105	10.92	339	35.25
23-07-72 1	101	10.50	310	32.24
23-07-72 2	103	10.71	308	32.03
28-07-72 1	141	14.63	436	45.25
28-07-72 2	140	14.53	428	44.42
28-07-72 3	149	15.46	436	45.25
29-07-72 1	146	15.15	446	46.29
29-07-72 2	148	15.36	446	46.29

Table XXVI. Yield Constants For Continuous Leaching At Dilution Rate = 0.0171 Hr^{-1}. (Corrected For Chemical Leaching)

Date	Net NH_4^+ Yield	Total Carbon Yield	Ratio
	$(\frac{mg\ NH_4^+}{g\ Zn})$	$(\frac{mg\ TC}{g\ Zn})$	$(\frac{mg\ TC}{mg\ NH_4^+})$
22-11-71	10.54	38.6	3.66
23-11-71	10.62	41.1	3.87
24-11-71	10.50	36.7	3.50
25-11-71	-----	38.0	----
26-11-71	10.60	39.1	3.69
27-11-71	10.51	37.5	3.57
15-12-71	12.14	44.1	3.63
16-12-71	11.91	45.3	3.80
17-12-71	12.07	43.9	3.64
17-12-72	10.72	42.8	3.99
18-12-72	9.79	37.6	3.84
19-12-72	9.97	35.7	3.58
20-12-72	10.47	35.4	3.38
21-12-72	10.80	34.9	3.23

Table XXVII. Yield Constants For Continuous Leaching At Dilution Rate = 0.0284 Hr^{-1}. (Corrected For Chemical Leaching)

Date	Net NH_4^+ Yield ($\frac{mg\ NH_4^+}{g\ Zn}$)	Total Carbon Yield ($\frac{mg\ TC}{g\ Zn}$)	Ratio ($\frac{mg\ TC}{mg\ NH_4^+}$)
24-02-72	12.10	49.2	4.06
25-02-72	13.32	48.2	3.62
26-02-72	12.15	45.3	3.73
27-02-72	13.01	46.7	3.59
28-02-72	13.02	51.2	3.93
11-04-72	12.26	47.9	3.91
12-04-72	13.28	49.9	3.76
13-04-72	12.53	44.6	3.56
14-04-72	12.50	46.8	3.74
4-05-72	12.93	45.2	3.50
5-05-72	11.85	43.7	3.75
6-05-72	12.08	44.7	3.70
7-05-72	11.25	42.1	3.74
8-05-72	12.62	45.0	3.56
9-05-72	11.16	40.8	3.66

Table XXVIII. Yield Constants For Continuous Leaching At Dilution Rate = 0.0595 Hr^{-1}. (Corrected For Chemical Leaching)

Date	Net NH_4^+ Yield ($\frac{mg\ NH_4^+}{g\ Zn}$)	Total Carbon Yield ($\frac{mg\ TC}{g\ Zn}$)	Ratio ($\frac{mg\ TC}{mg\ NH_4^+}$)
16-05-72 1	12.03	43.1	3.58
16-05-72 2	11.89	42.3	3.56
17-05-72 1	12.18	42.7	3.51
17-05-72 2	12.38	42.6	3.44
18-05-72 1	12.01	39.8	3.32
14-06-72 2	9.14	39.6	4.33
15-06-72 1	11.86	41.2	3.48
15-06-72 2	11.31	43.5	3.84
17-06-72 1	8.62	42.2	4.89
21-06-72 1	14.19	46.4	3.27
21-06-72 2	13.95	45.3	3.25
22-06-72 1	12.84	43.9	3.42
22-06-72 2	14.95	44.3	2.96
23-06-72 1	13.22	38.4	2.90

Table XXIX. Yield Constants For Continuous Leaching At Dilution Rate = 0.1038 Hr^{-1}. (Corrected For Chemical Leaching)

Date	Net NH_4^+ Yield ($\frac{mg\ NH_4^+}{g\ Zn}$)	Total Carbon Yield ($\frac{mg\ TC}{g\ Zn}$)	Ratio ($\frac{mg\ TC}{mg\ NH_4^+}$)
12-07-72 1	13.21	42.2	3.19
12-07-72 2	10.76	41.2	3.83
12-07-72 3	11.64	39.9	3.42
13-07-72 1	13.32	40.5	3.04
13-07-72 2	10.94	40.6	3.71
16-07-72 1	11.27	41.0	3.64
17-07-72 1	13.21	43.0	3.26
19-07-72 1	12.88	42.2	3.28
21-07-72 1	15.47	46.0	2.97
22-07-72 1	13.32	42.2	3.17
22-07-72 2	14.29	46.1	3.23
23-07-72 1	14.27	43.8	3.07
23-07-72 2	14.53	43.4	2.99
28-07-72 1	14.42	44.6	3.09
28-07-72 2	14.26	43.6	3.06
28-07-72 3	15.16	44.4	2.93
29-07-72 1	14.60	44.6	3.06
29-07-72 2	14.65	44.2	3.01

Table XXX. Results For Continuous Leaching At Dilution Rate = 0.0171 Hr^{-1}
(Zinc Values Uncorrected For Chemical Leaching)

Date	Pulp Density	Specific Surface Area	s	pH	[Fe]	[Zn]	r_Z	r_Z/s
	(%)	(m^2/g)	(m^2/l)		(g/l)	(g/l)	(g/l-hr)	(g/hr-m^2)
22-11-71	4.7304	1.5911	75.27	2.10	1.740	50.25	0.8608	0.0114
23-11-71	4.7164	1.5242	75.10	2.10	1.715	49.40	0.8462	0.0113
24-11-71	4.8720	1.6086	75.10	2.25	1.635	52.15	0.8933	0.0119
25-11-71	4.5588	1.6819	76.67	2.10	1.610	50.95	0.8728	0.0114
26-11-71	4.3080	1.5796	68.05	2.05	1.785	49.45	0.8471	0.0125
27-11-71	4.4242	1.5742	69.65	2.10	1.740	51.45	0.8813	0.0127
15-12-71	2.9900	1.6154	48.30	2.45	0.154	25.15	0.4187	0.0087
16-12-71	2.9164	1.6606	48.43	2.30	0.300	24.95	0.4154	0.0086
17-12-71	2.6142	1.5776	41.24	2.05	0.548	25.35	0.4221	0.0102
17-12-72	1.1184	1.6403	18.35	----	0.677	16.20	0.2767	0.0151
18-12-72	1.1168	1.6877	18.85	2.20	0.691	15.80	0.2699	0.0143
19-12-72	1.0568	1.4938	15.79	2.20	0.666	15.55	0.2656	0.0168
20-12-72	1.0800	1.6629	17.96	2.15	0.664	15.10	0.2579	0.0144
21-12-72	1.0782	1.6477	17.77	2.20	0.690	14.90	0.2545	0.0143

Table XXXI. Results For Continuous Leaching At Dilution Rate = 0.0284 Hr^{-1}
(Zinc Values Uncorrected For Chemical Leaching)

Date	Pulp Density	Specific Surface Area	s	pH	[Fe]	[Zn]	r_Z	r_Z/s
	(%)	(m^2/g)	(m^2/l)		(g/l)	(g/l)	(g/l-hr)	(g/hr-m^2)
24-02-72	3.2866	1.6257	53.43	2.35	0.190	22.45	0.6374	0.0119
25-02-72	3.5100	1.6920	59.39	2.50	0.175	20.70	0.5877	0.0099
26-02-72	3.3754	1.5765	53.21	2.45	0.203	22.05	0.6260	0.0118
27-02-72	3.2320	1.6480	53.26	2.40	0.246	21.10	0.5990	0.0113
28-02-72	3.3532	1.6895	56.65	2.40	0.288	20.70	0.5877	0.0104
11-04-72	5.0574	1.7929	90.67	2.25	0.735	40.25	1.0972	0.0121
12-04-72	5.0906	1.7391	88.53	2.40	0.743	37.85	1.0318	0.0117
13-04-72	5.2812	1.7278	91.25	2.25	0.770	40.10	1.0931	0.0120
14-04-72	5.3028	1.9896	105.51	2.25	0.749	40.25	1.0972	0.0104
4-05-72	1.9364	1.9229	37.24	2.50	0.256	13.94	0.4104	0.0110
5-05-72	1.8720	1.8774	35.15	2.45	0.247	14.05	0.4136	0.0118
6-05-72	1.9072	1.8906	36.06	2.55	0.242	13.66	0.4022	0.0112
7-05-72	1.9608	1.8081	35.45	2.45	0.239	14.21	0.4183	0.0118
8-05-72	2.1300	1.7999	38.34	2.40	0.236	14.38	0.4233	0.0110
9-05-72	2.0098	1.5944	32.04	2.40	0.280	15.02	0.4422	0.0138

Table XXXII. Results For Continuous Leaching At Dilution Rate = 0.0595 Hr^{-1}
(Zinc Values Uncorrected For Chemical Leaching)

Date	Pulp Density	Specific Surface Area	s	pH	[Fe]	[Zn]	r_Z	r_Z/s
	(%)	(m^2/g)	(m^2/l)		(g/l)	(g/l)	(g/l-hr)	($g/hr-m^2$)
16-05-72 1	4.5520	1.6045	73.04	2.40	0.464	20.08	1.2110	0.0166
16-05-72 2	4.4698	1.5980	71.43	2.40	0.479	20.53	1.2382	0.0173
17-05-72 1	4.5110	1.7566	79.24	2.40	0.487	20.21	1.2189	0.0154
17-05-72 2	4.8622	1.8313	89.04	2.45	0.454	20.26	1.2219	0.0137
18-05-72 1	4.7744	1.5437	73.70	2.40	0.467	21.45	1.2936	0.0176
14-06-72 2	1.3235	1.6583	21.95	2.10	0.402	6.310	0.3753	0.0171
15-06-72 1	1.4001	1.6764	23.47	2.05	0.424	6.540	0.3889	0.0166
15-06-72 2	1.3938	1.5374	21.43	2.05	0.434	6.720	0.3996	0.0187
17-06-72 1	1.2562	1.6264	20.43	2.00	0.425	6.395	0.3803	0.0186
21-06-72 1	3.1878	1.7311	55.18	2.30	0.689	12.75	0.7502	0.0136
21-06-72 2	3.2232	1.5770	50.83	2.50	0.677	13.43	0.7902	0.0156
22-06-72 1	3.0330	1.6366	49.64	2.35	0.700	13.06	0.7685	0.0155
22-06-72 2	2.9516	1.6451	48.56	2.35	0.703	12.96	0.7626	0.0157
23-06-72 1	2.9666	1.6570	49.16	2.40	0.737	13.36	0.7861	0.0160

Table XXXIII. Results For Continuous Leaching At Dilution Rate = 0.1038 Hr^{-1}
(Zinc Values Uncorrected For Chemical Leaching)

Date	Pulp Density	Specific Surface Area	s	pH	[Fe]	[Zn]	r_Z	r_Z/s
	(%)	(m^2/g)	(m^2/l)		(g/l)	(g/l)	(g/l-hr)	($g/hr-m^2$)
12-07-72 1	2.0710	1.6780	24.75	2.15	0.349	6.650	0.6916	0.0199
12-07-72 2	2.0836	1.6886	34.77	2.10	0.368	6.685	0.6952	0.0200
12-07-72 3	2.1960	1.8622	40.89	2.20	0.357	6.870	0.7145	0.0174
13-07-72 1	2.1361	1.7202	36.75	2.10	0.355	6.680	0.6947	0.0189
13-07-72 2	2.0155	1.6217	32.69	2.10	0.347	6.500	0.6760	0.0207
16-07-72 1	2.5272	1.7429	44.05	2.30	0.418	8.310	0.8593	0.0195
17-07-72 1	2.5577	1.7053	43.62	2.25	0.393	7.915	0.8184	0.0188
19-07-72 1	2.5797	2.0163	52.01	2.30	0.463	7.615	0.7874	0.0151
21-07-72 1	2.9350	2.0046	58.84	2.20	0.515	8.740	0.9090	0.0155
22-07-72 1	3.0692	1.9324	59.31	2.20	0.524	9.620	1.0005	0.0169
22-07-72 2	3.0468	2.3306	71.01	2.20	0.532	9.240	0.9610	0.0135
23-07-72 1	3.1262	2.1348	66.74	2.25	0.514	8.970	0.9329	0.0140
23-07-72 2	3.0590	2.3881	73.05	2.20	0.495	8.980	0.9339	0.0128
28-07-72 1	4.2682	1.9613	83.71	2.30	0.681	12.36	1.2830	0.0153
28-07-72 2	4.3786	2.0617	90.27	2.30	0.699	12.40	1.2871	0.0143
28-07-72 3	4.4136	1.9829	87.52	2.40	0.662	12.41	1.2882	0.0147
29-07-72 1	4.2328	1.8522	78.40	2.35	0.715	12.58	1.3058	0.0167
29-07-72 2	4.4098	2.1800	96.13	2.35	0.717	12.68	1.3162	0.0137

Table XXXIV. Results For Continuous Leaching At Dilution Rate = 0.0171 Hr^{-1}
(Zinc Values Corrected For Chemical Leaching)

Date	Pulp Density	Specific Surface Area	s	pH	[Fe]	[Zn]	r_Z	r_Z/s
	(%)	(m^2/g)	(m^2/l)		(g/l)	(g/l)	(g/l-hr)	(g/hr-m^2)
22-11-71	4.7304	1.5911	75.27	2.10	1.740	41.73	0.7148	0.0095
23-11-71	4.7164	1.5242	75.10	2.10	1.715	40.88	0.7003	0.0093
24-11-71	4.8720	1.6086	75.10	2.25	1.635	43.63	0.7474	0.0100
25-11-71	4.5588	1.6819	76.67	2.10	1.610	42.43	0.7268	0.0095
26-11-71	4.3080	1.5796	68.05	2.05	1.785	40.93	0.7011	0.0103
27-11-71	4.4242	1.5742	69.65	2.10	1.740	42.93	0.7354	0.0106
15-12-71	2.9900	1.6154	48.30	2.45	0.154	19.93	0.3318	0.0069
16-12-71	2.9164	1.6606	48.43	2.30	0.300	19.73	0.3285	0.0068
17-12-71	2.6142	1.5776	41.24	2.05	0.548	20.13	0.3352	0.0081
17-12-72	1.1184	1.6403	18.35	----	0.677	13.99	0.2389	0.0130
18-12-72	1.1168	1.6877	18.85	2.20	0.691	13.59	0.2321	0.0123
19-12-72	1.0568	1.4938	15.79	2.20	0.666	13.34	0.2278	0.0144
20-12-72	1.0800	1.6629	17.95	2.15	0.664	12.89	0.2202	0.0123
21-12-72	1.0782	1.6477	17.77	2.20	0.690	12.69	0.2167	0.0122

Table XXXV. Results For Continuous Leaching At Dilution Rate = 0.0284 Hr^{-1}
(Zinc Values Corrected For Chemical Leaching)

Date	Pulp Density	Specific Surface Area	s	pH	[Fe]	[Zn]	r_Z	r_Z/s
	(%)	(m^2/g)	(m^2/l)		(g/l)	(g/l)	(g/l-hr)	(g/hr-m^2)
24-02-72	3.2866	1.6257	53.43	2.35	0.190	18.34	0.5207	0.0097
25-02-72	3.5100	1.6920	59.39	2.50	0.175	16.59	0.4710	0.0079
26-02-72	3.3754	1.5765	53.21	2.45	0.203	17.94	0.5093	0.0096
27-02-72	3.2320	1.6480	53.26	2.40	0.246	16.99	0.4823	0.0091
28-02-72	3.3532	1.6895	56.65	2.40	0.288	16.59	0.4710	0.0083
11-04-72	5.0574	1.7929	90.67	2.25	0.735	33.12	0.9029	0.0100
12-04-72	5.0906	1.7391	88.53	2.40	0.743	30.72	0.8374	0.0095
13-04-72	5.2812	1.7278	91.25	2.25	0.770	32.97	0.8988	0.0099
14-04-72	5.3028	1.9896	105.51	2.25	0.749	33.12	0.9029	0.0086
4-05-72	1.9364	1.9229	37.24	2.50	0.256	11.37	0.3347	0.0090
5-05-72	1.8720	1.8774	35.15	2.45	0.247	11.48	0.3380	0.0096
6-05-72	1.9072	1.8906	36.06	2.55	0.242	11.09	0.3265	0.0091
7-05-72	1.9608	1.8081	35.45	2.45	0.239	11.64	0.3427	0.0097
8-05-72	2.1300	1.7999	38.34	2.40	0.236	11.81	0.3477	0.0091
9-05-72	2.0098	1.5944	32.04	2.40	0.280	12.45	0.3665	0.0114

Table XXXVI. Results For Continuous Leaching At Dilution Rate = 0.0595 Hr^{-1}
(Zinc Values Corrected For Chemical Leaching)

Date	Pulp Density	Specific Surface Area	s	pH	[Fe]	[Zn]	r_Z	r_Z/s
	(%)	(m^2/g)	(m^2/l)		(g/l)	(g/l)	(g/l-hr)	($g/hr-m^2$)
16-05-72 1	4.5520	1.6045	73.04	2.40	0.464	16.62	1.0024	0.0137
16-05-72 2	4.4698	1.5980	71.43	2.40	0.479	17.07	1.0295	0.0144
17-05-72 1	4.5110	1.7566	79.24	2.40	0.487	16.75	1.0102	0.0128
17-05-72 2	4.8622	1.8313	89.04	2.45	0.454	16.80	1.0132	0.0114
18-05-72 1	4.7744	1.5437	73.70	2.40	0.467	17.99	1.0850	0.0147
14-06-72 2	1.3235	1.6583	21.95	2.10	0.402	5.250	0.3122	0.0142
15-06-72 1	1.4001	1.6764	23.47	2.05	0.424	5.480	0.3259	0.0139
15-06-72 2	1.3938	1.5374	21.43	2.05	0.434	5.660	0.3366	0.0157
17-06-72 1	1.2562	1.6264	20.43	2.00	0.425	5.335	0.3173	0.0155
21-06-72 1	3.1878	1.7311	55.18	2.30	0.689	10.36	0.6096	0.0111
21-06-72 2	3.2232	1.5770	50.83	2.50	0.677	11.04	0.6496	0.0128
22-06-72 1	3.0330	1.6366	49.64	2.35	0.700	10.67	0.6278	0.0127
22-06-72 2	2.9516	1.6451	48.56	2.35	0.703	10.57	0.6219	0.0128
23-06-72 1	2.9666	1.6570	49.16	2.40	0.737	10.97	0.6455	0.0131

Table XXXVII. Results For Continuous Leaching At Dilution Rate = 0.1038 Hr^{-1}
(Zinc Values Corrected For Chemical Leaching)

Date	Pulp Density	Specific Surface Area	s	pH	[Fe]	[Zn]	r_Z	r_Z/s
	(%)	(m^2/g)	(m^2/l)		(g/l)	(g/l)	(g/l-hr)	(g/hr-m^2)
12-07-72 1	2.0710	1.6780	24.75	2.15	0.349	5.450	0.5668	0.0163
12-07-72 2	2.0836	1.6886	34.77	2.10	0.368	5.485	0.5704	0.0164
12-07-72 3	2.1960	1.8622	40.89	2.20	0.357	5.670	0.5897	0.0144
13-07-72 1	2.1361	1.7202	36.75	2.10	0.355	5.480	0.5699	0.0155
13-07-72 2	2.0155	1.6217	32.69	2.10	0.347	5.300	0.5512	0.0169
16-07-72 1	2.5272	1.7429	44.05	2.30	0.418	6.830	0.7062	0.0160
17-07-72 1	2.5577	1.7053	43.62	2.25	0.393	6.435	0.6654	0.0153
19-07-72 1	2.5797	2.0163	52.01	2.30	0.463	6.135	0.6344	0.0122
21-07-72 1	2.9350	2.0046	58.84	2.20	0.515	6.850	0.7124	0.0121
22-07-72 1	3.0692	1.9324	59.31	2.20	0.524	7.730	0.8039	0.0136
22-07-72 2	3.0468	2.3306	71.01	2.20	0.532	7.350	0.7644	0.0108
23-07-72 1	3.1262	2.1348	66.74	2.25	0.514	7.080	0.7363	0.0110
23-07-72 2	3.0590	2.3881	73.05	2.20	0.495	7.090	0.7374	0.0101
28-07-72 1	4.2682	1.9613	83.71	2.30	0.681	9.780	1.0152	0.0121
28-07-72 2	4.3786	2.0617	90.27	2.30	0.699	9.820	1.0193	0.0113
28-07-72 3	4.4136	1.9829	87.52	2.40	0.662	9.830	1.0204	0.0117
29-07-72 1	4.2328	1.8522	78.40	2.35	0.715	10.00	1.0380	0.0132
29-07-72 2	4.4098	2.1800	96.13	2.35	0.717	10.10	1.0484	0.0109

APPENDIX V

Calculations For Steady-State Achieved

22-11-71 To 27-11-71 Inclusive

1. Dilution Rate:

(a) Average Tank Depth With Air Off:

$$(2.54)\left(\frac{(11.25)(5) + 11.3125}{6.}\right) = 28.601 \text{ cm}$$

(b) Average Tank Volume For Test:

$$(0.63616)(28.601) - 0.020 = 18.175 \text{ l}$$

(c) Average Product Rate

Total Volume Collected

$= 22.8 + 22.5 + 20.4 = 65.70$ l

Total Time Span

20-11-71	29-11-71
1500	1030

$= 211.5$ hr

Subtract .5 Hr for Power Outage $= 211.0$ hr

Product Rate

$$= \frac{65.70}{211.} = 0.3114 \ \frac{1}{\text{hr}}$$

(D) Average Dilution Rate

$$= \frac{0.3114}{18.175} = 0.01713 \text{ hr}^{-1}$$

Residence Time $= 58.37$ hr

2. Specific Growth Rate:

By steady-State assumption, $\mu = D = 0.01713 \text{ hr}^{-1}$

$$t = \frac{\ln 2}{\mu} = 40.464 \text{ hr}$$

3. Surface Area Concentrations:

$$s = 10 \ (pd)(SSA)$$

Date	pd	SSA	s	
	%	(m^2/g)	(m^2/l)	
22-11-71	4.7304	1.5911	75.27	
23-11-71	4.7164	1.5242	75.10	*
24-11-71	4.8720	1.6086	75.10	
25-11-71	4.5588	1.6819	76.67	
26-11-71	4.3080	1.5796	68.05	
27-11-71	4.4242	1.5742	69.65	

* Not sure which pd goes with which SSA due to labelling error (23-11,24-11). Therefore average pulp densities and specific surface areas:

Average pd = 4.7942 % s = 75.10 m^2/l

Average SSA = 1.5664 m^2/g

4. Bacterial Growth Rate:

$$r_X = DX$$

Baseline Correction:

Net NH_4^+ = (13.68)(.72) = 10. mg/l

Total Carbon = (13.68)(7.26) = 99. mg/l

Corrected Values

Date	X_n	r_n	X_c	r_c
	(mg/l)	(mg/l-hr)	(mg/l)	(mg/l-hr)
22-11-71	440	7.53	1611	27.59
23-11-71	434	7.43	1681	28.79
24-11-71	458	7.84	1601	27.42
25-11-71	---	----	1611	27.60
26-11-71	434	7.43	1601	27.42
27-11-71	451	7.72	1609	27.56

5. Zinc Production Rate: (Dissolved Zinc)

$$r_Z = D[Zn]$$

Not Corrected For Chemical Leaching

Date	[Zn] (g/l)	r_Z (g/l-hr)	s (m^2/l)	r_Z/s (g/hr-m^2)
22-11-71	50.25	0.8608	75.27	0.0114
23-11-71	49.40	0.8462	75.10	0.0113
24-11-71	52.15	0.8933	75.10	0.0119
25-11-71	50.95	0.8728	76.67	0.0114
26-11-71	49.45	0.8471	68.05	0.0125
27-11-71	51.45	0.8813	69.65	0.0127

Correction For Chemical Leaching:

$$= \frac{(.001333)(73.31)}{(.01713)} + (.0206)(136.8) = 8.52 \text{ g/l}$$

Corrected For Chemical Leaching

Date	[Zn] (g/l)	r_Z (g/l-hr)	s (m^2/l)	r_Z/s (g/hr-m^2)
22-11-71	41.73	0.7148	75.27	0.0095
23-11-71	40.88	0.7003	75.10	0.0093
24-11-71	43.63	0.7474	75.10	0.0100
25-11-71	42.43	0.7268	76.67	0.0095
26-11-71	40.93	0.7011	68.05	0.0103
27-11-71	42.93	0.7354	69.65	0.0106

6. Yield Constants:

$$Y_n = \frac{r_n}{r_Z} \qquad Y_C = \frac{r_C}{r_Z}$$

Date	r_n $\frac{mg/l\ NH_4^+}{hr.}$	r_c $\frac{mg/l\ TC}{hr.}$	r_Z (g/l-hr)
22-11	7.709	29.29	0.861
23-11	7.606	30.49	0.846
24-11	8.017	29.12	0.893
25-11	-----	29.29	0.873
26-11	7.606	29.12	0.847
27-11	7.897	29.26	0.881

Date	Y_n $(\frac{mg\ NH_4^+}{g\ Zn})$	Y_c $(\frac{mg\ TC}{g\ Zn})$	Y_c/Y_n $(\frac{mg\ TC}{mg\ NH_4^+})$
22-11	10.54	38.6	3.66
23-11	10.62	41.1	3.87
24-11	10.50	36.7	3.50
25-11	-----	38.0	----
26-11	10.60	39.1	3.69
27-11	10.51	37.5	3.57

7. Volume Fraction Liquid In Tank

pd + (Volume Fracticn Liquid)(Density Of Liquid)

= (Density Of Slurry)

$$\therefore \text{(Volume Fraction Liquid)} = \frac{\text{(Density Of Slurry)} - pd}{\text{(Density Of Liquid)}}$$

Date	ρ_s (g/ml)	ρ_L (g/ml)	pd (g/ml)	Fraction Liquid
22-11	1.162	1.123	.0473	0.993
23-11	1.166	1.127	.0472	0.993
24-11	1.177	1.131	.0487	0.998
25-11	1.165	1.126	.0456	0.994
26-11	1.163	1.127	.0431	0.994
27-11	1.170	1.128	.0442	0.998

Note that this calculation ignores the weight of jarosite which is dissolved in the HCl wash of the pulp density sample.

8. Zinc Balance Over Tank: 20-11-71 ---- 29-11-71

Input:

Average Feed Rate

$$= \frac{((0.7671)(6) + 0.7392 + 0.7761 + 0.7290 + 0.7463)}{10.}$$

$$= .759 \text{ g/min}$$

Over 211 hr, Feed (211)(60)(0.7593)

= 9613 g Concentrate

Composition Of Concentrate = 55.69% Zn.

Therefore Total Weight Of Zinc Fed = (0.5569)(9613.)

= 5353 g Zinc

Output

Soluble Zinc:

22.8 l @ 49.00 g/l	=	1117 g
22.5 l @ 51.75 g/l	=	1164 g
20.4 l @ 48.40 g/l	=	987 g
Total	=	3268 g

Residue Analysis: Average Residue Analysis = 55.30% Zn.

Residue Production: 65.70 l @ 4.60% pd (average)

Total Residue Produced = (65.70)(0.0460)(1000)

= 3022 g

Total Zinc In Residue = (3022)(0.553) = 1671 g Zinc

Zinc Removed In Daily Sampling:

20 ml Centrifuged For Clear Sample And Analysis
10 ml Mixture For Dist. NH_4^+, TC, Density

10 ml Mixture For pH
4 ml For Kjeldahl Digestion
50 ml For Pulp Density

94 ml Daily

Removed 9 Samples Or 876 ml Containing

$$(49.72)(0.876)+(0.553)(46.0)(0.876)$$

$$= 65.8 \text{ g Zinc}$$

Total Zinc Output = (3268+1671+66) = 5005 g Zinc

Loss = (5353-5005)/5353 = 6.50%

9. Percent Extraction:

$$\text{Percent Extraction} = \frac{\text{Soluble Zinc Out}}{\text{Total Zinc Out}} \quad (100\%)$$

$$\frac{(3312)}{(5005)}(100\%) = 66.2\%$$

10. Concentration Of Surface Area In Feed:
(Feed Of 29-11-71)

Average Feed Rate Based On Recovered Zinc

$$= \frac{5005}{(.5569)(211)}$$

$$= 42.59 \text{ g/hr}$$

Product Rate = 0.3114 l/hr , >99% Liquid By Volume.

$$pd = \frac{42.59}{(0.3114)(10)} = 13.68\%$$

SSA Feed 29-11-71 = 3.2012 m^2/g

Therefore $s = (0.1368)(3.2012)(1000) = 437.9 \ m^2/l$

Table XXXVIII. Product Data For Sample Calculation.

Date	Time	Product Volume	[Zn]
		(l)	(g/l)
20-11	1500	0.0	
23-11	1445	22.8	49.00
23-11	1445	0.0	
26-11	1415	22.5	51.75
26-11	1415	0.0	
29-11	1030	20.4	48.40

Table XXXIX. Summary Of Daily Tank Data, 22-11-71 --- 27-11-71.

Date	pH	T	[Zn]
		(°C)	(g/l)
22-11	2.12	35.8	1.740
23-11	2.08	35.8	1.715
24-11	2.25	36.0	1.635
25-11	2.09	35.9	1.610
26-11	2.06	35.9	1.785
27-11	2.08	35.5	1.740

Table XL. Summary Of Tank Data For Sample Calculation.

Date	Depth	Solids Feed Rate	Slurry Density	Liquid Density
	(inches)	(g/min)	(g/ml)	(g/ml)
20-11	11.313	0.7392	1.159	1.118
21-11	11.250	0.7761	1.161	1.116
22-11	11.250	0.7859	1.162	1.123
23-11	11.313	0.8024	1.166	1.127
24-11	11.250	0.7588	1.177	1.131
25-11	11.250	0.7634	1.165	1.126
26-11	11.250	0.7660	1.163	1.127
27-11	11.250	0.7259	1.170	1.128
28-11	11.250	0.7290	1.168	1.114
29-11	11.250	0.7463	1.167	1.120

APPENDIX VI

Calculation Of Fractional Extraction Using Levenspiel's Model

Appendix VI. Calculation Of Fractional Extraction Using Levenspiel's Model.

A. Calculation From Bahco Size Distribution Of Feed

An attempt has been made to estimate the fractional extraction at various dilution rates using Levenspiel's shrinking sphere model for the case of chemical reaction controlling (17), by assuming that the feed consists of six fractions of monodisperse spheres corresponding to the six Bahco fractions (Figure 30). Using a release rate per unit surface area of 0.01 g/hr-m², the time for total reaction for particles of each size, τ , is calculated from

$$\tau = \frac{\rho d_o/2}{r_Z/s} \tag{76}$$

Using a dilution rate of 0.0595 hr^{-1} ($\bar{t}$ equals 16.8 hr), the fractional extraction for particles of each size is given by

$$X = 3\frac{\bar{t}}{\tau} - 6\left(\frac{\bar{t}}{\tau}\right)^2 + 6\left(\frac{\bar{t}}{\tau}\right)^3 \left(1 - e^{-\tau/\bar{t}}\right) \tag{77}$$

This equation has been plotted in Figure 31.

The mean fractional extraction for the feed is then calculated by summing the fractional extraction for each size times the fraction of the feed which is that size:

Figure 30
BAHCO SIZE DISTRIBUTION
ANALYSIS OF FEED CONCENTRATE

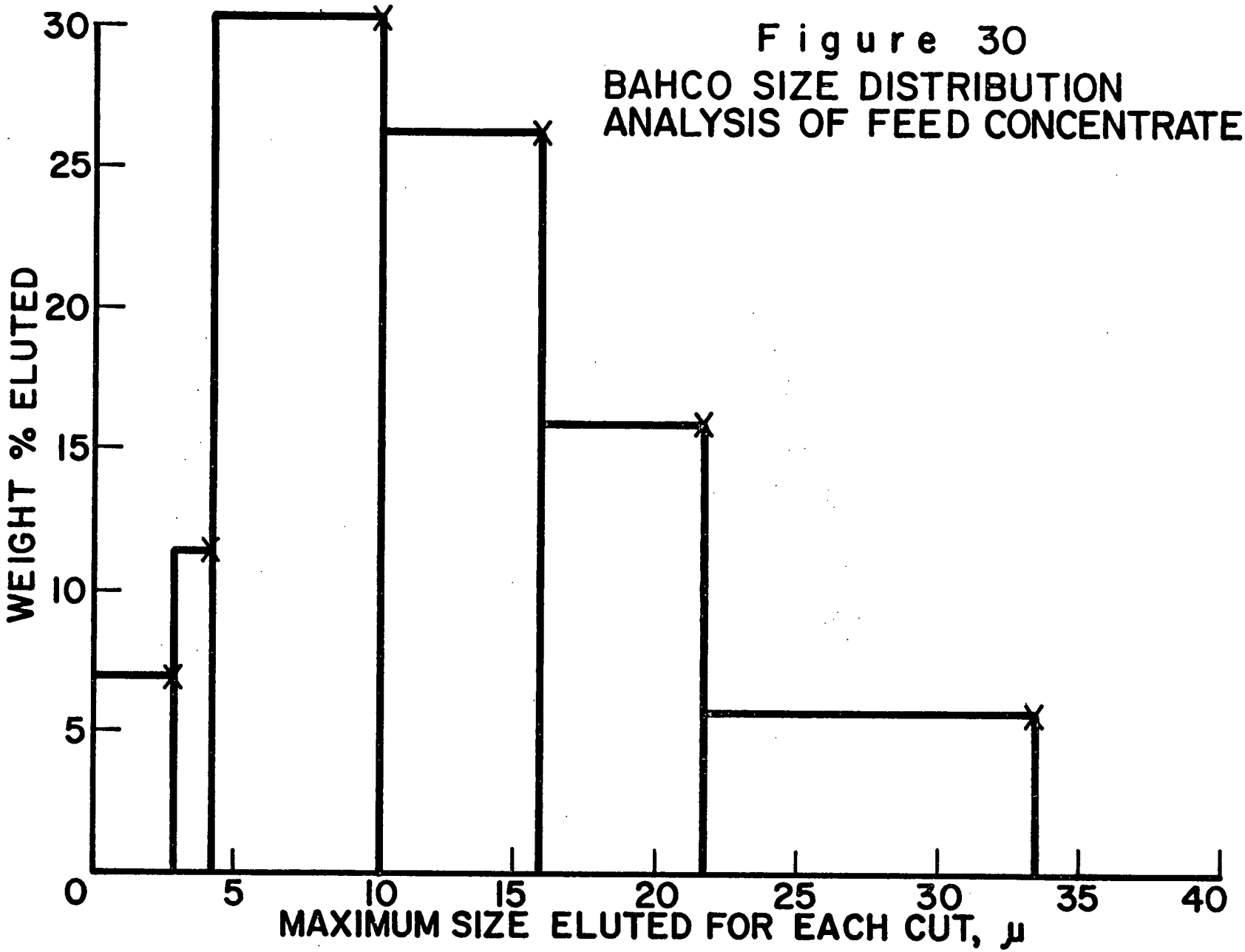

Figure 31

FRACTIONAL EXTRACTION Vs DIMENSIONLESS RESIDENCE TIME CALCULATED FROM LEVENSPIEL'S MODEL (17)

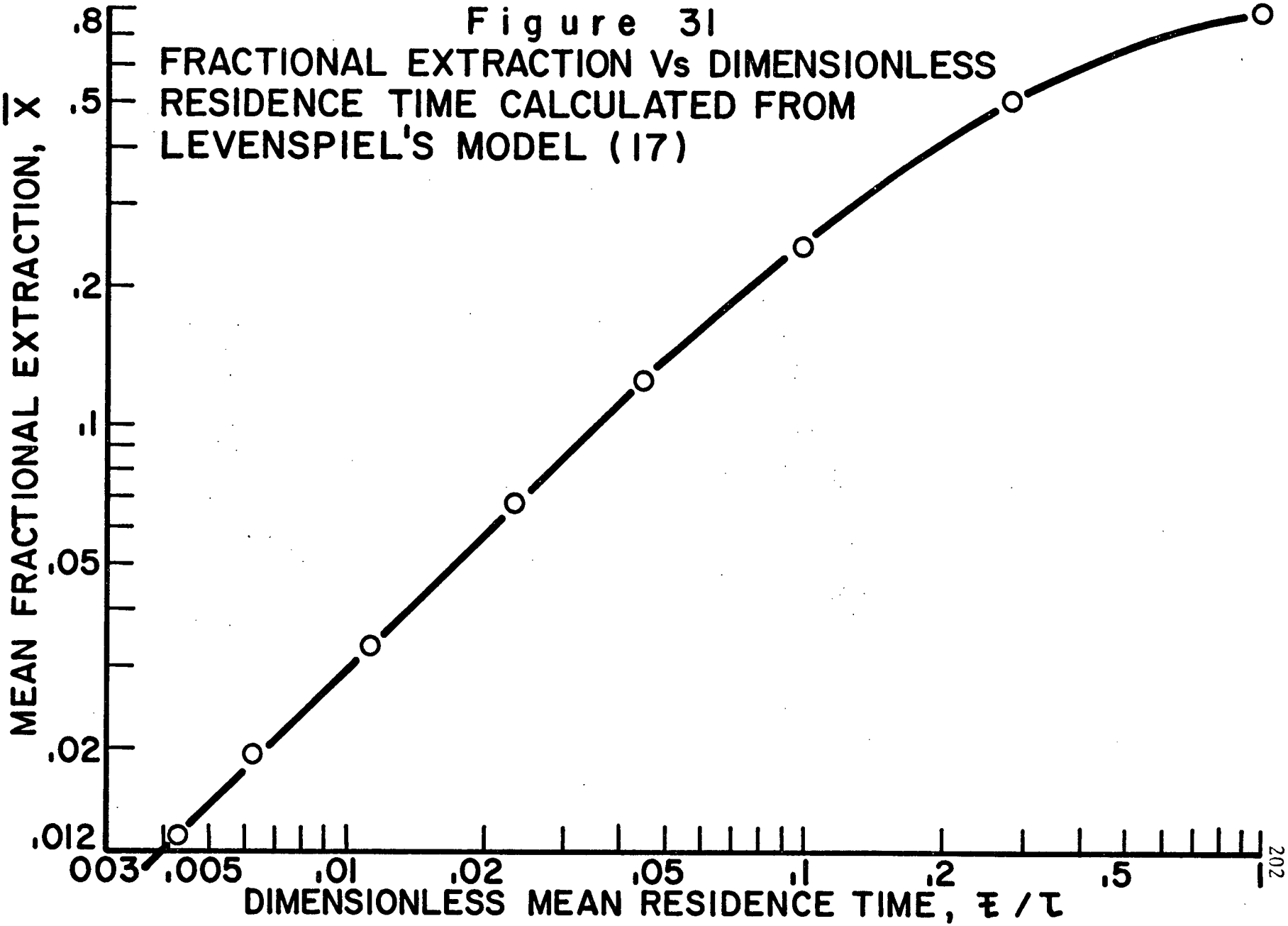

Table XLI. Calculation Of Fractional Extraction.

Size	Fraction Of Total	τ	$\frac{\bar{t}}{\tau}$	X	Overall Contribution
(μ)		(hr)			
1.8	0.091	369	0.0455	0.125	0.0114
3.5	0.116	718	0.0234	0.067	0.0081
7.2	0.308	1476	0.01138	0.033	0.0102
13.0	0.266	2665	0.00630	0.019	0.0051
19.0	0.161	3895	0.00431	0.013	0.0021
27.7	0.058	5679	0.00296	0.009	0.0005
					0.0374

$\bar{X}$ measured for this dilution rate is 0.427; $\bar{X}$ calculated by the above method is 0.037. Possible reasons for this discrepancy are:

The concentrate particles are of irregular shape and thus may have a greater surface area than spheres of the same diameter.

The sizes assigned to each fraction of material were the representative maximum sizes for that fraction. The smallest sized particles in each fraction may be completely eluted out of the equipment during the sizing operation, making it impossible to calculate a valid average particle size for the fraction. Consequently, the only thing one can do with any certainty is measure the dimensions of the largest particles one can find in a fraction.

The material fed to the Bahco sizer may not have been decaked to the point where each particle was classified individually. Clumps of small particles could report as larger particles.

Finally, the B. E. T. surface area may not represent the surface area on which the leaching reactions are occurring. If the B. E. T. surface area is too high an estimate, the reaction rate per unit surface used would be too low, and this could account for part of the discrepancy.

B. Calculation From Results Of A Continuous Run At One Dilution Rate

If we assume a monodisperse feed of spheres having the observed reaction rate per unit surface area, we can develop a

method to predict the extraction at other dilution rates once the extraction for one dilution rate is known.

To improve the accuracy of this method, we can express the extractions as fractions of the maximum amount of zinc extractable from the concentrate, not as fractions of the total amount of zinc in the concentrate.

The maximum fractional extraction obtainable from our sample of zinc concentrate was determined to be 0.886. On this basis, the extraction for the dilution rate of 0.0595 hr^{-1} is 0.482. Using Figure 31 we find τ = 64.6 hr, and d_o = 0.315 μ. Using this value of τ and Figure 31, we can get extractions for the three other dilution rates used and compare them with the achieved extractions.

A plot of measured extractions as a function of predicted extractions is given in Figure 32. The agreement is fair; thus, this method should prove helpful in making design decisions when solid substrate concentration is limiting the growth rate.

Figure 32

MEASURED FRACTIONAL EXTRACTION Vs FRACTIONAL EXTRACTION PREDICTED BY LEVENSPIEL'S MODEL (17)